

LOSS OF VENTROMEDIAL HYPOTHALAMIC LEPTIN RECEPTORS
RESULTS IN INCREASED ADIPOSITY AND A
METABOLIC SYNDROME

APPROVED BY SUPERVISORY COMMITTEE

Keith Parker, M.D., Ph.D.

Andrew Zinn, M.D., Ph.D.

Jane Johnson, Ph.D.

Lisa Monteggia, Ph.D.

“If you can dream it, you can do it. Always remember that this whole thing was started with a dream and a mouse.”

Walt Disney

DEDICATION

This work has not been done in a vacuum, and I owe thanks to many people. To labmates, past and present, who provided helping hands, know-how, encouragement, good advice and friendship – thank you. Suria, Liping, Yelena, Gareth, Tom, Goro, Carlotta, Anne, Nancy, and Kimmie, you have been a pleasure to work with. Last, this work would not have been possible without the support of my mentor Keith Parker, who provided the means and freedom to explore and learn. Thank you Keith, for the scientific foundation you have provided for me during my time in your lab.

On a personal note, I have been fortunate to be raised by loving parents, who have always given me the support I needed – financial, emotional, or spiritual. I count myself truly privileged to have grown up in the home they provided. Thank you, Mom and Dad. I would not be here without you.

The last five years have been an adventure, filled with high hopes and disappointments, enthusiasm and discouragement, excitement and drudgery. Through all the ups and down, twists and turns, it has been the great blessing of my life to have a beautiful and wonderful friend to love and support me, my wife Danielle. To you, Danielle, I give my sincere thanks and love. I look forward to many more years of your companionship. As well, the rough patches have always been made better by the smiles and hugs of my children. Chaid, Avram, and Kennis, thank you for making home such a sweet place to be.

LOSS OF VENTROMEDIAL HYPOTHALAMIC LEPTIN RECEPTORS
RESULTS IN INCREASED ADIPOSITY AND A
METABOLIC SYNDROME

by

NATHAN CHRISTIAN BINGHAM

DISSERTATION

Presented to the Faculty of the Graduate School of Biomedical Sciences

The University of Texas Southwestern Medical Center at Dallas

In Partial Fulfillment of the Requirements

For the Degree of

DOCTOR OF PHILOSOPHY

The University of Texas Southwestern Medical Center at Dallas

Dallas, Texas

May, 2008

Copyright

by

NATHAN CHRISTIAN BINGHAM, 2008

All Rights Reserved

LOSS OF VENTROMEDIAL HYPOTHALAMIC LEPTIN RECEPTORS
RESULTS IN INCREASED ADIPOSITY AND A
METABOLIC SYNDROME

NATHAN CHRISTIAN BINGHAM, M.D., Ph.D.

The University of Texas Southwestern Medical Center at Dallas, 2008

SUPERVISING PROFESSOR: KEITH L. PARKER, M.D., Ph.D.

Obesity is a leading health problem here in the United States and in other developing countries. Obesity is a risk factor for several life-threatening conditions including Type II diabetes, hypertension, and cardiovascular disease. Given the growing obesity epidemic, understanding the mechanisms whereby the central nervous system monitors and regulates energy homeostasis has become a major focus of scientific research in the last several decades. The discovery that

leptin, an adipocyte-derived hormone, acts on the brain to suppress appetite and stimulate energy expenditure greatly extended our understanding of such mechanisms. The leptin receptor is expressed in a number of hypothalamic nuclei known to play a role in energy homeostasis. While much work has focused on leptin's actions in the arcuate nucleus, other sites have received substantially less attention. Here, I report that mice lacking leptin receptors within the ventromedial hypothalamic nucleus ($\text{Lepr KO}^{\text{VMH}}$) develop increased adiposity and a metabolic syndrome. $\text{Lepr KO}^{\text{VMH}}$ mice fed high fat rodent chow show an increased sensitivity to diet-induced obesity, while $\text{Lepr KO}^{\text{VMH}}$ mice fed a low fat diet exhibit significantly increased adipose mass with no difference in weight compared to wild-type littermates. Further, these mice exhibit a metabolic syndrome including mild steatosis, dyslipidemia, and hyperleptinemia. From a young age, $\text{Lepr KO}^{\text{VMH}}$ mice are hyperinsulinemic and eventually become glucose intolerant. These data demonstrate that $\text{Lepr KO}^{\text{VMH}}$ mice are a novel genetic model of obesity and may be used for the study of energy partitioning, lipogenesis, and central leptin signaling.

TABLE OF CONTENTS

DEDICATION	iii
TABLE OF CONTENTS	viii
PRIOR PUBLICATIONS	x
LIST OF FIGURES.....	xi
LIST OF TABLES	xii
LIST OF DEFINITIONS.....	xiii
CHAPTER ONE Introduction.....	1
A GROWING PROBLEM.....	1
CENTRAL CONTROL OF ENERGY HOMEOSTASIS	4
<i>Hypothalamic Development and Anatomy</i>	6
<i>The Hypothalamus and Energy Homeostasis</i>	8
THE VENTROMEDIAL HYPOTHALAMIC NUCLEUS (VMH)	9
<i>Ventromedial Hypothalamic Development</i>	9
<i>Neuronal Circuitry of the VMH</i>	11
<i>Functional Studies of the Ventromedial Hypothalamus</i>	12
<i>The Myth of the Ventromedial Nucleus</i>	15
MOLECULAR GENETICS OF OBESITY	16
<i>Yellow agouti (A^y)</i>	16
<i>obese and diabetes</i>	21
<i>Steroidogenic Factor 1</i>	34
RATIONALE OF PRESENT WORK	36
CHAPTER TWO Materials & Methods.....	39
CONSTRUCTION OF THE SF-1/CRE BAC.....	39
GENERATION OF SF-1/CRE TRANSGENIC MICE	39
ANIMAL CARE	40
<i>Husbandry</i>	40
<i>Genotyping</i>	40
<i>Body weight and composition</i>	41
<i>Tissue and plasma collection</i>	41
SOUTHERN ANALYSIS	42
LIVER AND PLASMA TRIGLYCERIDE MEASUREMENTS	43
ISOLATION OF TISSUE MRNA AND QRT-PCR.....	43
HISTOLOGY	44
<i>H&E Staining</i>	44
<i>pSTAT3 immunohistochemistry</i>	45
<i>Oil Red O staining</i>	47
<i>β-galactosidase stain</i>	47
PLASMA HORMONE MEASUREMENTS	49
ASSESSMENT OF FEMALE ESTRUS CYCLE.....	49
ENERGY EXPENDITURE	50
<i>Indirect calorimetry and fine locomotor activity</i>	50
<i>Wheel running</i>	50
GLUCOSE TOLERANCE TESTS	51

CHAPTER THREE Development of a steroidogenic factor 1/Cre transgenic mouse line	52
INTRODUCTION.....	52
RESULTS.....	53
<i>SF-1/Cre transgene</i>	53
<i>ROSA26R Studies</i>	54
CONCLUSION	63
CHAPTER FOUR Cre mediated deletion of Lepr from the Ventromedial Hypothalamic Nucleus.....	64
INTRODUCTION.....	64
RESULTS.....	65
<i>Generation of Lepr KO^{VMH} mice</i>	65
<i>Selective deletion of VMH LEPRs</i>	65
<i>Lepr KO^{VMH} mice are sensitive to diet-induced obesity (DIO)</i>	67
<i>Body composition of Lepr KO^{VMH} mice</i>	67
<i>Hepatic pathology and dyslipidemia</i>	70
<i>Neuroendocrine function of Lepr KO^{VMH} mice</i>	72
<i>Food Intake</i>	78
<i>Energy Expenditure</i>	80
<i>Glucose Homeostasis</i>	84
CONCLUSION	88
CHAPTER 5 Conclusions and Future directions	91
CONCLUSIONS	91
<i>Other VMH leptin models</i>	92
<i>Comparison of Lepr KO^{VMH} and MC3R KO mice</i>	93
<i>Hyperinsulinemia of Lepr KO^{VMH} mice</i>	95
FUTURE DIRECTIONS	97
<i>Diet-induced thermogenesis</i>	98
<i>Lipogenesis</i>	99
<i>Neuronal Circuitry of VMH LEPRs – Role of MC3R</i>	100
<i>Hyperinsulinemia</i>	101
<i>Other gene knockouts</i>	102
BIBLIOGRAPHY	104
VITAE.....	122

PRIOR PUBLICATIONS

- Busath, D. D., Thulin, C. D., Hendershot, R. W., Phillips, L. R., Maughan, P., Cole, C. D., Bingham, N. C., Morrison, S., Baird, L. C., Hendershot, R. J., *et al.* (1998). Noncontact dipole effects on channel permeation. I. Experiments with (5F-indole)Trp13 gramicidin A channels. *Biophys J* 75, 2830-2844.
- Bingham, N. C., Smith, N. E., Cross, T. A. and Busath, D. D. (2003). Molecular dynamics simulations of Trp side-chain conformational flexibility in the gramicidin A channel. *Biopolymers* 71, 593-600.
- Correa, R. V., Domenice, S., Bingham, N. C., Billerbeck, A. E., Rainey, W. E., Parker, K. L. and Mendonca, B. B. (2004). A microdeletion in the ligand binding domain of human steroidogenic factor 1 causes XY sex reversal without adrenal insufficiency. *J Clin Endocr Metab* 89, 1767-1772.
- Li, Y., Choi, M., Cavey, G., Daugherty, J., Suino, K., Kovach, A., Bingham, N. C., Kliewer, S. A. and Xu, H. E. (2005). Crystallographic identification and functional characterization of phospholipids as ligands for the orphan nuclear receptor steroidogenic factor-1. *Mol Cell* 17, 491-502.
- Bingham, N. C., Verma-Kurvari, S., Parada, L. F. and Parker, K. L. (2006). Development of a steroidogenic factor 1/Cre transgenic mouse line. *Genesis* 44, 419-424.
- Reuter, A.L., Goji, K., Bingham, N.C., Matsuo, M., and Parker, K.L. (2007). A novel mutation in the accessory DNA-binding domain of human steroidogenic factor 1 causes XY gonadal dysgenesis without adrenal insufficiency. *Eur J Endocrinol* 157, 233-238.
- Kim, Y., Bingham, N., Sekido, R., Parker, K.L., Lovell-Badge, R., and Capel, B. (2007). Fibroblast growth factor receptor 2 regulates proliferation and Sertoli differentiation during male sex determination. *Proc Natl Acad Sci U S A* 104, 16558-16563.

LIST OF FIGURES

FIGURE 1. ENERGY BALANCE.....	6
FIGURE 2. HYPOTHALAMIC NUCLEI.....	8
FIGURE 3. MEDIAL HYPOTHALAMUS.	10
FIGURE 4. PARABIOSIS OF DB/DB AND OB/OB MICE WITH NORMAL MICE.	24
FIGURE 5. LEPTIN SIGNAL TRANSDUCTION.....	29
FIGURE 6. LEPTIN-MELANOCORTIN CIRCUIT OF THE ARCUATE NUCLEUS.....	34
FIGURE 7. SF-1/CRE BAC TRANSGENE AND TRANSGENE COPY OF TRANSGENIC FOUNDERS.	54
FIGURE 8. B-GALACTOSIDASE EXPRESSION IN TISSUES OF ADULT SF-1/CRE/ROSA26R MICE.	56
FIGURE 9. B-GALACTOSIDASE EXPRESSION IN THE BRAIN OF ADULT SF-1/CRE/ROSA26R MICE.	59
FIGURE 10. B-GALACTOSIDASE EXPRESSION DURING EMBRYONIC DEVELOPMENT.	61
FIGURE 11. PSTAT3 IMMUNOHISTOCHEMICAL ANALYSIS OF LEPR KO ^{VMH} BRAINS.....	67
FIGURE 12. BODY WEIGHT OF LEPR KO ^{VMH} MICE.	68
FIGURE 13. ADIPOSE HISTOLOGY OF LEPR KO ^{VMH} MICE.	70
FIGURE 14. LIVER PATHOLOGY OF LEPR KO ^{VMH} MICE.	72
FIGURE 15. DYSLIPIDEMIA OF LEPR KO ^{VMH} MICE FED A LF DIET.....	73
FIGURE 16. GONADAL MORPHOLOGY OF LEPR KO ^{VMH} MICE.....	75
FIGURE 17. ADRENAL MORPHOLOGY OF LEPR KO ^{VMH} MICE.	78
FIGURE 18. CALORIC INTAKE OF LEPR KO ^{VMH} MICE.	80
FIGURE 19. WHEEL RUNNING ACTIVITY OF LEPR KO ^{VMH} MICE.	82
FIGURE 20. FINE LOCOMOTOR ACTIVITY OF LEPR KO ^{VMH} MICE.....	83
FIGURE 21. METABOLIC RATE AND RESPIRATORY EXCHANGE RATIO OF LEPR KO ^{VMH} MICE.....	84
FIGURE 22. GLUCOSE TOLERANCE OF ADULT LEPR KO ^{VMH} MICE.....	85
FIGURE 23. FED AND FASTING GLUCOSE AND INSULIN LEVELS OF LEPR KO ^{VMH} MICE.....	87
FIGURE 24. GLUCOSE TOLERANCE OF WEANLING LEPR KO ^{VMH} MICE.	88

LIST OF TABLES

TABLE 1. COMPLICATIONS OF OBESITY.	2
TABLE 2. pSTAT3 IMMUNOHISTOCHEMISTRY PROTOCOL.	46
TABLE 3. BODY COMPOSITION OF LEPR KO ^{VMH} MICE.	69
TABLE 4. NEUROENDOCRINE FUNCTION OF LEPR KO ^{VMH} MICE.....	74

LIST OF DEFINITIONS

ACTH	adrenocorticotropin hormone
AgRP	agouti related protein
AH	anterior hypothalamus
α -MSH	α -melanocyte stimulating hormone; melanocortin agonist
ARC	arcuate nucleus
A^y	<i>yellow</i> allele of the agouti locus
BAC	bacterial artificial chromosome
BAT	brown adipose tissue
BDNF	brain-derived neurotrophic factor
BMI	body mass index (kg/m ²)
BST	bed nuclei of the stria terminalis
CART	cocaine and amphetamine-regulated transcript
Cre	"causes recombination"; recombinase from P1 bacteriophage
DAB	3,3'-diaminobenzidine
<i>db</i>	<i>diabetes</i> allele of the leptin receptor
DGAT	diacylglycerol O-acyltransferase
DIO	diet-induced obesity
DMH	dorsomedial hypothalamic nucleus
eGFP	enhanced green fluorescent protein
FAS	fatty acid synthase

GTT	glucose tolerance test
HF	high fat
i.p.	intraperitoneal
ICV	intracerebroventricular
KO	knockout
LEPR	leptin receptor
Lepr KO ^{VMH}	VMH-specific leptin receptor knockout using the SF-1/Cre transgene; genotype of Cre ⁺ , Lepr ^{fl/fl}
Lepr WT	cre negative littermate of Lepr KO ^{VMH} mice; genotype Lepr ^{fl/fl} or Lepr ^{fl/+}
Lepr ^{fl/fl}	conditional allele of leptin receptor; exon 1 flanked by loxP sites
LF	low fat
loxP	"locus of crossing over"; DNA sequence recognized by the P1 recombinase Cre
MB	mammillary body
MC1R	melanocortin 1 receptor
MC3R	melanocortin 3 receptor
MC4R	melanocortin 4 receptor
mpPVH	medial parvocellular PVH
MTII	melanocortin agonist
NHANES	National Health and Nutrition Examination Survey
NPY	neuropeptide Y

Nr5a1	nuclear receptor subfamily 5, group A, member 1; SF-1
<i>ob</i>	<i>obese</i> allele of leptin
PAG	periaqueductal gray
PGC-1	peroxisome proliferative activated receptor, gamma, coactivator 1
PH	posterior hypothalamic nucleus
PMN	polymorphonuclear leukocytes
POMC	pro-opiomelanocortin
PPAR	proliferative activated receptor
pSTAT3	phospho-STAT3
PVH	paraventricular hypothalamic nucleus
qRT-PCR	quantitative reverse transcription polymerase chain reaction
RER	respiratory exchange ratio (VCO_2/VO_2)
ROSA26R	transgenic mouse line in which Cre-mediated recombination activates expression of a β -galactosidase reporter gene
SCD-1	stearoyl-Coenzyme A desaturase 1
SCN	suprachiasmatic hypothalamic nucleus
SF-1	steroidogenic factor 1; Nr5a1
SHU9119	melanocortin antagonist
SNA	sympathetic nerve activity
SOCS3	suppressor of cytokine signaling 3
SON	supraoptic hypothalamic nucleus

SREBP	sterol regulatory element binding protein
STAT3	signal transducer and activator of transcription 3
UCP	uncoupling protein
VMH	ventromedial hypothalamic nucleus
VMHc	central VMH
VMHdm	dorsomedial VMH
VMHvl	ventrolateral VMH
VNAB	ventral noradrenergic bundle
WAT	white adipose tissue
WT	wild-type
X-gal	5-bromo-4-chloro-3-indolyl-beta-D-galactopyranoside; chromogenic substrate for β -galactosidase

CHAPTER ONE

Introduction

A GROWING PROBLEM

It comes as no surprise to most Americans to learn that the prevalence of overweight and obesity is rising at an alarming rate. One need only sit in a public space to realize the pervasiveness of obesity in our society. Concerned with the health and nutritional status of Americans, the Centers for Disease Control and Prevention instituted the National Health and Nutrition Examination Survey (NHANES). Beginning in 1960, the NHANE surveys reveal a disturbing trend in the prevalence of overweight and obesity in the United States.

After remaining relatively stable through 1980, the NHANES III (1988-1994) showed an increase of 8% in the prevalence of obesity – defined as a body mass index (BMI, kg/m^2) greater than 30. The most recent NHANES statistics (1999-2000) show a 7.6% increase of obesity over NHANES III levels. As a result of such trends, the National Center for Health Statistics currently estimates that approximately 64% of all Americans are overweight ($\text{BMI} \geq 25$) and/or obese (Flegal et al., 2002). Of particular alarm is the rise in prevalence of childhood obesity, with a 5% rise in overweight adolescents over the last ten years (Ogden et al., 2002). With many of these obese children destined to become obese adults, there are certain to be significant increases in the adverse sequelae associated with obesity.

Obesity is a primary risk factor for a number of chronic conditions and has negative effects on most physiological systems (Table 1). Insulin resistance, in particular, is a common consequence of obesity and is thought to be the central pathophysiological process leading to the constellation of metabolic disturbances known as the ‘metabolic syndrome,’ the ultimate outcome of which is cardiovascular disease (Reilly and Rader, 2003).

Cardiovascular Disease Atherosclerosis Heart Disease Stroke High Blood Pressure	Intestinal Disease Cirrhosis Steatosis Gallstones Gastric Reflux
Respiratory Disease Sleep Apnea Asthma Respiratory Insufficiency	Cancer Prostate Colon Breast
Orthopedic Arthritis Gout	Reproductive Infertility Uterine Bleeding
Pancreatic Disease Diabetes mellitus	Mental Depression

Table 1. Complications of obesity.

The adverse health consequences of obesity translate into extensive economic and social costs. It has been estimated that medical spending attributable to overweight and obesity accounts for approximately 10% of all U.S. medical expenditures, almost \$100 billion annually. For the average obese adult, this equates to a nearly 40% increase in annual medical expenditures compared to non-obese individuals.

Unfortunately, the impact of obesity extends far beyond the pocketbook. While the prevalence of obesity continues to increase in most western societies, these societies concomitantly harbor deep-rooted social stigmas towards the obese. The obese are perceived as gluttonous, lazy, and lacking in self-discipline – not just physically handicapped, but mentally ineffectual as well. Consequently, the obese are often the subject of prejudice and bias in the workplace as well as healthcare and educational settings. The effect of such discrimination is often a self-perpetuating cycle of isolation and depression leading to over-eating and sedentary activity, exacerbating their obesity and resulting in a further decline in physical and mental well-being (Carpenter et al., 2000; Puhl and Brownell, 2003).

When it comes to obesity, however, current scientific evidence directly counters the prevailing public attitudes – namely, that rather than simply being a result of poor choice, obesity is largely a result of one's genetic make-up. Though it may be difficult to parse the relative influence that environmental and genetic

factors contribute to a complex disorder, a number of studies have demonstrated that BMI, more so than many other disorders including cancer and heart disease, is highly heritable (Allison et al., 1996). We now know that though environment and the glut of available calories have contributed to the rise in incidence of obesity, the variance in individual weight is primarily a genetic outcome (reviewed in Friedman, 2004).

The disturbing escalation in obesity and its resulting co-morbidities, coupled with the knowledge that obesity is often a genetic disorder, has initiated a renaissance of interest in the regulation of body weight. As a result, work over the last fifteen years has transformed our understanding of the genetics and physiology of energy homeostasis.

CENTRAL CONTROL OF ENERGY HOMEOSTASIS

Because caloric scarcity has been the more prevalent condition historically, evolution has equipped most organisms with a robust physiologic system to guard against the acute consequences of starvation. In response to a caloric shortage, an organism must be able to efficiently mobilize needed calories from fat depots, reduce energy expenditure via decreases in metabolic rate and activity level, as well as initiate hunger and food-seeking behavior. If the caloric deficit is sufficient, other physiological activities such as reproduction must be curtailed. Further, most organisms efficiently convert excess calories into fat

stores in anticipation of future deficiencies. Unfortunately, most organisms are less ably equipped to protect against the more chronic sequelae of excess adiposity.

To maintain energy balance, organisms must match energy expenditure with energy intake over the long term (Figure 1). The complex behavioral and physiological responses necessary to maintain such balance requires the integration of a myriad of afferent signals, communicating the status of both short term and long term energy stores. Further, compensatory efferent responses must be vectorial, appropriate in direction and magnitude. Given these requirements, it is somewhat intuitive that the central nervous system would play a primary role in the control and regulation of energy homeostasis. Thus, hunger is not just a visceral discomfort, but a centrally controlled compulsion. Similarly, satiety consists of more than the cessation of hunger pains but includes the activation of cerebral pleasure and reward centers (Saper et al., 2002). In rodents and humans, a large body of work has revealed the hypothalamus to be the primary locus for the integration of signals that influence energy balance.

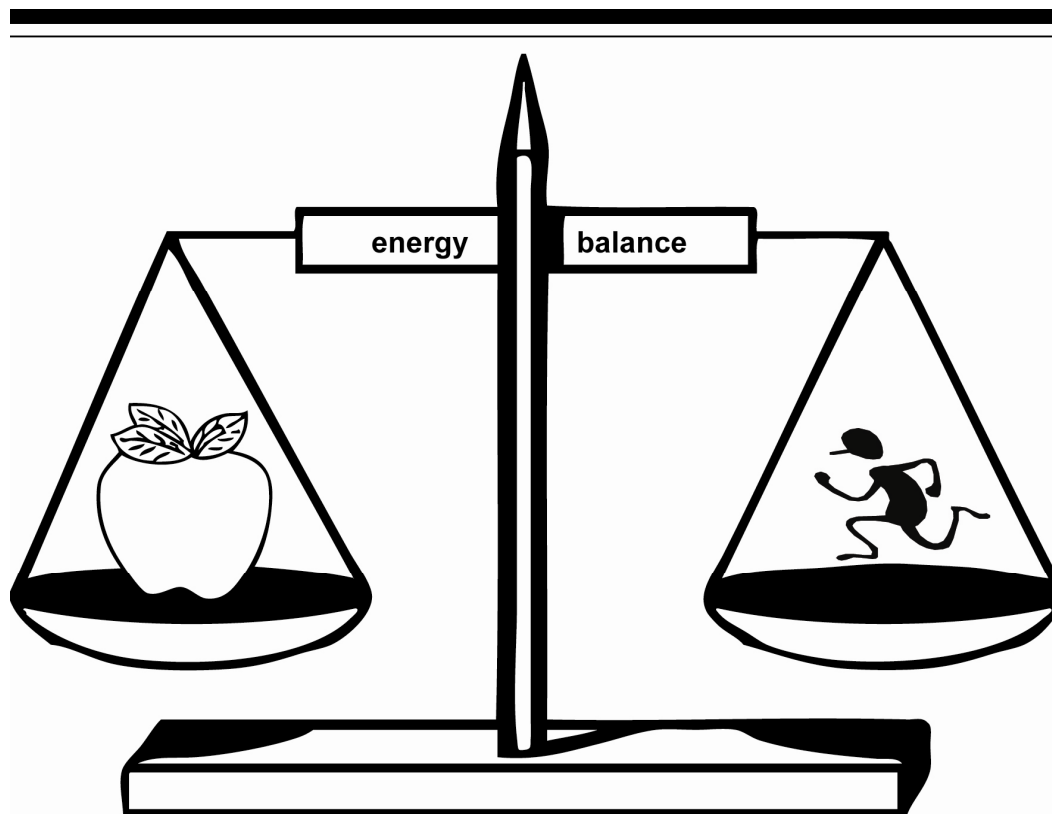


Figure 1. Energy Balance. The maintenance of sufficient energy stores requires that an organism match energy intake to energy expenditure over the long term.

Hypothalamic Development and Anatomy

Following neurulation, the hypothalamus arises as a subdivision of the diencephalon. During development, the paired telencephalic vesicles expand laterally and rostrally resulting in rearward overgrowth of the diencephalon by the developing cortex cerebri. Consequently, in the developed brain, the hypothalamus is located at the basomedial margin of the forebrain and forms the walls and floor of the ventral 3rd ventricle. As its name suggests, the hypothalamus is limited dorsally by the thalamus and is bounded by the optic

chiasm and the mammillary bodies at the anterior and posterior, respectively. Ventrally, the hypothalamus maintains a functional and physical connection to the pituitary via the infundibulum.

In contrast to the cortex, which is organized in layers, the hypothalamus is anatomically and functionally organized into nuclei, discrete groups of neuronal somata, each with its own unique configuration of intra- and extrahypothalamic connections as well as distinct but overlapping set of functions. Hypothalamic nuclei are grouped and identified according to their location along medial-lateral and anterior-posterior axes (Figure 2). Along the anterior-posterior axis the nuclei are organized into the preoptic, anterior, tuberal and posterior regions and subdivided into medial or lateral nuclear groups.

The Hypothalamus and Energy Homeostasis

We now understand the hypothalamus to be responsible for producing many of the behaviors necessary to meet the basic needs of an organism such as feeding, sleeping, sexual responsiveness, and maternal care. It monitors the body's internal milieu, integrating a variety of hormonal and neuronal inputs and directing an assortment of sympathetic and parasympathetic outputs in an attempt to maintain factors such as blood pressure, body temperature, fluid and electrolyte balance, as well as body weight within acceptable limits.

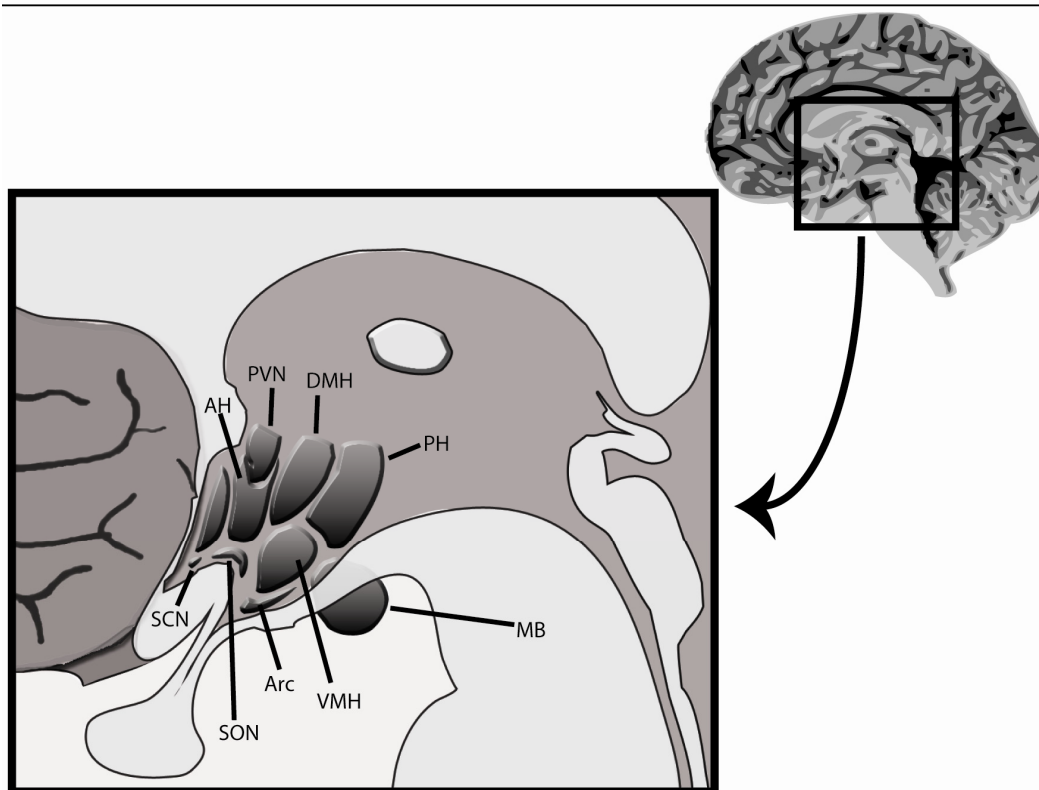


Figure 2. Hypothalamic nuclei. Diagram showing a sagittal section of the hypothalamus and spatial relationship of various hypothalamic nuclei. AH, anterior hypothalamic nucleus; Arc, arcuate nucleus; DMH, dorsomedial hypothalamic nucleus; MB, mammillary body; PH, posterior hypothalamic nucleus; PVN, paraventricular nucleus; SCN, suprachiasmatic nucleus; SON, supraoptic nucleus.

The association of diencephalic lesions with pathologic adiposity has been recognized for well over 100 years. In humans, physicians observed marked hyperphagia and weight gain in patients with tumors at the base of the brain. During the early 20th century, experimentalists demonstrated that basomedial lesions of the hypothalamus in dogs produced a similar phenomenon (Bailey and Bremer, 1921). It has thus become evident that within the hypothalamus there resides a receptor field for adiposity signals whose constituent neurons are

responsible for effecting the physiological changes necessary for the maintenance of energy homeostasis.

Major advances in defining the hypothalamic nuclei responsible for energy homeostasis were made with introduction of stereotaxic surgical technique. Employing such technique, Hetherington and Ranson described the correlation of severe weight gain with discrete hypothalamic lesions in rats. In a series of seminal articles published in the early 1940s, they reported that obesity resulted most readily from bilateral lesions to the medial hypothalamus (Hetherington and Ranson, 1940, 1941, 1942a, b, 1944). From their observations, they concluded that the hypothalamic systems controlling adiposity seemed to “arise rostrally in, or in the neighborhood of the ventromedial hypothalamic nucleus, and to proceed caudally into the midbrain in the company of the medial forebrain bundle” (Hetherington and Ranson, 1942b).

THE VENTROMEDIAL HYPOTHALAMIC NUCLEUS (VMH)

Ventromedial Hypothalamic Development

The VMH is a medial tuberal cell group located at the base of the diencephalon sandwiched between the more ventral arcuate (ARC) and dorsomedial (DMH) hypothalamic nuclei. Its medial border abuts the third ventricle while its elliptical shape extends ventro-laterally to the base of the hypothalamus (Figure 3).

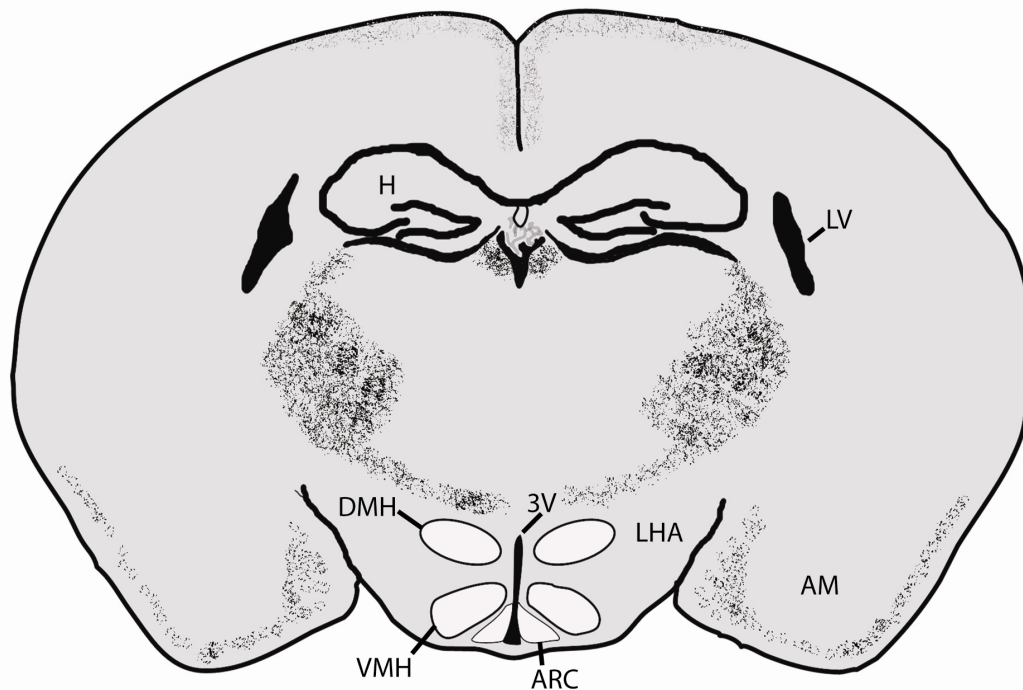


Figure 3. Medial hypothalamus. Diagram of a coronal section of the mouse brain showing the major medial-basal hypothalamic nuclei involved in energy homeostasis. 3V, 3rd ventricle; AM, amygdala; ARC, arcuate nucleus; DMH, dorsomedial hypothalamic nucleus; H, hippocampus; LHA, lateral hypothalamic area; LV, lateral ventricle; VMH, ventromedial hypothalamic nucleus.

In the mouse, cells destined to reside in the VMH arise from precursor cells in the proliferative zone proximate to the third ventricle between E10 and E15 and migrate in a dorsomedial to ventrolateral direction (Altman and Bayer, 1986; reviewed in McClellan et al., 2006). By E16 to E17, the distinct structure of the VMH is recognizable, the boundaries of which are demarcated by the cell-poor, fiber-rich zone which circumscribes the cell-rich nucleus proper. Despite lacking a defined structure before this time, cells identified by expression of

factors expressed in the mature VMH can be identified as early as E9 to E10 (Bingham et al., 2006; Luo et al., 1999; McClellan et al., 2006).

Neuronal Circuitry of the VMH

Based on cytoarchitecture and the region-specific expression of various proteins, the VMH may be anatomically subdivided into several distinct regions – ventrolateral (VMHvl), central (VMHc), and dorsomedial (VMHdm) – each with its own distinct pattern of axonal projections and functions.

The VMH makes extensive intrahypothalamic connections. Within the hypothalamus the most common axonal target of VMH neurons is the VMH itself, with each region's projections tending to remain segregated within itself (Canteras et al., 1994; Nishizuka and Pfaff, 1989). The VMH also shares a dense reciprocal innervation with the anterior hypothalamic nucleus (AH) (Cullinan and Zaborszky, 1991). As well, the VMH innervates other anterior hypothalamic structures including the retrochiasmatic, perifornical, and suprachiasmatic regions. Within the medial hypothalamus, the dorsomedial hypothalamic nucleus (DMH) is the recipient of a majority of VMH innervation with very few projections reaching the periventricular zone (Canteras et al., 1994).

Outside of the hypothalamus, the VMH is known to project axons to several thalamic nuclei and the bed nuclei of the stria terminalis (BST). The ventrolateral VMH (VMHvl), which is densely populated with cells expressing

estrogen receptors, has been shown to have extensive connections to the periaqueductal gray of the dorsal midbrain (PAG) – an area known to be involved in female copulatory behavior (Cohen and Pfaff, 1992). The VMHdm has been also shown to connect to the PAG and also has significant amygdalar connections. This particular circuit has been shown to mediate the fear response to predatory stimuli while simultaneously down regulating mating behavior in the rat (Choi et al., 2005; Dielenberg et al., 2001).

Although a large number of studies have implicated the VMH in the regulation of autonomic processes (see discussion below), the VMH is not known to provide direct input to sympathetic or parasympathetic preganglionic cell groups. The VMH influence over such processes is likely via intermediary connections to the BST, thalamic nuclei, amygdala, and PAG, which are known to provide massive inputs to the dorsal vagal complex and/or spinal cord (Canteras et al., 1994).

Functional Studies of the Ventromedial Hypothalamus

Subsequent to the work of Hetherington and Ranson, a number of reports substantiating and/or slightly modifying their observations were published (Anand and Brobeck, 1951; Brobeck et al., 1943; Kennedy, 1950). Work by John Brobeck and others seemed to establish a substantial increase in food intake as the etiology of the increased adiposity in VMH lesioned animals (Brobeck et al., 1943). Such

hyperphagia was characterized by an increase in meal size as well as frequency. As well, VMH lesioned rats often exhibited a disturbance in the light-entrained circadian meal patterns – ingesting an abnormally elevated proportion of their calories during the light cycle (reviewed in King, 2006).

The hyperphagia of VMH lesioned animals quickly led to the hypothesis that the principle function of the VMH was “the prevention of an excessive calorie intake, that is, it acted as a calorimetric satiety center” (Kennedy, 1953). In what became known as the lipostatic theory of energy homeostasis, Gordon Kennedy proposed that chemo-sensitive neurons within the VMH induced satiety in response to some fat-derived, circulating metabolite (Kennedy, 1953). An alternative to the lipostatic theory, set forth by Jean Mayer, held that the hypothalamus regulates satiety in response to blood glucose concentrations (Mayer, 1952, 1955). Current evidence suggests that both the lipo- and glucostatic theories are at least partially correct – indeed the relative contribution of lipostatic and glucostatic mechanisms to the regulation of satiety and body weight is still an area of active research and debate (Campfield et al., 1995; Levin et al., 1999; Melanson et al., 1999; Woods et al., 1998).

Evidence that the VMH does in fact monitor one or more blood borne satiety signals was persuasively provided by Hervey by using parabiotic rats – rats that have been surgically joined so as to create a shared circulation. Lesioning of

the VMH in one parabiont led to hyperphagia and obesity in the lesioned animal with concomitant hypophagia and emaciation in the parabiotic partner. Hervey concluded that the hypothalamic satiety centers of the unlesioned partner were responding to some anorexic signal transmitted via the shared circulation from the obese partner. Hervey confirmed the role of the VMH in the process by showing that the severe cachexia of the unlesioned animal could be rescued if it too was given bilateral VMH lesions (Hervey, 1959).

During the decades following the work of Hetherington and Ranson, the VMH was the central focus of research regarding central control of appetite and food intake. By the mid-1950s the VMH along with the lateral hypothalamus (LH) – which had subsequently been shown to stimulate feeding – became the paradigmatic example of the dual-center control of motivated behavior (Anand and Brobeck, 1951; Stellar, 1954).

With a number of groups focused on understanding the role of the VMH in ingestive behavior, it also became evident that the VMH was involved in the regulation of a variety of other physiological processes and behaviors. A number of groups recognized that VMH lesions in female mammals appeared to have consequences for reproductive physiology and behavior – in particular the lordosis response (Chateau et al., 1981; Cohen and Pfaff, 1992; Emery and Moss, 1984; Leedy and Hart, 1985). In addition, the VMH has been implicated in the

modulation of the affective component of fear and pain (Borszcz, 2006; Fuchs et al., 1985a, b), cardiovascular function (Hirasawa et al., 1996a, b), as well as the counter-regulatory response to hypoglycemia (Borg et al., 1994; Borg et al., 1995).

The Myth of the Ventromedial Nucleus

Three decades after the original VMH lesions performed by Hetherington and Ranson the VMH “satiety center” hypothesis was generally accepted. Over those same decades, however, a slow accumulation of inconsistent evidence began to cast doubt on the role of the VMH in food intake (reviewed in King, 2006). Primarily, a number of groups were unable to reproduce the hyperphagia and obesity seen by Hetherington and Ranson (Bernardis and Skelton, 1965; Han et al., 1965; Joseph and Knigge, 1968; Rosen, 1968). The ebb in the status of the VMH “satiety center” came to an abrupt halt in 1973 when Richard Gold published his paper, “Hypothalamic obesity: the myth of the ventromedial nucleus” (Gold, 1973). Gold attributed the obesity in VMH lesioned rats not to ablation of the VMH but the severing of the ventral noradrenergic bundle (VNAB) – which had already been shown to lead to obesity when lesioned at the level of the midbrain (Ahlskog and Hoebel, 1973).

In two pages, Gold dismissed 30 years of research and consigned the study of the VMH to the backwater of obesity research. He concluded that the VMH

was “merely a prominent landmark in the vicinity of effective loci” (Gold, 1973). By the early 1980s, many investigators, recognizing the oversimplification of the dual-center model, moved on to study the role of other hypothalamic nuclei in the regulation of food intake and obesity (Aravich and Sclafani, 1983; Leibowitz et al., 1981). As the work and conclusions of Hetherington and Ranson were dismissed, similarly the techniques they perfected and which had been the mainstay of neuroanatomists for thirty years fell in to decline. The 1980s saw a decline in hypothalamic lesion studies as the Horsley-Clarke stereotaxic instrument was superseded by the tools of molecular biology and genetics.

MOLECULAR GENETICS OF OBESITY

Yellow agouti (A^y)

Yellow agouti mice develop a dominantly-inherited, mature-onset, moderate obesity syndrome with increased somatic growth that is more pronounced in females. The obesity appears to result from hyperphagia, although A^y mice pair-fed to control levels maintain higher body fat content despite weighing the same as controls. In addition, A^y mice exhibit aberrant carbohydrate metabolism including hyperglycemia with concomitant hyperinsulinemia (Herberg and Coleman, 1977).

The molecular basis for the pleiotropic effects of the *agouti* gene – including the yellow pelage, obesity, increased tumor susceptibility, and homozygous lethality – remained elusive until two groups simultaneously

reported the isolation and characterization of the mouse *agouti* gene in the early 1990s (Bultman et al., 1992; Miller et al., 1993). The coding sequence of the *agouti* gene produces a secreted, 131 amino acid protein whose expression is normally limited to testis and neonatal skin. Examination of the A^y mutation revealed the juxtaposition of novel 5' sequence to the protein-coding region of the normal *agouti* gene. Further, this anomalous promoter sequence resulted in expression of *agouti* mRNA in nearly all tissues of the body. Bultman et al. hypothesized that such deregulated overexpression of the agouti protein may well account for the dominant pleiotropic effects of the A^y allele (Bultman et al., 1992).

Subsequently, Lu et al. demonstrated that the agouti protein functioned as a high affinity antagonist of the receptor for melanocyte-stimulating hormone, a member of the melanocortin receptor family – designated MC1R. Binding of the agouti protein to the MC1R prevents stimulation of adenylyl cyclase by α -MSH – the endogenous MC1R ligand. In the absence of α -MSH, melanocytes fail to produce eumelanin, resulting in the characteristic yellow coat of A^y mice (Lu et al., 1994).

More pertinent to the obesity phenotype, however, was the localization of several of the melanocortin receptor family members, designated MC3R and MC4R, within hypothalamic nuclei responsible for energy homeostasis (Gantz et al., 1993b; Mountjoy et al., 1994; Roselli-Reh fuss et al., 1993). This led to the

hypothesis that ectopic overexpression of the agouti protein resulting in pathologic inhibition of these central melanocortin receptors may account for the obesity and other metabolic abnormalities of the A^y mouse.

Central melanocortin signaling

Melanocortin receptors are seven-transmembrane, αG_s -coupled receptors whose downstream effects are mediated through the activation of adenylyl cyclase and the resulting rise in cAMP and activation of downstream protein phosphorylation cascades (Gantz et al., 1993a; Gantz et al., 1993b; Mountjoy et al., 1992). The natural ligands of these receptors are the cleavage products of pro-opiomelanocortin (POMC), including α -, β -, and γ -MSH. Within the central nervous system, the activity of MC3 and MC4 receptors is antagonized by an agouti homologue, designated Agouti-related protein (AgRP). The activity of this agouti-like protein is best demonstrated in mice where transgenic overexpression of AgRP results in hyperphagia and obesity without the altered pigmentation characteristic of A^y mice (Ollmann et al., 1997). Thus, the central melanocortin system is composed of neurons expressing POMC or AgRP as well as the post-synaptic neurons expressing melanocortin receptors whose activity is modulated by these peptides.

Over the last fifteen years, a series of pharmacologic and genetic experiments have identified the MC3 and MC4 receptors as mediators of the

agouti syndrome and regulators of energy homeostasis. The demonstration that agouti protein could in fact inhibit activation of the MC4R was a first step in establishing the relationship between central melanocortin signaling and the agouti obesity syndrome (Lu et al., 1994). Further advances in understanding melanocortin signaling came with the development of synthetic melanocortin agonists and antagonists. Fan et al. demonstrated that the intracerebroventricular (ICV) injection of MTII, a cyclic melanocortin analogue and MC3R/MC4R agonist, was able to inhibit feeding in *A^y* mice while injection of SHU9119, an agouti-mimetic was able to stimulate feeding (Fan et al., 1997).

Rats given an ICV injection of SHU9119 for eleven days doubled their food intake and increased their body weight by 14% and their fat content by 90%. These body composition changes were accompanied by significant increases in plasma insulin (250%), glucagon (80%), and leptin (490%) whereas spontaneous locomotor activity and body temperature were reduced. Restricting the food intake of such animals to WT levels normalized plasma insulin and glucagon, partially reversed the elevations in leptin and body fat content (Adage et al., 2001). Thus, melanocortin signaling inhibits fat deposition via both food intake-dependent and -independent mechanisms.

Given the relatively non-specific nature of melanocortin agonists and antagonists, pharmacologic data alone have proven unable to distinguish the

relative contribution of these receptors to the agouti obesity syndrome. To this end, genetic experiments, often combined with pharmacologic methods, have proven most useful. Targeted disruption of the *Mc4r* gene, for example, has demonstrated that the MC4R is required for the normal control of food intake. Mice lacking the *Mc4r* develop maturity onset obesity associated with an impressive hyperphagia, hyperinsulinemia, and hyperglycemia (Huszar et al., 1997). This melanocortin syndrome is nearly identical to the agouti syndrome described a century earlier.

Deletion of the *Mc3r* receptor results in a primary metabolic syndrome without directly influencing food intake. While MC4R KO mice are hyperphagic and weigh more than WT mice, the body weight and appetite of MC3R KO mice remain relatively normal (Butler et al., 2000; Chen et al., 2000). Despite relatively equivalent weight, MC3R KO mice exhibit significantly increased adiposity and feeding efficiency. Thus, MC3R appears to promote the partitioning of calories toward lean body mass and away from fat stores. In addition, MC3R KO mice exhibit a mild impairment in locomotor activity (Butler et al., 2000). Mice lacking MC3R are also hyperinsulinemic though they appear to have normal plasma glucose.

The evidence indicates that the melanocortin system is an important component of the central control of energy homeostasis via the regulation of

caloric intake and expenditure as well as substrate oxidation (Butler, 2006; Cummings and Schwartz, 2000). The melanocortin system is itself contained within the central nervous system – including centrally produced ligands. Intuitively, such a system would be downstream of any humoral factor transmitting information from body energy stores and thus must be but a part in a larger satiety system (Cone, 2005).

obese and diabetes

In 1950, Ingalls et al. described “some very plump mice” that were observed in the mouse colony of Jackson Laboratory in Bar Harbor, Maine (Ingalls et al., 1996). By age four to six weeks these mice were visibly different than their normal littermates – with a shorter, square body and “expansive hind quarters.” By three months of age, these mice weighed twice as much as their non-obese litter mates. Though the obese mice were infertile, they occurred in a 1:3 ratio with non-obese littermates, characteristic of a recessive disorder. The as-yet unidentified mutant gene was designated *ob* for obese.

In 1966, Douglas Coleman and his associates described a new mouse obesity model which they termed *diabetes (db)* (Hummel et al., 1966). Though *db/db* and *ob/ob* mice exhibit a similar phenotype, mating between the two produced no offspring with increased adiposity – demonstrating the *ob* and *db* mutations to be distinct genes.

Both *db/db* and *ob/ob* mice exhibit a severe, early-onset, complex metabolic syndrome. The most prominent feature of these mutations is the marked hyperphagia and accelerated weight gain, which is often perceptible as early as weaning (Hummel et al., 1966; Ingalls et al., 1996). Studies of body composition reveal that 90% of the weight gain is accounted for by increases in body fat (Bates et al., 1955). Even when placed on a diet matched to non-obese siblings, *db/db* mice gain more weight than normal mice and maintain the same fat-to-weight ratio as *db/db* mice fed ad libitum (Cox and Powley, 1977). Biochemical studies reveal that these mice exhibit augmented liver and adipose lipogenesis with elevated rates of glucose incorporation into lipid (Loten et al., 1974) with concomitant diminished oxidation of glucose and other substrates (Hughes and Tolbert, 1958). This state of hypometabolism results in decreased energy expenditure and defective thermoregulation (Campfield, 2000).

Further assessment shows *db/db* and *ob/ob* mice to have aberrant carbohydrate metabolism as well. As early as 10 days old, *db/db* mice show a marked hyperinsulinemia, and though hypoglycemic early on, quickly develop hyperglycemia (Coleman and Hummel, 1974; Herberg and Coleman, 1977). The result of this hyperinsulinemic hyperglycemia is a diabetic state characterized by insulin resistance, glycosuria, polydipsia, polyuria, as well as morphological

changes in pancreas – specifically β -cell hyperplasia and hypertrophy (Coleman and Hummel, 1967; Herberg and Coleman, 1977).

In addition to these primary metabolic disturbances, *db/db* and *ob/ob* have defects in a broad array of neuroendocrine systems which compound and contribute to the metabolic problems. These mice exhibit hypercorticosteronemia (Naeser, 1974), are hypothyroid (van der Kroon et al., 1982), and infertile due to hypogonadotropic hypogonadism (Swerdloff et al., 1976). Despite the excess of caloric stores, it is evident from such broad behavioral, metabolic, and neuroendocrine defects that the central satiety center of *db/db* and *ob/ob* mice is responding to a perceived state of starvation (Ahima et al., 1996).

Parabiosis studies of ob/ob and db/db mice

Ten years after Hervey published his experiments on VMH lesioned parabiotic rats, Douglas Coleman used the same technique to elucidate the molecular character of the *ob* and *db* genes (Coleman, 1973; Coleman and Hummel, 1969). In parabiotic pairs consisting of a *db/db* and WT mouse, the *db/db* mouse continued to gain weight while the WT partner became hypophagic, hypoglycemic and usually died within 3-4 weeks from apparent starvation (Figure 4A). Unions between *ob/ob* and WT mice ended very differently, with no change in the WT mouse and a reduction in the weight and hyperglycemia of the *ob/ob* mouse (Figure 4B). The third experiment consisted of a parabiotic union between

db/db and *ob/ob* mice. These unions resulted in continued weight gain and hyperglycemia in the *db/db* mice while the *ob/ob* mice ceased eating, became emaciated and eventually died of starvation (Figure 4C). From these results, Coleman concluded:

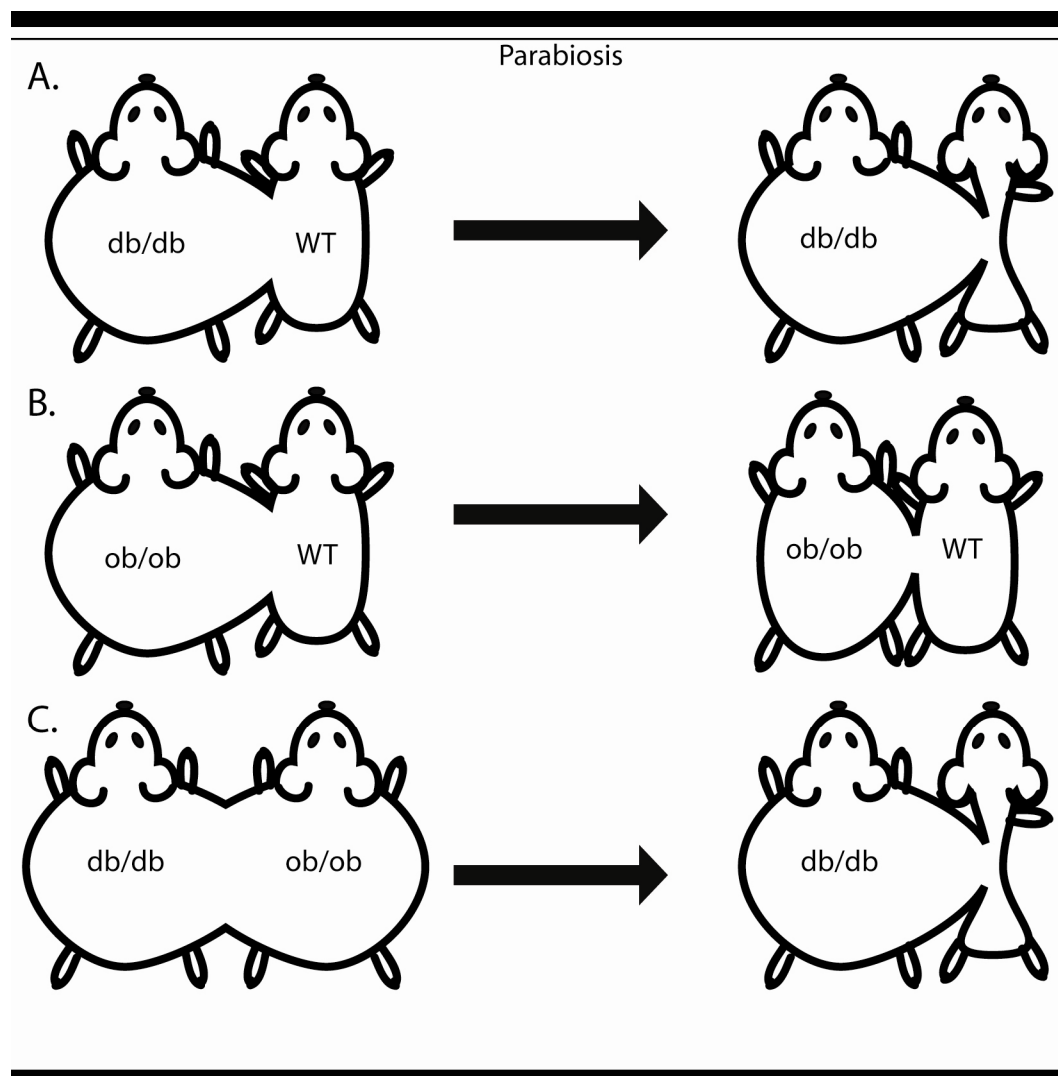


Figure 4. Parabiosis of *db/db* and *ob/ob* mice with normal mice. Diagram showing the various parabiotic experiments performed on the left and the resulting outcomes on the right.

...that the diabetes partner produces, but does not respond to, a satiety factor that prevents overeating. In parabiosis this factor crosses the circulation of the normal partner where it acts on the normal partner's satiety centre to inhibit eating, producing subsequent starvation and death... the obese partner, unlike the diabetes mouse, does not produce sufficient satiety factor to turn off the normal partner's eating drive.

The seminal work performed by Coleman and colleagues reconfirmed the hypotheses made by Kennedy and Mayer twenty years earlier that the central satiety center responds to some circulating, humoral factor. Coleman's work suggested that the product of the *ob* gene may be such a factor, while the *db* gene product was in some way responsible for reception of the humoral signal.

Leptin

While the parabiosis experiments of Hervey, Coleman, and others demonstrated the existence of a humoral satiety factor, the exact nature of this putative factor remained undetermined for another twenty years. In 1994, Zhang et al., using positional cloning techniques, cloned the *ob* gene and demonstrated its expression was limited to white adipose tissue (WAT) (Zhang et al., 1994). The *ob* gene product is a 16 kD protein that circulates in the blood in concentrations proportional to the mass of body adipose stores (Matkovic et al., 1997; Saad et al., 1997). This new hormone was aptly named leptin from the Greek *leptos*, meaning thin.

Peripheral or central administration of recombinantly-expressed leptin resulted in increased energy expenditure, normalized food intake, and reduced

body weight and fat content in *ob/ob* and WT mice while *db/db* mice remained unaffected (Campfield et al., 1995; Halaas et al., 1995). The fat depots of rats made hyperleptinemic by infusion of leptin-expressing, recombinant adenovirus were completely ablated while control pair-fed rats retained ~50% of their fat (Chen et al., 1996). Further, these rats saw a significant reduction in plasma triglycerides and insulin. Chehab et al. demonstrated that peripheral administration of leptin rescues the normal reproductive function in *ob/ob* females (Chehab et al., 1996) and induces precocious reproductive function in normal mice (Chehab et al., 1997).

The physiological and behavioral adaptations induced by leptin correlate with molecular changes within the basal hypothalamus. Peripheral and central leptin administration modulates the presence and release of a number of hypothalamic neurotransmitters associated with the regulation of appetite and/or energy homeostasis (Wilding et al., 1993). In harmony with its role as an anorexigenic signal, leptin injection has been shown to inhibit the expression of the orexigenic peptides neuropeptide Y (NPY) and AgRP within the hypothalamus while augmenting the expression of the anorexigenic peptides POMC (precursor to α -MSH) and cocaine and amphetamine-regulated transcript (CART) (Ahima and Hileman, 2000).

The current evidence regarding leptin corroborates the lipostatic theory of weight regulation proposed by Gordon Kennedy over fifty years ago. In short, leptin acts as a lipostat – providing information regarding long term energy stores to central satiety centers. The effects of leptin on metabolic physiology are pleiotropic, and it has often been difficult to distinguish primary defects from secondary effects of leptin signaling. Key to understanding the mechanisms by which leptin modulates metabolic homeostasis is an understanding of the signal transduction pathways activated and inhibited by leptin.

Leptin Receptor – signal transduction

A year after Jeff Friedman published his paper on the cloning of leptin, Tartaglia et al. from Millenium Pharmaceuticals, Inc. described the cloning of a high affinity receptor for leptin (Tartaglia et al., 1995). Using a leptin-alkaline phosphatase fusion protein they identified significant leptin binding in the choroid plexus of the lateral ventricles. A cDNA library, derived from the choroid plexus of 300 mice, was subsequently used to transfect COS7 cells and identify the clone responsible for the observed binding. Genetic analysis subsequently demonstrated that the newly discovered *Lepr* and the *db* genes are the same (Chua et al., 1996).

Sequencing of the putative leptin receptor cDNA revealed a protein with domain homology similar to members of the class I cytokine receptors, including gp130, G-CSF receptor and the leukemia inhibitory factor receptor (Tartaglia, 1997). While the original sequence revealed a receptor with a large extracellular

and short intracellular domain, subsequent screening of cDNA libraries proved this cDNA to be one of several different splice variants, one of which possessed an extensive intracellular domain (Figure 5A). Currently, as many as six different splice variants of the leptin receptor (LEPR) have been identified (Ahima and Osei, 2004). All share a common extracellular leptin binding domain, but differ in the length of their intracellular carboxyl-termini. Analysis of the *db* allele reveals an abnormally spliced LEPR isoform which produces a premature termination codon and truncated protein lacking much the intracellular region, suggesting that the metabolic phenotype of the *db/db* mouse may result from an inability of the LEPR to effect downstream signaling cascades (Lee et al., 1996).

Like other members of the class I cytokine receptor family, the LEPR signals through the Jak/STAT signaling pathway (Myers, 2004). Upon leptin binding to the LEPR, Jak2 kinase is recruited to the box 1 motif of the receptor, though the box 2 motif has proven essential for the binding and specificity of Jak2 (Figure 5B)(Kloek et al., 2002). Thus, the LEPRb isoform is the only known splice variant to activate the Jak/STAT pathway, known to be essential for the metabolic and weight reducing effects of leptin (Bjorbaek et al., 1997; Buettner et al., 2006). Further, the LEPRs of *db/db* mice were shown to be unable to activate STAT3 (Ghilardi et al., 1996; Vaisse et al., 1996).

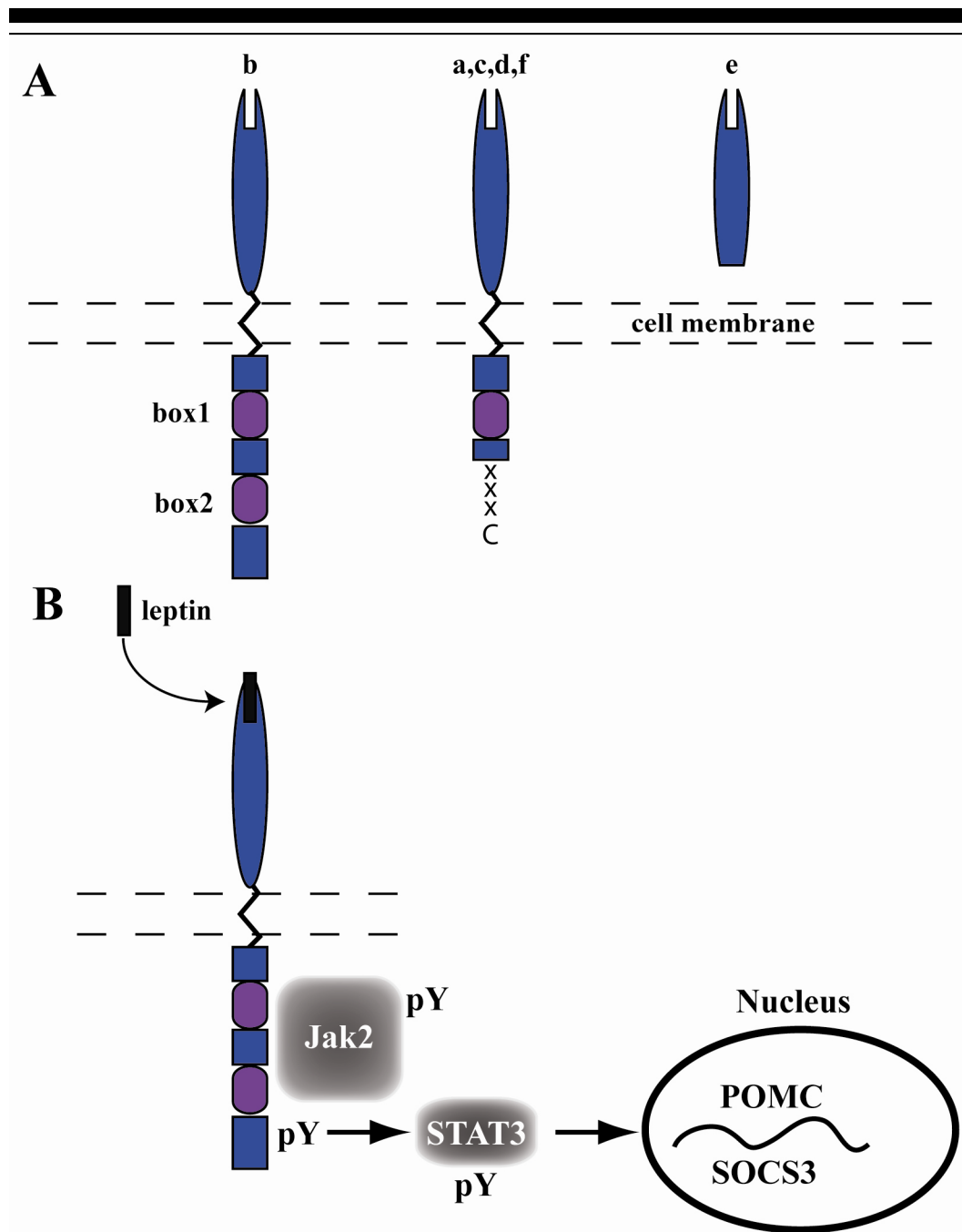


Figure 5. Leptin signal transduction. (A) Diagram showing the various LEPRe isoforms. The short isoforms (a,c,d,f) all truncate following the Box1 motif and are unable to activate STAT3 signaling. LEPRe consists of only the extracellular ligand bind domain and is secreted from cells. LEPReb, or long form, contains all the protein domains necessary for intracellular signaling and has been shown to be responsible for the weight regulating effects of leptin. (B) Simplified

diagram showing leptin signal transduction. Leptin binding leads to recruitment of Jak2 and tyrosine phosphorylation (pY) of the LEPR. STAT3 binds the phosphorylated receptor and is itself activated by phosphorylation. Activated STAT3 translocates to the nucleus where it is responsible for transcriptional regulation of leptin target genes such as POMC and SOCS3.

Binding of Jak2 kinase leads to its autophosphorylation and phosphorylation of several tyrosine residues on the cytoplasmic tail of the LEPR. This cascade of events leads to the recruitment, phosphorylation and dimerization of the signal transducer and activator of transcription 3 (STAT3). Dimerized STAT3 translocates to the nucleus where it modulates the transcription of several genes including POMC and suppressor of cytokine signaling 3 (SOCS3), an endogenous inhibitor of LEPR signaling.

In addition to its genomic effects, leptin has been shown to have rapid effects on neuronal membrane potential. Spanswick et al. showed that leptin, applied to acute hypothalamic slices was able to decrease the firing rate of action potentials and increase the input resistance of a subset of neurons. This decreased action potential frequency results from increased potassium current resulting in membrane hyperpolarization. Further, many leptin sensitive neurons are also glucose responsive with leptin antagonizing the effects of glucose on these neurons (Spanswick et al., 1997).

Anatomic distribution of leptin receptors

In order to understand the basis for leptin action, a number of groups have documented the anatomic distribution of LEPRs (Elmqvist et al., 1998b; Fei et al., 1997), with particular attention paid to those locations where the long, or signal-

competent, isoform is expressed. Using *in situ* hybridization, Elmquist et al. reported the LEPRb isoform distributed within several hypothalamic nuclei, including dense hybridization within the ARC, VMH, and DMH. Outside of the hypothalamus, the LEPR – mostly short non-signaling isoforms – has a broad range of distribution including the olfactory tract, thalamus, and cerebellum (Elmquist et al., 1998b).

The functionality of LEPRs within the hypothalamus has been examined using pharmacological and histological techniques to identify and follow the activation of downstream effectors of leptin signaling. Using such a technique, Elmquist et al. demonstrated the induction of Fos, an immediate early gene product, in the basal hypothalamus of rats following a leptin injection. Fos immunoreactivity was seen in the paraventricular (PVH) and dorsomedial nuclei (DMH) as well as VMH. In addition, the induction of SOCS-3 and phosphorylation of STAT3 has been histologically demonstrated in a number of hypothalamic nuclei (Bjorbaek et al., 1999; Hubschle et al., 2001). Such studies have not only revealed the anatomic distribution of leptin responsive neurons, but have helped expose the larger neuronal circuitry to which they belong.

Intersection of leptin and melanocortin signaling

As mentioned above, leptin is known to modulate the levels of orexigenic and anorexigenic peptides within the hypothalamus. The common anatomic distribution of LEPRs with several of these neuropeptides implies that leptin may

be upstream of one or more of these neuronal circuits. Thus, leptin acts as a peripheral signal to inhibit feeding by regulating the release of anorexigenic or orexigenic neurotransmitters from the first-order neurons of central feeding circuits. The best documented case of this paradigm is the role of leptin in regulating the melanocortin system within the arcuate nucleus.

The arcuate nucleus of the hypothalamus contains two neuronal populations known to regulate appetite. The first, part of an orexigenic circuit, coexpresses NPY and AgRP. The second is part of an anorexigenic circuit and coexpresses POMC and CART. Both these neuronal populations are known to coexpress LEPRs and modulate melanocortin signaling – the first by expressing AgRP, a melanocortin antagonist, and the second by expressing α -MSH, a melanocortin agonist and proteolytic cleavage product of POMC (Cheung et al., 1997; Hakansson et al., 1998; Mercer et al., 1996).

The AgRP neurons of the arcuate nucleus are coexpressed with NPY – another molecule with clearly demonstrated orexigenic properties (Clark et al., 1984; Stanley et al., 1985). Both AgRP and NPY expression is stimulated in states of energy deficiency or increased metabolic demand (Chen et al., 1999; Mizuno et al., 1999). The converse effect is seen in response to leptin injections (Mizuno and Mobbs, 1999). The POMC neurons inhibit food intake and energy storage, primarily through their production and release of α -MSH. Cowley et al. elegantly

demonstrated that leptin activates POMC neurons both directly, by increasing depolarizing cation flux, and indirectly, by decreasing inhibitory GABAergic input on the POMC neurons from arcuate NPY neurons (Cowley et al., 2001).

Integration of counterregulatory signals is necessary for the function of any homeostatic system. Thus, the interplay of α -MSH excitatory signals and AgRP inhibitory signals on second-order neurons expressing MCRs leads to the physiological effects of leptin. The anatomic basis of this regulatory circuit was provided by confocal microscopic analysis of neurons within the medial parvocellular PVH (mpPVH) expressing MC4R. Using double label immunohistochemistry, Cowley et al. have demonstrated the physical proximity of NPY/AgRP neuronal fibers, α -MSH containing fibers, and single-cell bodies within the mpPVH. The functional consequences of this spatial proximity were demonstrated pharmacologically, with preinjection of the melanocortin antagonist SHU9119 completely abrogating the inhibition of feeding by the melanocortin agonist MTII. Showing integration of NPY signals with melanocortin signals, preinjection of MTII into the mpPVH was able to completely suppress the orexigenic effects of NPY (Cowley et al., 1999; Marks and Cone, 2001). Such studies make it clear that the melanocortin system is a critical interface between peripheral lipostatic signals and higher centers responsible for the implementation of leptin physiological effects (Figure 6).

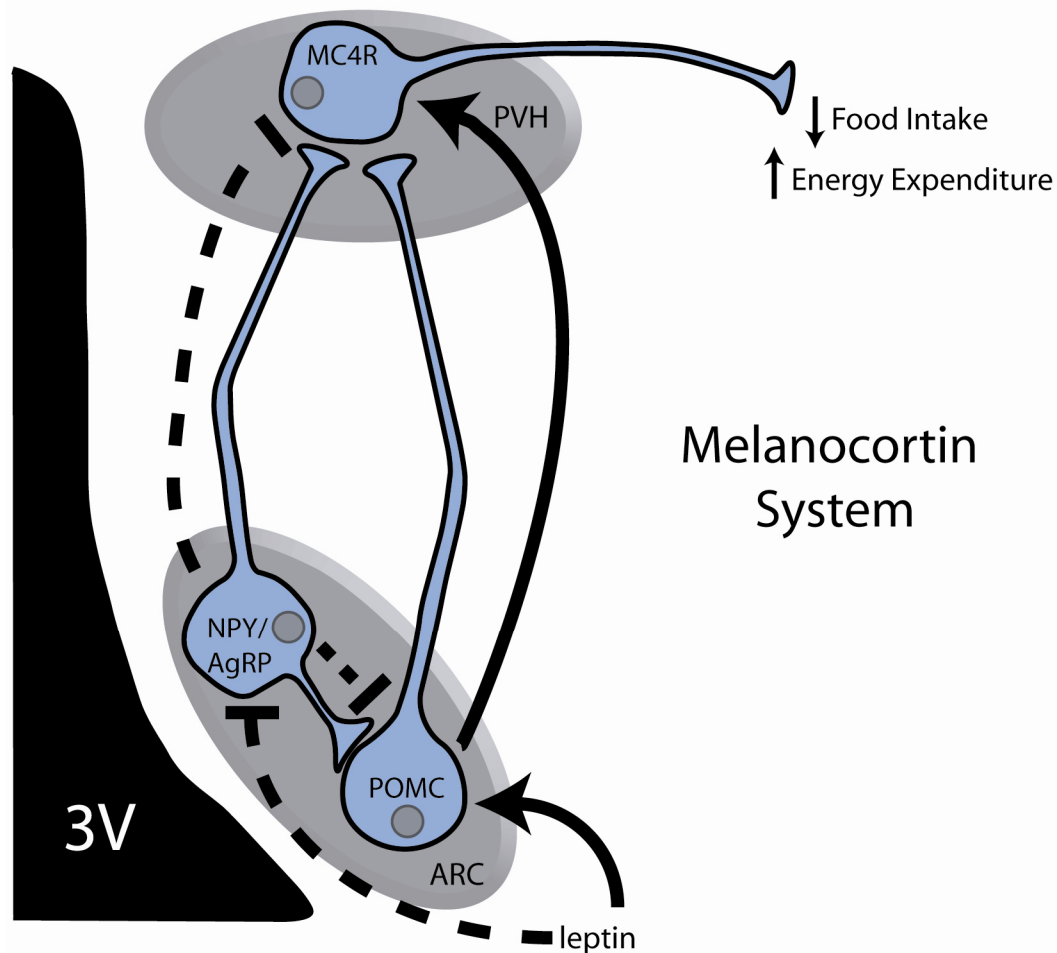


Figure 6. Leptin-melanocortin circuit of the arcuate nucleus. Leptin binds to neurons of the ARC where it activates POMC neurons and inhibits NPY/AgRP neurons. These neurons in turn modulate melanocortin receptor activity on 2nd-order neurons in regions such as the PVH. 3V, 3rd ventricle; ARC, arcuate nucleus; PVH, paraventricular nucleus.

Steroidogenic Factor 1

Though not a classic obesity model, its relevance to the current work necessitates a brief discussion of the Steroidogenic factor 1 (SF-1, officially designated Nr5a1) knockout mouse. SF-1 is a member of the nuclear receptor

family of transcription factors and was originally identified as a common binding factor in the promoters of the cytochrome P450 genes involved in steroidogenesis (Bogerd et al., 1990; Rice et al., 1991) and proved to be a key regulator of these genes (Ikeda et al., 1993).

Genetic ablation of the *SF-1* gene in mice demonstrated SF-1 to be involved, not only in the regulation, but in the development of the endocrine system. All SF-1 KO mice die perinatally and closer examination reveals that KO mice show adrenal and gonadal agenesis resulting in glucocorticoid and mineralocorticoid deficiency as well as male-to-female sex reversal of both internal and external genitalia (Luo et al., 1994). In addition, SF-1 is essential for expression of the pituitary gonadotrope phenotype (Shinoda et al., 1995; Zhao et al., 2001). Most pertinent to the current work, however, was the revelation that SF-1 expression in the brain is limited to the VMH.

Histological examination of the hypothalamus in SF-1 KO mice reveals marked disruption of the cellular architecture and absence of distinct nuclear structure in the area normally occupied by the VMH (Ikeda et al., 1995; Shinoda et al., 1995). Immunohistochemical analysis also reveals an altered distribution of neuronal phenotypes within the area, with cells expressing estrogen receptor α (ER α) and galanin being displaced from their normal positions (Dellovade et al.,

2000). As well, the immunoreactive fibers for NPY and GABA extending through the VMH exhibited an aberrant distribution.

The study of energy homeostasis in SF-1 KO mice has proven to be technically difficult due to the adrenal insufficiency of the knockouts. However, Majdic et al. proved successful in rescuing the adrenal insufficiency of SF-1 KO mice with corticosterone injections and adrenal transplants from WT littermates, restoring normal ACTH and corticosterone levels (Majdic et al., 2002). Despite normal adrenal function, SF-1 KO mice showed significant differences in body weight beginning at eight weeks of age. By six months of age, KO mice weighed almost twice as much as WT mice, with no changes in somatic growth. MRI analysis showed the increased weight to be due to an increase in the percent body fat ($42 \pm 1.3\%$ vs. $20 \pm 1.3\%$).

While analysis of SF-1 KO mice showed no difference in food intake, examination of voluntary locomotor activity, as assessed by revolutions on a running wheel, showed a significant decrease in the activity of the SF-1 KO mice. SF-1 KO mice were also hyperleptinemic and hyperinsulinemic, though euglycemic.

RATIONALE OF PRESENT WORK

The early hypothalamic lesion studies performed by Hetherington, Ranson, and others strongly implicated the VMH in the regulation of body

weight, though the precision and accuracy of these studies were later called into question. The examination of the *db* and *ob* models of obesity and the discovery of leptin and its receptor have further shifted attention away from the VMH as investigators have focused on the arcuate nucleus, the primary center for leptin's appetite suppression. As the SF-1 KO mouse model indicates, however, it is likely that the VMH may still play a role in energy homeostasis. In addition, analysis of LEPRs in the hypothalamus has shown that LEPRs are present in the VMH and are capable of responding to circulating leptin.

The dissection of the *ob/ob* and *db/db* phenotype has revolutionized the study of obesity and energy homeostasis. Leptin has been shown to be a major component of the homeostatic system regulating appetite, weight, and metabolism. However, given the complex metabolic phenotype of the *ob/ob* and *db/db* mice and the pleiotropic effects of leptin, it is improbable that a single region of the brain is responsible for producing such wide-ranging physiological effects. In order to understand the anatomical basis for leptin's effects, it is necessary to experimentally isolate each region.

The Cre-LoxP strategy is ideal for creating tissue specific gene knockouts and has also proven useful for region-specific gene ablation within the brain (Balthasar et al., 2004). In order to investigate the function of LEPRs within the

VMH, I report here the development of an SF-1/Cre mouse line and the use of that line to ablate *Lepr* within the SF-1 neurons of the VMH.

CHAPTER TWO

Materials & Methods

CONSTRUCTION OF THE SF-1/CRE BAC

The *SF-1* BAC clone was obtained from the CT7 mouse library (clone id: 572J24, Invitrogen, Carlsbad, CA). Two 500 bp fragments flanking the SF-1 initiator methionine were cloned into pBluescript KS(-) (Stratagene, La Jolla, CA) with an intervening *FseI* site. A fragment containing the Cre cDNA and the bovine Growth Hormone (bGH) polyadenylation sequence was inserted at the *FseI* site using the In-Fusion PCR Cloning System (Clontech, Mountain View, CA). This recombination cassette was inserted into the *SalI* site of the pSV1.RecA shuttle vector, and this shuttle vector was then introduced into *E. coli* containing the unmodified SF-1 BAC. Following homologous recombination and resolution as described (Yang et al., 1997), the Cre cDNA was inserted at the SF-1 initiator methionine in the second exon. Modified BACs were identified and characterized by Southern blotting, PCR, and restriction digest analysis. The loxP site in the pBeloBAC11 vector backbone was replaced with an *AscI* site using homologous recombination.

GENERATION OF SF-1/CRE TRANSGENIC MICE

BAC DNA for pronuclear injection was prepared by alkaline lysis followed by purification on a CsCl gradient (Sambrook and Russell, 2001). Ethidium bromide was removed using an AG 50W-X8 resin (Bio-Rad).

Laboratories, Hercules, CA). The DNA was resuspended in microinjection buffer (10 mM Tris, pH 7.4; 0.25 mM EDTA) and injected as circular DNA into fertilized ova (B6D2F1/J background). After weaning at 3–4 weeks of age, transgene-positive pups were identified by PCR (see below). Transgenic mice were maintained in the heterozygous state and bred on the C57BL/6J background (Jackson Laboratory, Bar Harbor, ME).

ANIMAL CARE

Husbandry

Mice were housed 2-4 per cage in a temperature-controlled room with a 12 hour light/dark cycle. Fresh water and standard diet (LF; Teklad 7001 diet, 2.94 kcal/g, 9.4% kcal from fat, Harlan Teklad, Madison, WI) were available *ad libitum*. For high fat studies, mice were given a 60% kcal fat diet (HF; Research Diets D12492, 5.24 kcal/g, 60% kcal from fat, New Brunswick, NJ). For food intake experiments, 12-week-old female *Lepr* KO^{VMH} and *Lepr* WT mice were transitioned from LF to HF diet, with food being weighed daily. For all other studies, mice were fed a LF diet unless otherwise indicated. Littermates were used as controls for all studies.

Genotyping

Genotyping for the SF-1/Cre transgene by PCR was carried out using the following conditions: 94°C, 45 sec.; 55°C, 45 sec.; 72°C, 1 min for a total of 40 cycles (primers: 5'GAGTGAACGAACCTGGTCGAAATCAGTGCG3';

5'GCATTACCGGTCGATGCAACGAGTGATGAG3'), producing a 408 bp product. ROSA26R and Lepr^{fl/fl} mice were genotyped as described (Cohen et al., 2001; Soriano, 1999).

Body weight and composition

Male and female Lepr WT and Lepr KO^{VMH} mice were placed on LF or HF diet beginning at weaning. Body weight was measured every 14 days beginning at 4 weeks of age. Naso-anal length was measured with digital calipers at 20 weeks of age (Fisher). Body fat was quantified using the Bruker Minispec mq10 NMR Analyzer (The Woodlands, TX).

Tissue and plasma collection

Twenty-week-old mice were sacrificed by decapitation without anesthesia within 30 seconds of handling. Trunk blood was collected in 50 ml conical tubes that had been coated with trace amounts of 7.5% K₃-EDTA (Sigma-Aldrich E0270, St Louis, MO). Blood was centrifuged at 2000 x g for 20 minutes, plasma was collected and frozen on dry ice, and stored at -80°C until used for analysis. Gonads, adrenals, and liver were simultaneously harvested, weighed, and rapidly frozen in liquid nitrogen.

For female estrus measurements, blood was collected from the retro-orbital sinus of anesthetized mice using heparinized natelson blood collecting

tubes (Fisher Hampton, NH). While still anesthetized, mice were subsequently sacrificed and blood processed as described above.

SOUTHERN ANALYSIS

Genotyping of transgenic founders was confirmed by Southern blot analysis (Fig. 1C). A probe was generated by PCR from the original SF-1 BAC (primers: 5'TGCTTACCAGACCTTGGGATGC3'; 5'AAAACCACGGAGACACAGAATCAG3') and labeled with ^{32}P using the Rediprime II random-prime labeling system (Amersham Biosciences, Pittsburgh, PA). 5 μg of mouse liver DNA was purified, digested with EcoRI, EcoRV, and NcoI, and resolved on a 1.5% agarose gel in TAE buffer. The DNA was transferred to a Nytran nylon membrane using the Turboblotter transfer system according to the manufacturer's protocol (Whatman, Florham Park, NJ), and the DNA was crosslinked to the membrane using 120 mJ/cm² in the UV Stratalinker (Stratagene). The probe was hybridized with the membrane at 68°C for 12 hrs using ExpressHyb solution (Clontech). The membrane was then washed and exposed to a phosphorimager screen for ~3hrs. The screen was scanned using a Storm 820 scanner (Molecular Dynamics, Sunnyvale, CA) and the transgene copy number was quantified using ImageQuant software (Molecular Dynamics).

LIVER AND PLASMA TRIGLYCERIDE MEASUREMENTS

Approximately 100 mg of liver from 20-week-old female Lepr KO^{VMH} and Lepr WT mice was homogenized in 4 ml of chloroform / methanol (2:1 v/v) using a Polytron tissue homogenizer. Homogenate was washed with 1 ml of 50 mM NaCl, vortexed, and centrifuged at 1500 x g for 10 minutes. The resulting organic phase was transferred to a new tube, washed with 1 ml of 0.36 M CaCl₂ / methanol (1:1: v/v), vortexed, and again centrifuged at 1500 x g for 10 minutes. The organic phase was once again removed to a new tube and the CaCl₂ / methanol wash repeated. Following centrifugation, the organic phase was placed in a fresh tube and the volume brought to 5 ml with chloroform. For cholesterol content determination, 10 µl of 50% Triton X-100 was added to 100 µl of liver homogenate and allowed to dry down under nitrogen. The cholesterol assay was performed using the Roche Cholesterol Enzymatic Reagent (Roche Applied Science, Indianapolis, IN). For triglyceride content determination, 10 µl of 50% Triton X-100 was added to 50 µl of liver homogenate and allowed to dry down under nitrogen. The triglyceride assay was performed using the Sigma Triglycerides Enzymatic Reagent (Sigma-Aldrich).

ISOLATION OF TISSUE MRNA AND QRT-PCR

Tissues were homogenized in Trizol Reagent (Invitrogen) and total RNA was isolated according to the manufacturer's instructions. Isolated RNA was cleaned of DNA via DNase treatment and then reverse transcribed using random

hexamer primers (Roche) and Superscript III reverse transcriptase (Invitrogen). *Lepr* cDNA was amplified on an ABI Prism 7700 Sequence Detection System (Applied Biosystems, Foster City, CA) and quantified using a Taqman probe specific to the first exon of *Lepr* (Applied Biosystems, Assay ID Mm01265205_m1).

HISTOLOGY

H&E Staining

To obtain adult tissues, mice were anesthetized and fixed via transcardial perfusion with ice cold 4% paraformaldehyde (PFA). Following perfusion, tissues were removed and post-fixed overnight in Bouin's fixative, rinsed twice for 30 minutes with phosphate buffered saline (PBS, pH 7.4), and infiltrated with paraffin following standard protocols. Tissues were stored at 4°C, embedded in 100% paraffin (Paraplast Plus Tissue Embedding Medium, Fisher), until sectioning. Eight µm sections were cut on a Microm HM 330 rotary microtome (Microm, Heidelberg, Germany) and floated on a 42°C water bath before mounting on Superfrost/Plus microscope slides (Fisher). Slides were then allowed to dry overnight at 37°C. H&E staining was performed following standard protocols. Stains, clarifier, and blueing reagent were purchased from Richard-Allen Scientific (Kalamazoo, MI). Following staining procedure, slides were coverslipped using a non-aqueous mounting medium (Richard-Allen Scientific).

Images were captured on a Nikon Eclipse e1000m microscope and Nikon DXM1200F digital camera with ACT-1 software (Nikon, Melville, NY).

pSTAT3 immunohistochemistry

Twelve-week old female Lepr KO^{VMH} and Lepr WT mice were each given an injection of 100 µg recombinant mouse leptin (obtained from the National Hormone and Peptide Program, NIDDK, and Dr. Parlow) or control PBS injection. Forty-five minutes after injections, mice were anesthetized and fixed via transcardial perfusion with PBS followed by 10% neutral buffered formalin. Brains were removed, post-fixed in the same fixative overnight, and then cryoprotected in a PBS-buffered 20% sucrose solution for 24 hours. Fifty µm sections were cut using a vibrating microtome (Vibratome, St. Louis, MO) and stored in a PBS-buffered, 30% ethylene glycol, 30% glycerol solution at -20°C until further processing.

pSTAT3 immunohistochemistry was performed as described (Munzberg et al., 2003) and outlined in Table 2. The anti-pSTAT3 antibody (Cell Signaling Technology #9131: lot 6, Danvers, MA) was diluted 1:3000. The biotin-conjugated donkey anti-rabbit IgG secondary antibody (Jackson ImmunoResearch #711-065-152: lot70285, West Grove, PA) was diluted 1:1000. An avidin biotinylated-peroxidase complex (ABC) combined with 3,3'-diaminobenzidine (DAB) peroxidase substrate was used for detection (Vector Laboratories,

Burlingame, CA). Normal donkey serum was purchased from Equitech-Bio, Inc. (Kerrville, TX). All other chemicals were purchased from Sigma-Aldrich.

solution	repititions	time
PBS	6 x	10 min
1%NaOH / 1%H ₂ O ₂	1 x	20 min
PBS	3 x	10 min
0.3% glycine in PBS	1 x	10 min
PBS	3 x	10 min
0.03% SDS in PBS	1 x	10 min
NDS Blocking soln.	1 x	2 hrs
primary antibody soln.	1 x	24 hrs
primary antibody soln. (4°C)	1 x	48 hrs
PBS	6 x	10 min
secondary antibody soln.	1 x	2 hrs
PBS	3 x	10 min
ABC complex	1 x	1 hr
PBS	2 x	10 min
DAB soln.	1 x	as needed
PBS	2 x	10 min

Table 2. pSTAT3 immunohistochemistry protocol. PBS = Phosphate-buffered saline, pH 7.4; NDS Blocking soln. = PBS + 0.02% sodium azide + 0.25% Triton X-100; primary antibody soln, = NDS blocking soln. + anti-pSTAT3 antibody (1:3000); secondary antibody soln. = PBS + 0.025% Triton X-100 + donkey anti-rabbit IgG; ABC complex = Vectastain ABC system (Vector laboratories); DAB soln. = chromographic peroxidase substrate (Vector Laboratories).

Following chromographic development, sections were mounted on to Superfrost/Plus microscope slides (Fisher). Slides were dried at 37°C overnight and subsequently left at room temperature until further processing. Slides were subsequently dehydrated in graded EtOH series and cleared in xylenes for 48

hours before coverslipping using a non-aqueous mounting media. Images were captured as detailed above.

Oil Red O staining

Twenty-week-old Lepr KO^{VMH} and Lepr WT mice were perfused and livers harvested and processed as described for mouse brains under pSTAT3 immunohistochemistry above. Following cryoprotection, livers were embedded in OCT compound and stored -80°C for further processing. Ten µm sections were cut using a Leica CM1900 cryostat, placed on Superfrost/Plus microscope slides (Fisher), and allowed to dry at room temperature. Sections were subsequently fixed to the slide in formalin and rinsed in three changes of distilled water. To stain, sections were rinsed in absolute propylene glycol for 5 minutes and then placed in Oil Red O solution (propylene glycol + 0.5% Oil Red O) at 60°C for 10 minutes. Sections were then rinsed in 85% propylene glycol for five minutes, rinsed in distilled water and counterstained in hematoxylin for 2 minutes. Finally, sections were rinsed in running water for 3 minutes and coverslipped using an aqueous mounting medium. Images were captured as detailed above.

β-galactosidase stain

For whole-mount staining, embryos were collected from timed-pregnant females, washed in cold PBS, and fixed in cold 4% paraformaldehyde in PBS (PFA) for 2-3 hrs. Embryos were subsequently rinsed three times for 30 minutes

at room temperature in rinse buffer (PBS, 2 mM MgCl₂, 0.01% sodium deoxycholate, 0.02% NP-40) and incubated overnight in X-gal staining solution (rinse buffer + 5 mM K₃Fe(CN)₆, 5 mM K₄Fe(CN)₆, 1 mg/ml X-gal) at 37°C. Following staining, embryos were rinsed in PBS and fixed overnight in 4% PFA at 4°C. Embryos were then dehydrated in a graded alcohol series and cleared by incubating in methyl salicylate for several hours at room temperature. Images were captured using a dissecting microscope and digital camera as described above.

For sectioning, embryos were processed as described above, embedded in OCT compound (Sakura FineTek U.S.A., Torrance, CA), and stored at -80°C. Twenty-five µm sections were cut using a Leica CM1900 cryostat, placed on Superfrost/Plus microscope slides (Fisher), and allowed to dry at room temperature. Slides were rinsed in PBS and incubated in X-gal staining solution (without detergent) at 37°C. Sections were counterstained with Nuclear Fast Red (Vector laboratories) for 5 minutes, rinsed, and dehydrated in a graded alcohol/xylene series and coverslipped using a non-aqueous mounting medium. Images were captured as described above.

To obtain adult tissues, mice were anesthetized and fixed via transcardial perfusion with ice cold 4% PFA. Following perfusion, tissues were removed and post-fixed for an additional 1-2 hrs in cold 4% PFA. Tissues were rinsed in

copious amounts of cold PBS, generally overnight. Brains were cryoprotected in 30% sucrose in PBS. Sectioning, staining, and processing were performed as described above.

PLASMA HORMONE MEASUREMENTS

Plasma was used for all assays. Leptin and insulin levels were determined using ELISA kits from Crystal Chem, Inc. (Downers Grove, IL). Corticosterone, estradiol, and testosterone levels were determined using RIA kits from MP Biomedicals (Solon, OH). All assays were performed following manufacturer's suggested protocol.

ASSESSMENT OF FEMALE ESTRUS CYCLE

Female estrus cycles were monitored by microscopic analysis of vaginal smears taken every morning from 12-week-old female *Lepr* KO^{VMH} and *Lepr* WT mice. Twenty μ l of PBS was pipetted several times into each mouse vagina, placed on microscope slides, and coverslipped. A mouse was determined to be in proestrus when the majority cells present were nucleated epithelial cells. The estrus phase was identified when the majority of cells were cornified anucleated epithelial cells. Both proestrus and estrus were further characterized by the absence of polymorphonuclear leukocytes (PMN). The presence of PMNs led to the phase classification of metestrus or diestrus. Estrus cycles were followed for 3 full cycles prior to blood collection and sacrifice at which time ovaries were

harvested and weighed. The percent of time spent in the follicular phase (proestrus and estrus) versus luteal phase (metestrus and diestrus) was calculated.

ENERGY EXPENDITURE

Indirect calorimetry and fine locomotor activity

Twelve-week-old female Lepr KO^{VMH} and Lepr WT mice were placed in chambers of an OXYMAX system (Columbus Instruments, Columbus, OH). Food and water were supplied ad libitum. Room temperature was maintained at 22°C with a 12 hour light-dark cycle. Air flow into each chamber was maintained at 0.6 L/min and exhaust air from each chamber was sampled every 39 minutes for 3 minutes. Mice were allowed to acclimatize to the chamber for 24 hours before data was collected. O₂ consumption and CO₂ production were measured for 72 hours on LF diet and 72 hours on HF diet. The respiratory exchange ratio (RER) is a ratio of volume of CO₂ produced (ml/kg/hr) per volume of O₂ consumed (ml/kg/hr). Fine locomotor movements were measured in the same chambers which were equipped with photobeam sensors to measure movement in the horizontal and vertical direction. Each photobeam interruption was counted as an ambulatory event and is reported as the average number of events per day.

Wheel running

Mice were placed in individual cages containing a running wheel with a 24 cm diameter. Mice were allowed to acclimatize to the cages for five days before data collection was started. Wheel turns were collected every 30 minutes

for 10 days. Animals were fed LF diet for 5 days before being transitioned to HF diet. Each revolution was counted by magnetic switch closures and data was acquired using Vitalview Software from Mini Mitter Company, Inc. (Bend, Oregon).

GLUCOSE TOLERANCE TESTS

Mice were maintained in a 12 hour light-dark cycle room. All tests were done using littermate controls. Mice were fasted overnight (14 -16 hours) but given water ad libitum. The day of the test, the mice were weighed and given a small nick at the end of the tail with a clean razor blade for blood collection. Blood glucose concentrations were determined via the glucose oxidase method using a OneTouch Ultra glucometer (Lifescan, Inc., Milpitas, CA). A baseline glucose concentration was obtained, after which the mice were given an intraperitoneal injection of glucose. Each mouse was given one unit of glucose per gram of body weight using an insulin syringe (1.5g/kg body weight). Blood glucose levels were sampled from the tail nick at 10, 20, 30, 60, and 120 minutes post-injection. Data are reported as mmol/L and analyzed using a 2-way ANOVA with genotype and time as parameters.

CHAPTER THREE

Development of a Steroidogenic Factor 1/Cre Transgenic Mouse Line

INTRODUCTION

The Cre-loxP strategy was developed to circumvent limitations of global gene knockouts such as embryonic lethality or secondary effects in one tissue due to absence of expression at distant site(s) (Lewandoski, 2001). Cre is a site-specific recombinase encoded by bacteriophage P1 that excises DNA between direct repeats of its recognition motif, termed loxP sites for “locus of crossing over” (Sauer and Henderson, 1988). An advance came with the demonstration that recombinantly-expressed Cre could be used to inactivate genes that were modified (or “floxed”) to place loxP sites around regions critical for function (Branda and Dymecki, 2004; Gossen and Bujard, 2002; Lewandoski, 2001)

A limitation to the general application of this strategy is the paucity of transgenes that target Cre expression to specific cell types at desired stages of development. Increasingly, Bacterial Artificial Chromosomes (BAC) are being used to provide position-independent, copy number-dependent transgenic expression (Giraldo and Montoliu, 2001; Heintz, 2000). Stallings et al. previously reported the use of a BAC containing sequences from Steroidogenic Factor 1 (SF-1) to direct expression of enhanced green fluorescent protein (eGFP) to the gonads, adrenal cortex, spleen, and VMH (Stallings et al., 2002). Subsequent studies suggested that this 47 kb BAC transgene—which contains

sequences from the 5'-flanking region and first two exons—lacks important sequences for expression of SF-1 in the hypothalamus and pituitary (Karpova et al., 2005; Shima et al., 2005).

Reported here is the use of an 111 kb BAC containing the SF-1 locus to target Cre expression to somatic cells of the gonads, adrenal cortex, anterior pituitary, spleen, and the VMH. This BAC transgene, containing 23 kb 5' of the SF-1 transcriptional initiation site and 88 kb of the SF-1 gene and 3' region, includes a regulatory element in the 6th intron that is absent from the 47 kb SF-1/eGFP transgene (Shima et al., 2005; Stallings et al., 2002).

RESULTS

SF-1/Cre transgene

A cassette containing the Cre coding sequence and the 3'-splice/transcription termination signals from bovine growth hormone (bGH) was inserted into the *SF-1* locus at the ATG initiator methionine (Figure 7). Transgenic mice were generated by pronuclear injection of supercoiled BAC DNA, and founders were identified by PCR genotyping. As shown in Figure 7, two transgenic lines were established that had 1 and 5 copies of the transgene, respectively. Based on its higher levels of Cre expression and more consistent expression pattern, the results using line 2 have been reported here.

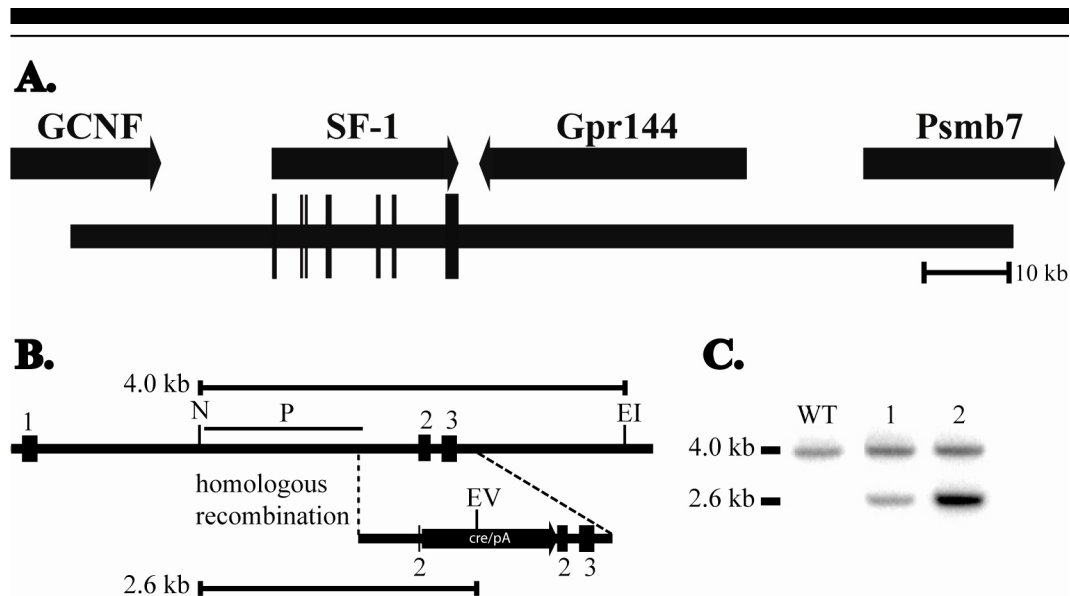


Figure 7. SF-1/Cre BAC transgene and transgene copy of transgenic founders. (A) Schematic diagram showing the position and orientation of genes within the 111 kb mouse SF-1 BAC clone. The BAC contains the SF-1 structural gene and 23 kb of 5'-flanking region and 88 kb of 3'-flanking region. (B) The recombination cassette containing the Cre coding sequence flanked by 500 bp homologous arms. The probe used for Southern blotting analysis of transgene copy number is indicated (P). Exons are labeled 1-3 and cre/pA is the fusion between Cre cDNA and bGH polyadenylation sequence. (C) Copy number of the SF-1/Cre transgenic lines. Genomic DNA was digested EcoRI (EI), EcoRV (EV) and NcoI (N), the Southern blot was hybridized with a ^{32}P -labeled probe as described in Materials and Methods. The endogenous band is 4.0 kb whereas the transgene derived band is 2.6 kb.

ROSA26R Studies

Adult studies

To determine the spatial and temporal expression profiles of the Cre transgene, SF-1/Cre transgenic mice were crossed with mice carrying the Rosa26-Cre reporter allele (Rosa26R) (Soriano, 1999). Both male and female SF-1/Cre transgenic mice appeared to have normal fertility and were readily crossed with

other lines. Expression of the Cre transgene has remained stable through seven generations.

β -galactosidase expression was first assessed in adult SF-1/Cre transgenic mice. Consistent with endogenous SF-1 expression, blue staining was seen in the adrenal cortex, testes, and ovaries (Figure 8). Within the adrenal gland, staining was limited to the cortex, with no staining in the chromaffin cells of the medulla or capsular fibroblasts (Figure 8, arrowhead).

In the ovary, theca cells (both interna and externa) stained deep blue (Figure 8, arrowhead), while there was mottled staining in the corpora lutea (Figure 8C). β -galactosidase staining was also seen in the granulosa cells, which normally express endogenous SF-1, but not all cells appeared blue (Figure 8D, data not shown). No staining was seen in oocytes (Figure 8D).

SF-1/Cre males showed β -galactosidase expression within the interstitial Leydig cells (Figure 8E, arrowhead), which normally express high levels of SF-1. The intense blue staining of the entire interstitium made it difficult to assess specific cell types, but it is likely that the peritubular myoid cells and other interstitial cell types also express the Cre transgene. Blue staining was also seen within Sertoli cells at the periphery of the seminiferous tubules, which express lower levels of SF-1 (Figure 8E, arrow).

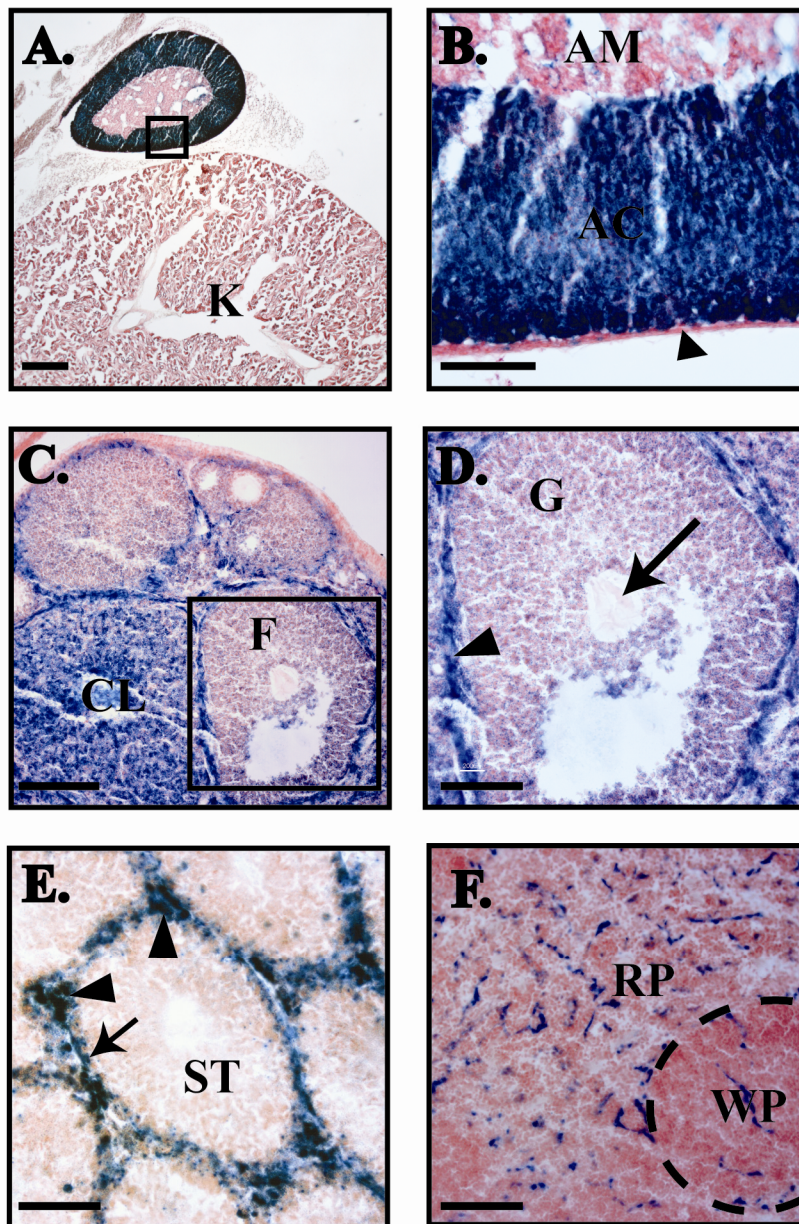


Figure 8. β -galactosidase expression in tissues of adult SF-1/Cre/ROSA26R mice. Sections were stained with X-gal and counterstained with Nuclear Fast Red as described in Materials and Methods. (A) Adrenal gland (low magnification). (B) Adrenal gland (high magnification). The arrowhead indicates the adrenal capsule. (C) Ovary (low magnification). (D) Ovarian follicle (high magnification of box in 2C). The arrow indicates an oocyte, while the arrowhead indicates the

theca interna. (E) Testis. Leydig cells are indicated by an arrowhead, and Sertoli cells by an arrow. (F) Spleen. Scale Bars = 1mm (A), 100 μ m (B,D,E,F), and 200 μ m (C). AC, adrenal cortex; AM, adrenal medulla; CL, corpus luteum; F, follicle; G, granulosa cells; K, kidney; RP, red pulp, ST, seminiferous tubule; WP, white pulp.

In contrast, male germ cells in the interior of the seminiferous tubules lacked β -galactosidase expression. Moreover, in multiple crosses of mice carrying both the SF-1/Cre transgene and a floxed allele of the *LEPR*, ectopic recombination of the *Lepr* allele was not observed in genomic DNA from tail samples (data not shown). These data suggest that the SF-1/Cre transgene in the ovaries and testes is expressed only in the somatic cells.

SF-1 is expressed in specialized endothelial cells that form the walls of the splenic venous sinuses and is necessary for splenic development and function (Morohashi et al., 1999). Consistent with this, SF-1/Cre/ROSA26R mice showed X-gal staining in the red pulp of the spleen (Figure 8F).

β -galactosidase expression in the hypothalamus of SF-1/Cre transgenic mice again was consistent with that of endogenous SF-1. The VMH showed intense staining with a gradient from dorsomedial (highest) to ventrolateral (lowest), while adjacent nuclei such as the arcuate (ARC) and dorsomedial nuclei (DMH) were largely unstained. (Figure 9A, inset). Some staining was also observed in sites where SF-1 expression has not previously been described. The most intense staining was seen within the choroid plexus of the lateral ventricles (Figure 9H). More variegated staining was also visible in the hippocampus,

predominately in the CA1 layer, and the cerebral cortex (Figure 9B, C). Although these sites may express endogenous SF-1 at levels below the sensitivity of the immunohistochemical/*in situ* hybridization approaches or may express SF-1 transiently during development, the Cre expression may also reflect transgene-directed ectopic expression.

SF-1 is also expressed in gonadotropes of the anterior pituitary. A subset of cells in the anterior pituitary had definite β -galactosidase staining, consistent with the known representation of gonadotropes in the anterior pituitary (Figure 9D). During development, some staining was apparent within the remnants of Rathke's pouch at E12.5 (data not shown). By E13.5, distinct blue staining was clearly discernible within the developing pituitary (Figure 10K, arrowhead).

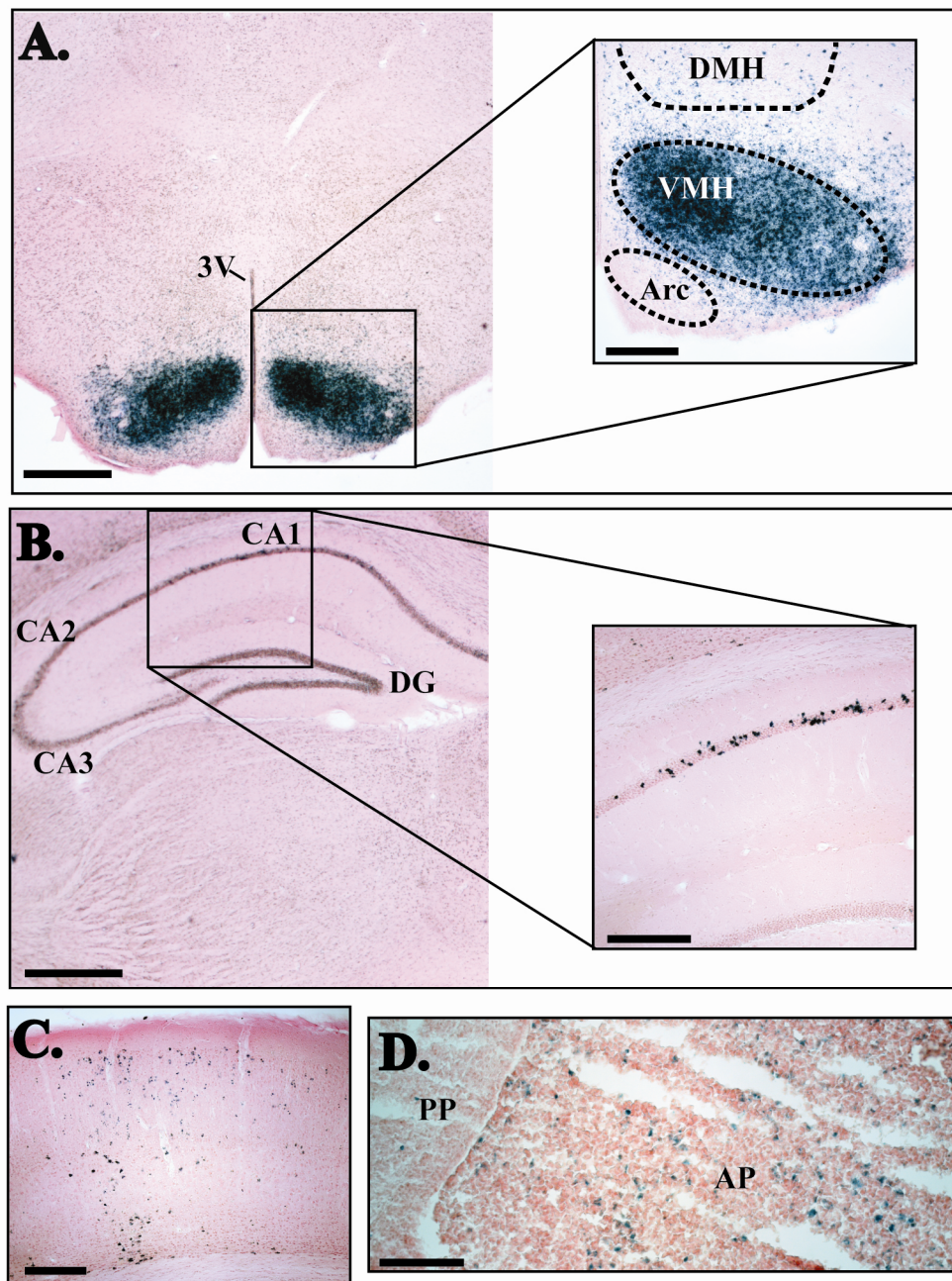


Figure 9. β -galactosidase expression in the brain of adult SF-1/Cre/ROSA26R mice. Sections were stained with X-gal and counterstained with Nuclear Fast Red. (A). Coronal section through hypothalamus. Inset shows a part of the mediobasal hypothalamus. (B) Coronal section through hippocampus; inset shows CA1 at higher magnification. (C) Coronal section through cerebral cortex at the level of the VMH. (D) Anterior pituitary. Scale bars = 500 μ m (A,B), 200 μ m (inset)

in A,B, C), and 100 μ m (D). 3V, third ventricle; AP, anterior pituitary; Arc, Arcuate nucleus; DG, dentate gyrus; DMH, dorsomedial hypothalamic nucleus; PP, posterior pituitary; VMH, ventromedial hypothalamus.

Developmental Studies

To determine when Cre expression commenced in the SF-1/Cre transgenic mice, β -galactosidase expression was examined at different developmental stages by staining of whole mount embryos and sections (Figure 10). While endogenous SF-1 transcripts can be detected in the developing gonad by E9.5 (Ikeda et al., 1994), β -galactosidase expression was not readily detected until E10.5 in the gonadal ridge of SF-1/Cre/ROSA26R male (Figure 10A,C) and female embryos (data not shown). This apparent delay most likely reflects the time necessary for Cre-dependent recombination of the ROSA26R allele and subsequent transcription, translation, and accumulation of β -galactosidase.

Staining of the gonadal ridge was definitive and consistent by E11.5 (Figure 10D, F), and was restricted to the gonadal-adrenal primordium, with no staining in the mesonephros at any ages examined. By E12.5, X-gal staining began to demarcate testicular cords within the developing testis, with the interstitial Leydig and Sertoli cell compartments continuing to robustly express β -galactosidase while germ cells within the cords failed to stain (data not shown, Figure 10L). The ovaries continued to stain more diffusely throughout development (Figure 10I).

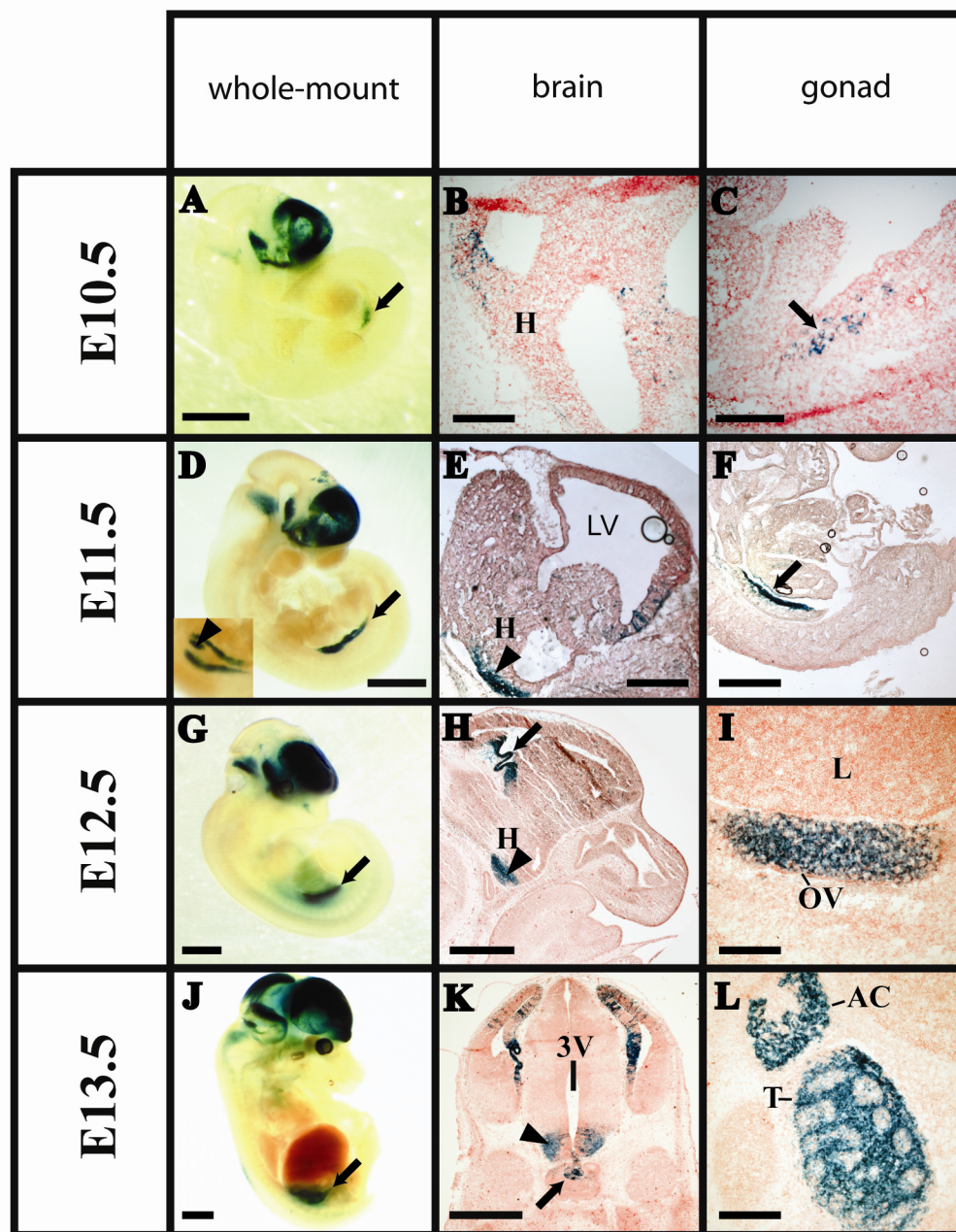


Figure 10. β -galactosidase expression during embryonic development. SF-1/Cre/ROSA26R embryos were harvested at the indicated stages. Sections were stained with X-gal and counterstained with Nuclear Fast Red. (A-C) E10.5 embryos. (A) Whole mount X-gal stained embryo. Arrow indicates gonadal ridge. (B) Sagittal section through diencephalon and telencephalon. (C) Sagittal section through the gonadal ridge (arrow). (D-F) E11.5 embryos. (D)

Whole mount X-gal stained embryo. Arrow indicates gonadal ridge. Inset shows gonadal and adrenal anlage (arrowhead). (E) Sagittal section through hypothalamus and telencephalon. Arrowhead indicates developing VMH. (F) Sagittal section through gonadal ridge (arrow). (G-I) E12.5 embryos. (G) Whole mount X-gal stained embryo. (H) Sagittal section through choroid plexus (arrow). (I) Sagittal section through ovary. (J-L) E13.5 embryos. (J) Whole mount X-gal stained embryo. (K) Coronal section through the brain at the level of the hypothalamus (arrow) and pituitary (arrowhead). (L) Sagittal section through the adrenal and testis. Scale bars = 1mm (A, D, G, H, J, K), 500 μ m (E, F), and 200 μ m (B, C, I, L). 3V, 3rd ventricle; AC, adrenal cortex; H, hypothalamus; LV, lateral ventricle; L, liver; Ov, ovary; T, testis.

A subset of β -galactosidase positive cells distinct from the gonadal primordium was identified at E11.5, situated close to the rostral end of the primordium Figure 10 (D, inset, arrowhead). While the identity of these cells was not characterized, a separate group of cells reportedly gives rise to the adrenal primordium at this developmental stage (Hatano et al., 1996). By E13.5, a distinct signal of β -galactosidase expression was clearly detected in the adrenal cortex (Figure 10L). Thereafter, as distinct cortex and medulla emerged, β -galactosidase was expressed only in the cortex.

The earliest SF-1/Cre expression in the embryonic brain was at E9.5, when expression was confined to the telencephalon (data not shown). By E10.5, expression was also observed in the diencephalon (Figure 10B). Beginning at E11.5, staining in the diencephalon acquired a distinct structure (Figure 10E). At E13.5, many cells resided in the region of the future VMH (Figure 10K, arrowhead) and could be distinguished from the cells of the more mediobasal arcuate nucleus.

Similar to the diencephalon, staining within the telencephalon became associated with distinct structures as development progressed. At E10.5, individual blue cells were dispersed within the telencephalon (Figure 10B). By E12.5, the darkest staining was found in the choroid plexus of the lateral ventricle and associated structures such as the hippocampus (Figure 10H, arrow).

CONCLUSION

In summary, the SF-1/Cre transgene directs Cre expression to specific cell lineages in the gonads, adrenal cortex, VMH, anterior pituitary, and spleen. As revealed by activation of a Cre-dependent reporter allele, Cre expression driven by the SF-1 BAC generally correlates closely with the known spatial and temporal patterns of SF-1 expression. Taken together, data presented here suggest that the SF-1/Cre transgene will provide a valuable tool for gene inactivation in the adrenal cortex, Leydig and theca cells of the gonads, the VMH, and a subset of cells in the anterior pituitary. The utility of the SF-1/Cre transgene for conditional gene knockouts in Sertoli/granulosa cells remains to be determined.

CHAPTER FOUR

Cre mediated deletion of *Lepr* from the ventromedial hypothalamic nucleus

INTRODUCTION

The cloning of leptin and its receptor revolutionized the study of obesity and metabolism. In particular, the role of leptin in modulating the melanocortin system via its actions on POMC neurons of the arcuate nucleus has received a great deal of attention. It has become apparent, however, that this “arcuocentric” approach cannot explain all aspects of the *ob/ob* or *db/db* phenotype. For example, specific deletion of *Lepr* in POMC neurons fails to recapitulate the severe obesity of the *db/db* mice and results rather in hyperphagia, hyperleptinemia, and mild obesity (Balthasar et al., 2004). Therefore, to more fully understand the mechanisms by which leptin regulates energy homeostasis, it is necessary to investigate its functions in brain regions outside the arcuate nucleus.

Though the work of Richard Gold and others has thrown a disparaging light on the role of the VMH in energy homeostasis, there is ample evidence that this region contributes to regulation of body energy stores. First, mice lacking SF-1 have an abnormal VMH and develop obesity (Dellovade et al., 2000; Majdic et al., 2002). Further, a number of factors implicated in metabolism and energy homeostasis are known to be expressed in VMH neurons including BDNF, the

MC3R, and most importantly LEPRs (Chen et al., 2000; Elmquist et al., 1998a; Rios et al., 2001; Xu et al., 2003).

In order to investigate the function of LEPRs within the VMH, I have selectively deleted *Lepr* within SF-1 neurons using the SF-1/cre mouse, previously described. Characterization of these mice has shown that leptin signaling within the VMH is essential to normal energy homeostasis.

RESULTS

Generation of *Lepr* KO^{VMH} mice

Mice homozygous for a conditional *Lepr* allele were obtained from Jeffrey Friedman at Rockefeller University (Cohen et al., 2001). Exon 1 of the *Lepr* gene in these mice is flanked by loxP sites (floxed). Excision of exon 1 results in a null allele with deletion of all LEPR isoforms. Mice lacking LEPRs in the SF-1 neurons of the VMH were generated by the successive crossing of SF-1/Cre positive mice with *Lepr*^{fl/fl} mice to obtain SF-1/Cre, *Lepr*^{fl/fl} mice – designated as *Lepr* KO^{VMH} mice, hereafter. Cre negative, *Lepr*^{fl/+}, or Cre negative, *Lepr*^{fl/fl} mice were used as WT controls and are designated as *Lepr* WT mice.

Selective deletion of VMH LEPRs

To confirm the deletion of LEPRs within the SF-1 neurons of the VMH, immunohistochemistry for phosphorylated STAT3 (pSTAT3) was performed on the brain sections from *Lepr* KO^{VMH} and *Lepr* WT mice that had previously

received intraperitoneal (i.p.) injections of recombinant mouse leptin. As phosphorylation of STAT3 follows binding of leptin to its receptor, pSTAT3 immunohistochemistry can be used as a marker for activated LEPRs (Munzberg et al., 2003). As seen in Figure 11, i.p. injection of leptin into a Lepr WT mouse produces pSTAT3-immunoreactivity (pSTAT3-IR) in the ARC, DMH, as well as VMH (Figure 11B). Little pSTAT3-IR is seen in the VMH of Lepr KO^{VMH} mice given the same dose of leptin, while expression in other sites is preserved (Figure 11D).

Lepr KO^{VMH} mice are sensitive to diet-induced obesity (DIO)

To investigate the role of VMH LEPRs in the regulation of body weight, the weights of Lepr KO^{VMH} mice was compared to that of Lepr WT littermates. Mice were weaned at 4 weeks of age and placed on either normal mouse chow (LF, 9.4% kcal from fat) or a high fat (HF, 60% kcal from fat) and weighed every 14 days. On normal chow, neither male nor female Lepr KO^{VMH} mice showed a significant weight increase over their WT littermates (Figure 12). However, both male and female Lepr KO^{VMH} mice showed sensitivity to diet-induced obesity. By 20 weeks of age, female Lepr KO^{VMH} mice on the HF diet were 20% heavier than WT littermates (40.5 ± 1.8 g vs. 33.5 ± 1.5 g). Males were less severely affected, with the Lepr KO^{VMH} males weighing 12% more than WT littermates, at 20 weeks (52.2 ± 1.9 g vs. 46.7 ± 1.3 g). It appears that VMH LEPRs do not play

a role in somatic growth as there was no difference in the length of male or female mice on either diet (data not shown).

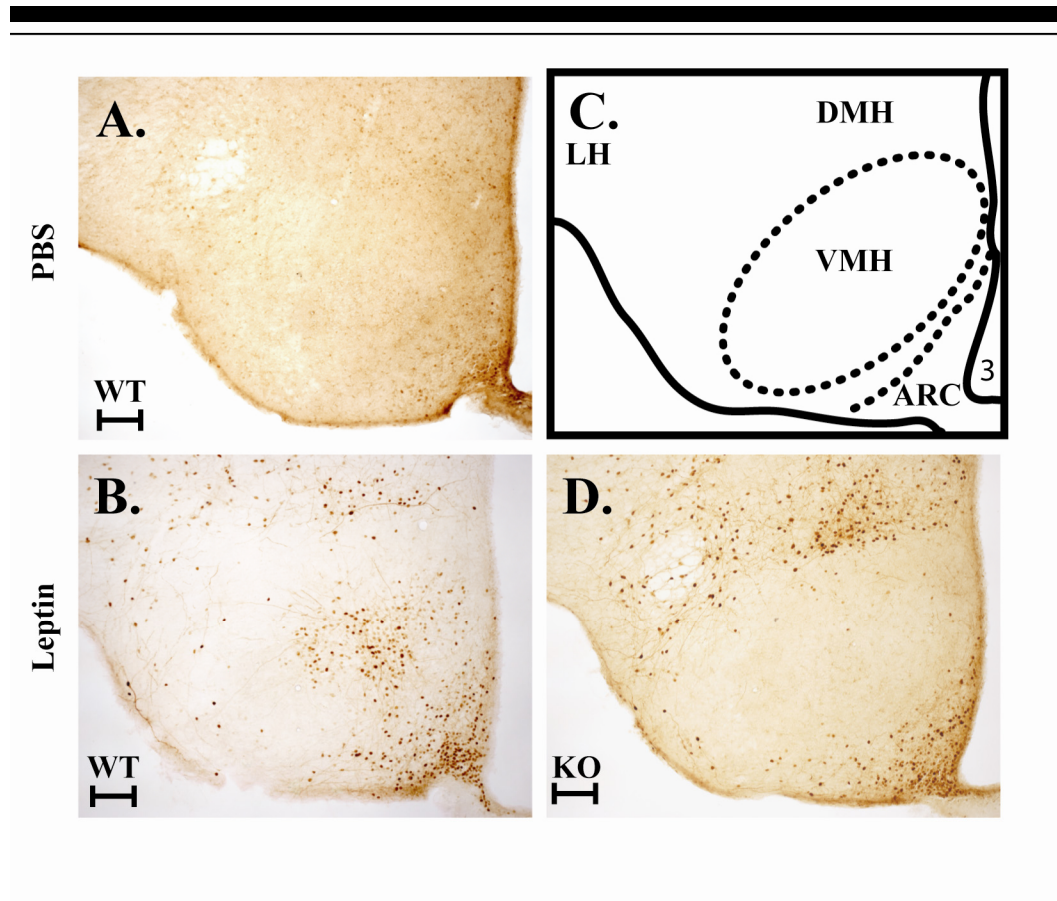


Figure 11. pSTAT3 immunohistochemical analysis of Lepr KO^{VMH} brains. pSTAT3 immunohistochemistry on 50mm brain sections from Lepr WT mice injected with PBS (A) or leptin (B) and a Lepr KO^{VMH} mouse, also injected with leptin (D). (E) schematic of basal hypothalamus. Scale bars = 100mm. ARC, arcuate nucleus; DMH, dorsomedial hypothalamic nucleus; LH, lateral hypothalamus; VMH, ventromedial hypothalamic nucleus.

Body composition of Lepr KO^{VMH} mice

The increased weight of Lepr KO^{VMH} mice is wholly due to an increase in adipose tissue mass (Table 3). On HF diet, the percent body fat is increased by

15% and 21% in male and female $\text{Lepr KO}^{\text{VMH}}$ mice compared to their Lepr WT littermates. Interestingly, while $\text{Lepr KO}^{\text{VMH}}$ mice show no significant increase in total body weight on LF diet, both males and females exhibit even greater increases in percent body fat than on HF diet – 55% and 30%, respectively, compared to Lepr WT controls.

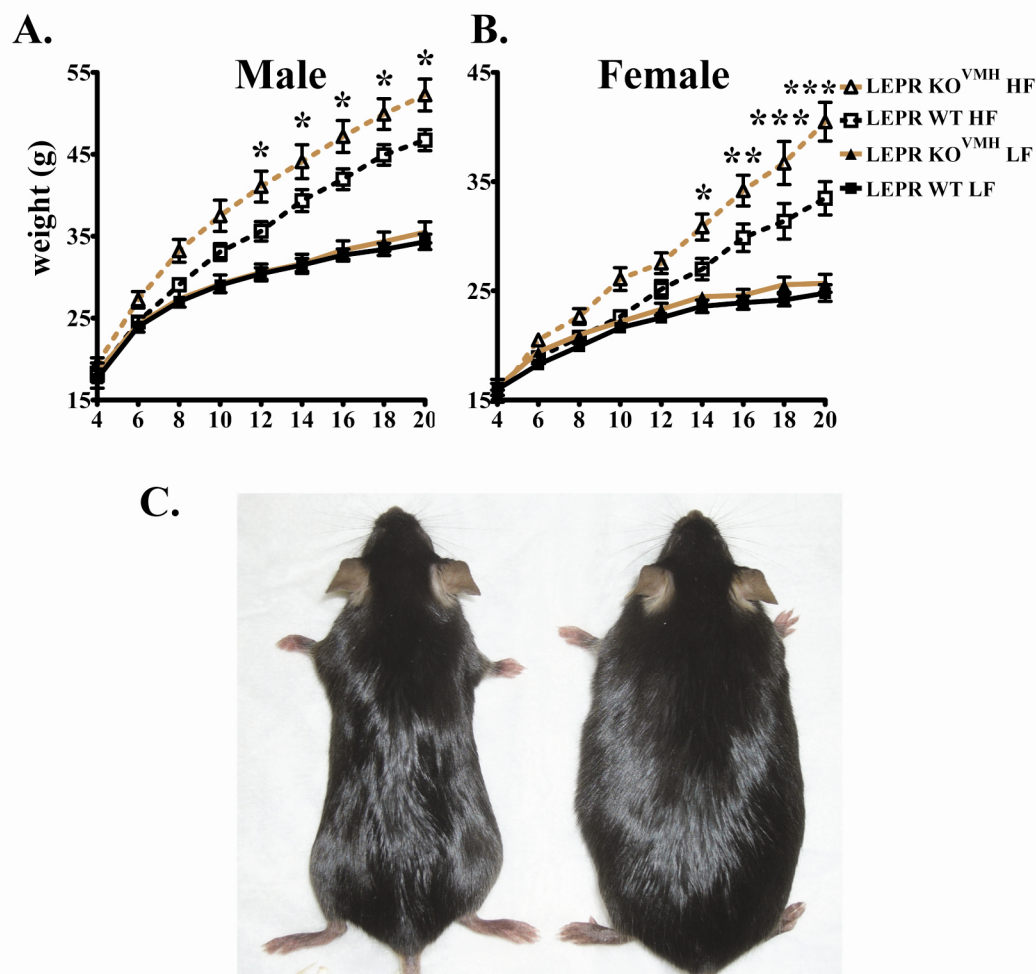


Figure 12. Body weight of $\text{Lepr KO}^{\text{VMH}}$ mice. The weights of male (A) and female (B) $\text{Lepr KO}^{\text{VMH}}$ mice were compared to that of Lepr WT littermates on both LF and HF diet. (C) Photo of

twenty-week-old female Lepr WT (left) and Lepr KO^{VMH} (right) littermates on HF diet. Results represent the mean \pm S.E.M. of at least 10 mice of each sex in each genotype. *P<0.05, **P<0.01, ***P<0.001 Lepr KO^{VMH} HF versus Lepr WT by two-way ANOVA.

Histological evidence supports the body composition data obtained by NMR. Examination of white adipose tissue (WAT) from Lepr KO^{VMH} mice fed a LF diet revealed a marked cellular hypertrophy (Figure 13A,B), while examination of BAT shows a significant increase in the size of cellular vacuoles, presumable filled with excess lipid (Figure 13C,D). Thus, on a LF diet, Lepr KO^{VMH} mice demonstrate an increased accumulation of lipid stores in fat depots compared to Lepr WT littermates, despite comparable body weights.

	Low Fat		High Fat	
	Lepr WT	Lepr KO ^{VMH}	Lepr WT	Lepr KO ^{VMH}
Percent fat mass				
Male	11.7 \pm 1.1 (6)	18.1 \pm 1.9 (8) ^a	38.1 \pm 1.1 (9)	43.7 \pm 1.7 (9) ^a
Female	13.8 \pm 0.9 (10)	18.0 \pm 0.7 (9) ^c	39.2 \pm 3.4 (7)	47.6 \pm 2.2 (8) ^a
Percent lean mass				
Male	74.4 \pm 1.6 (6)	69.2 \pm 1.5 (8) ^a	53.5 \pm 1.0 (9)	48.1 \pm 0.8 (9) ^b
Female	72.1 \pm 0.7 (10)	69.2 \pm 0.7 (9) ^c	53.2 \pm 2.6 (7)	46.6 \pm 1.5 (8) ^a
Percent water mass				
Male	1.4 \pm 0.1 (6)	1.7 \pm 0.1 (8)	2.9 \pm 0.2 (9)	3.3 \pm 0.1 (9)
Female	1.3 \pm 0.1 (10)	1.3 \pm 0.1 (9)	2.4 \pm 0.2 (7)	2.9 \pm 0.2 (8)

Table 3. Body composition of Lepr KO^{VMH} mice. Fat, lean and water mass of twenty-week-old Lepr KO^{VMH} and Lepr WT mice was measured by NMR spectroscopy and normalized to total body mass. All data represent the mean \pm SEM, with the sample size in parentheses. ^aP < 0.05; ^bP<0.01; ^cP < .001 versus Lepr WT on same the same diet in an unpaired, two-tailed Student's t test.

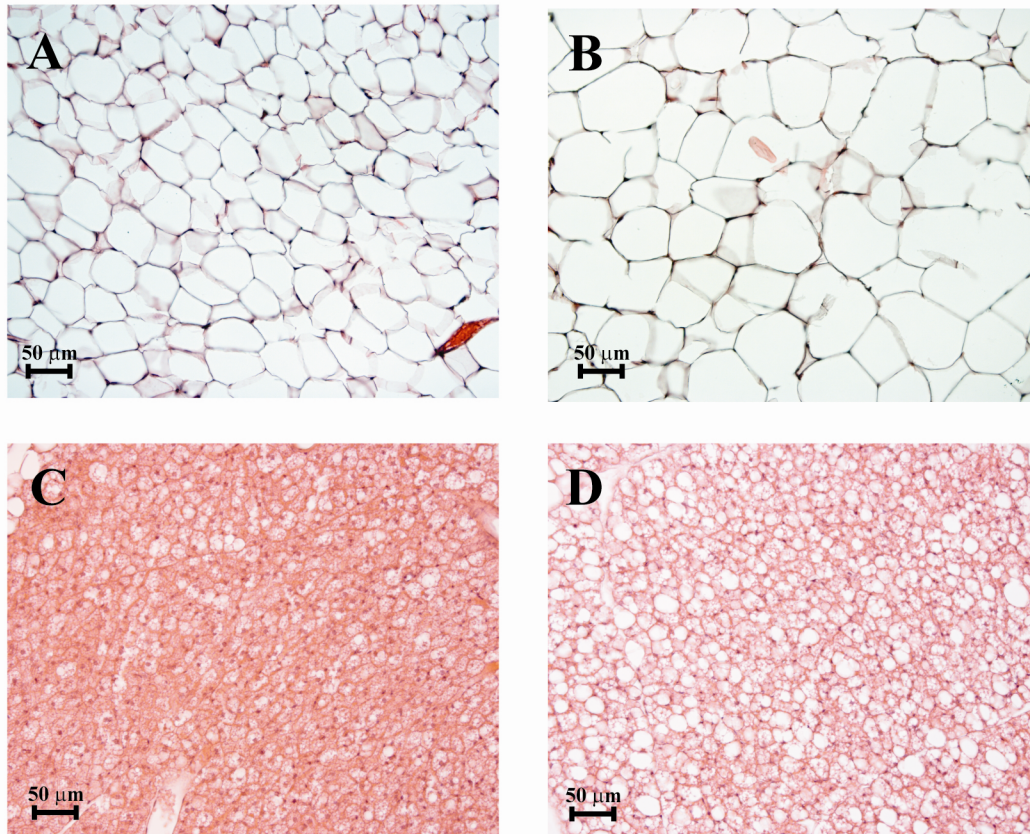


Figure 13. Adipose histology of *Lepr* KO^{VMH} mice. Comparison of H&E stained WAT from the gonadal fat pad of 20-week-old female *Lepr* WT (A) and *Lepr* KO^{VMH} (B) on LF diet shows marked cellular hypertrophy. Comparison of H&E stained BAT from the same animals (C, *Lepr* WT; D, *Lepr* KO^{VMH}), shows large, clear vacuoles in BAT of *Lepr* KO^{VMH} mice, presumably from lipid accumulation.

Hepatic pathology and dyslipidemia

Liver steatosis is a characteristic sequela of disrupted central leptin signaling (Cohen et al., 2001; Yen et al., 1976), and has been shown to be largely independent of the hyperphagia associated with leptin deficiency (Levin et al., 1996). In order to determine if the increased adiposity in *Lepr* KO^{VMH} mice fed a

LF diet was limited to adipocytes or more generalized, the lipid content of *Lepr* KO^{VMH} livers was assayed by both histological and biochemical methods (Figure 14). By twenty weeks of age, the livers of *Lepr* KO^{VMH} mice fed weighed approximately 50% more than *Lepr* WT controls and contained approximately 50% more triacylglycerol (Figure 14C). This increased lipid content is readily apparent on histological sections stained with oil red O (Figure 14A). In contrast, there is no difference in liver cholesterol levels (Figure 14D). To rule out ectopic Cre expression and primary loss of *Lepr* expression in the liver, hepatic *Lepr* transcripts were assayed by quantitative reverse transcription PCR (qRT-PCR), with no difference seen in mRNA levels (Figure 14E). Paralleling the increased liver triacylglycerol content, *Lepr* KO^{VMH} mice fed a LF diet also exhibit hypertriglyceridemia without concomitant hypercholesterolemia (Figure 15).

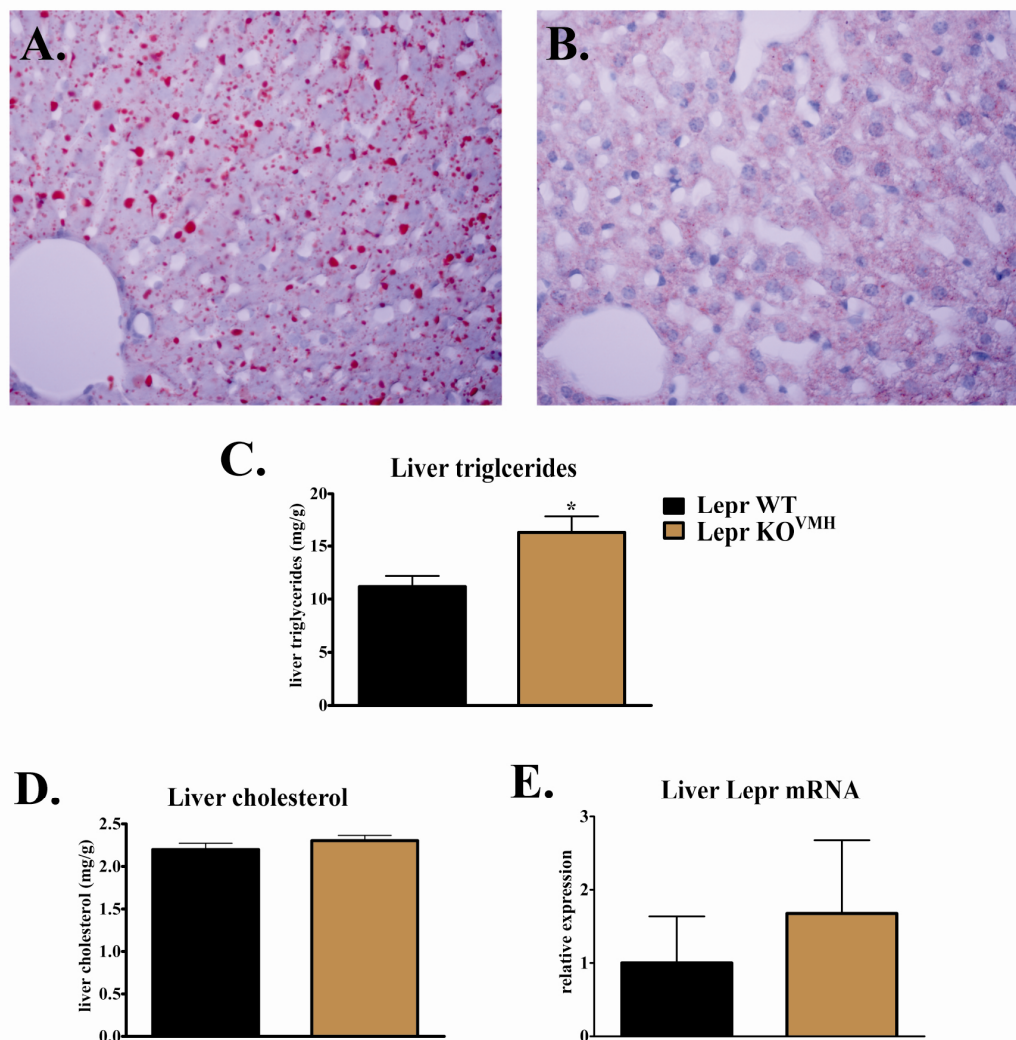


Figure 14. Liver pathology of Lepr KO^{VMH} mice. (A,B) Oil red O staining of liver sections shows increased hepatic lipid levels in livers of Lepr KO^{VMH} (A) mice compared to Lepr WT (B) mice. (C) Liver triglyceride levels were measured for Lepr KO^{VMH} and Lepr WT mice. (D) Liver cholesterol was measured for Lepr KO^{VMH} and Lepr WT mice. (E) Expression levels of Lepr transcripts were determined by qRT-PCR. Results represent the mean \pm S.E.M. Animals were sacrificed at 0900 under free feeding conditions. $n = 9$ of each genotype in C,D. $n = 3$ of each genotype in E. * $P < 0.05$ versus Lepr WT in an unpaired, two-tailed Student's t test.

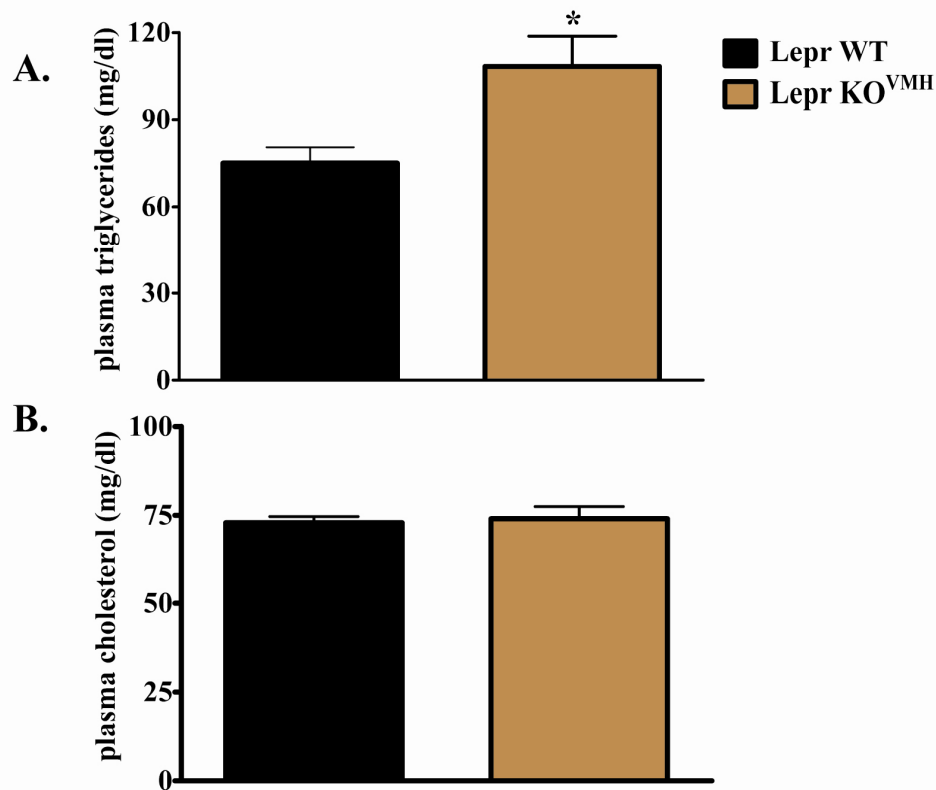


Figure 15. Dyslipidemia of Lepr KO^{VMH} mice fed a LF diet. (A) Plasma triglycerides of twenty-week-old female Lepr KO^{VMH} and Lepr WT mice. (B) Plasma cholesterol of twenty-week-old female Lepr KO^{VMH} and Lepr WT mice. Mice were sacrificed at 0900 under free feeding conditions using LF chow. Results represent the mean \pm S.E.M. $n = 9$ of each genotype. * $P < 0.05$ versus Lepr WT in an unpaired, two-tailed Student's t test.

Neuroendocrine function of Lepr KO^{VMH} mice

Ob/ob and *db/db* mice are known to exhibit aberrant neuroendocrine function including hypogonadotropic hypogonadism, hypercorticonemia, and hyperinsulinemia (Coleman and Hummel, 1974; Naeser, 1974; Swerdloff et al., 1976). In addition, the SF-1/Cre transgene is expressed the adrenal, gonads, and pituitary gonadotropes of Lepr KO^{VMH} mice (Bingham et al., 2006; Stallings et al., 2002) deleting *Lepr* in these tissues. Therefore, the Lepr KO^{VMH} mice were

analyzed with respect to endocrine abnormalities associated with the *db/db* phenotype (Table 4).

	Lepr WT	Lepr KO^{VMH}
leptin (ng/ml)	2.4 ± 0.4 (9)	6.3 ± 1.1 (10)^b
insulin (ng/ml)	0.8 ± 0.1 (8)	1.9 ± 0.3 (8)^b
glucose (mmol/L)	13.4 ± 0.5 (13)	13.3 ± 0.4 (14)
AM corticosterone (ng/ml)	7.3 ± 1.2 (12)	14.0 ± 3.5 (14)
estradiol (pg/ml)	26.0 ± 1.4 (10)	29.4 ± 2.5 (8)
testosterone (ng/ml)	1.2 ± 0.5 (12)	2.0 ± 0.7 (8)

Table 4. Neuroendocrine function of Lepr KO^{VMH} mice. For leptin, insulin, glucose, and corticosterone measurements, twenty-week-old female Lepr KO^{VMH} and Lepr WT mice raised on LF diet were sacrificed by decapitation at 0900 under free feeding conditions. Plasma for testosterone measurements was obtained similarly from male mice. Plasma for estradiol measurement was collected from twelve-week-old females in estrus phase as determined by vaginal cytology. ^bP<.01 versus Lepr WT in an unpaired, two-tailed Student's t test.

Adrenal and Gonadal Function

Though the presence and function of LEPRs in the adrenal and gonads is unclear (Banks et al., 1999; Hoggard et al., 1997; Ryan et al., 2003; Ryan et al., 2002), the adrenal and gonadal function of Lepr KO^{VMH} mice was assessed to evaluate any primary or secondary defects in these endocrine organs. The gonadal weights of both male and female Lepr KO^{VMH} was comparable to values for Lepr WT mice of the same sex (data not shown), and histological inspection of ovaries and testes revealed no obvious morphological abnormalities (Figure 16). The sex

steroid hormones of both male and female *Lepr* KO^{VMH} mice were measured, with no significant difference being seen in either male or females (Table 4).

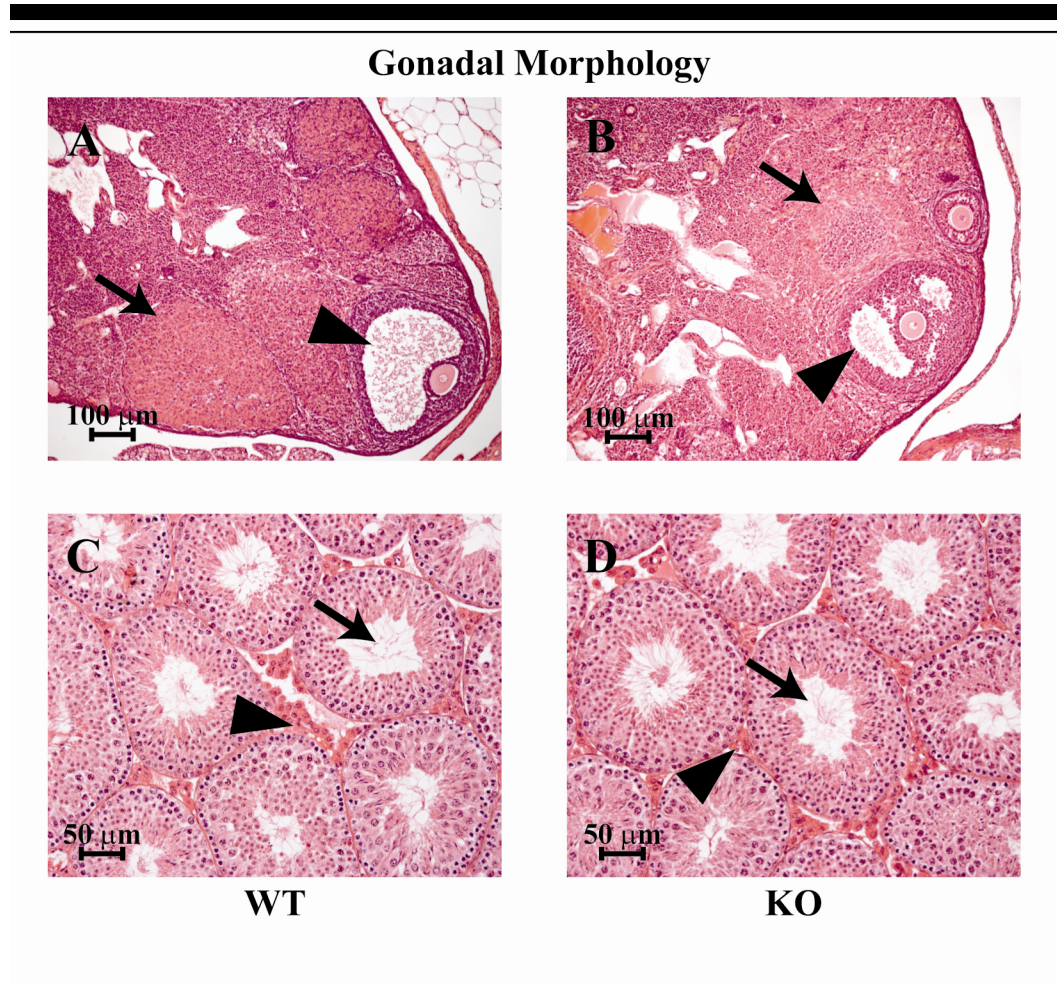


Figure 16. Gonadal morphology of *Lepr* KO^{VMH} mice. (A,B) H&E stained sections of *Lepr* WT (A) and *Lepr* KO^{VMH} ovaries. Arrowhead indicates mature antral follicles while arrow indicates corpus lutei. (C,D) H&E stained sections of *Lepr* WT (C) and *Lepr* KO^{VMH} (D) testes. Arrowhead indicates interstitial space with Leydig cells while arrow indicates open lumen with mature spermatids.

The estrus cycle of female *Lepr* KO^{VMH} mice was evaluated by monitoring changes in vaginal cytology. Vaginal smears were taken daily from *Lepr* KO^{VMH}

and Lepr WT mice over three complete cycles and the percent of time spent in the follicular phase (proestrus and estrus) versus the luteal phase (metestrus and diestrus) was calculated. Lepr KO^{VMH} mice cycle regularly and there was no apparent difference in cycle length, with Lepr KO^{VMH} spending slightly more time in the follicular phase (41%) than Lepr WT mice (32%). In addition, both male and female Lepr KO^{VMH} were regularly used as breeders in the mouse colony and appeared to produce regularly spaced and sized litters, though this was not strictly quantitated. Thus, although subtle defects may exist, these results indicate that there are no significant perturbations in the male or female reproductive capacity.

The adrenal glands function to regulate fluid and electrolyte balance as well as the stress response through the production and secretion of mineralocorticoids and glucocorticoids, respectively. Severe defects in mineralocorticoid secretion result in hypotension, culminating in death. Given that Lepr KO^{VMH} mice appear healthy with no signs of hypotension, it is unlikely that they have any severe defects in mineralocorticoid production. Glucocorticoids are secreted acutely in response to stress as well as in a normal diurnal rhythm, with a morning nadir and evening apex in nocturnal animals such as mice. Hyposecretion of glucocorticoids results in fatigue, muscle weakness, and loss of weight and appetite, while hypersecretion of glucocorticoids results in increased adiposity.

Db/db mice have been shown to have increased levels of plasma corticosterone, the primary glucocorticoid produced by the mouse adrenal (Naeser, 1974). Therefore, to assess for hypercorticosteronemia, A.M. corticosterone levels of *Lepr* KO^{VMH} females were measured. Though corticosterone levels trended higher in the *Lepr* KO^{VMH} mice, variation between individuals made it difficult to establish statistical significance, though it is possible that with a larger cohort of animals these levels may prove significantly different (Table 4). In addition, adrenal weight of *Lepr* KO^{VMH} mice did not differ significantly from *Lepr* WT mice (data not shown) and histological examination showed normal zonation of the adrenal (Figure 17).

Leptin, Insulin, and Glucose

In order to further assess the endocrine status of *Lepr* KO^{VMH} mice, plasma leptin, insulin, and glucose levels were measured. Twenty week old, female *Lepr* KO^{VMH} mice fed a LF diet were hyperleptinemic, with a 2 to 3-fold increase in plasma leptin levels relative to *Lepr* WT controls (Table 4). As well, *Lepr* KO^{VMH} mice on LF diet were slightly hyperinsulinemic (~2-fold), while remaining euglycemic (Table 4).

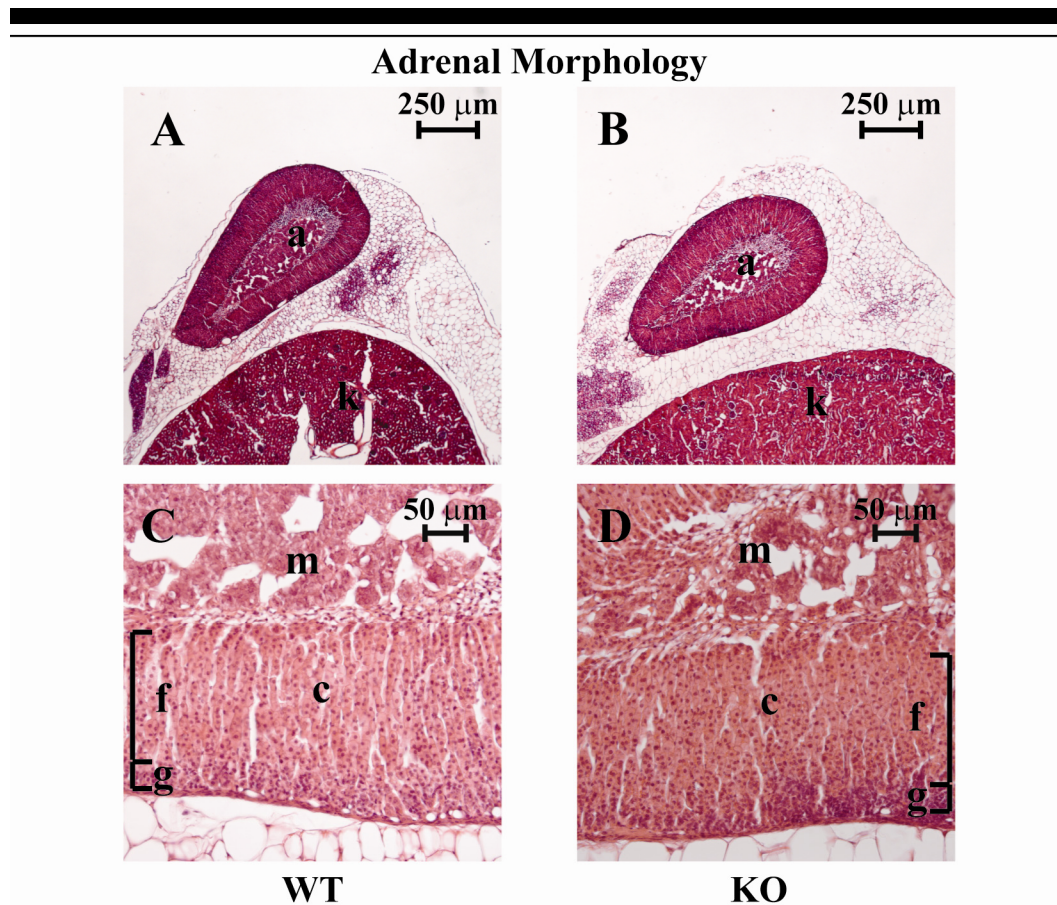


Figure 17. Adrenal morphology of Lepr KO^{VMH} mice. (A,B) H&E stained sections of twenty-week-old female Lepr WT (A) and Lepr KO^{VMH} adrenal glands (low power). (C,D) H&E stained sections of twenty-week-old Lepr WT (C) and Lepr KO^{VMH} (D) adrenal glands (high power), showing zonation of adrenal cortex. a, adrenal; c, adrenal cortex; f, zona fasciculata; g, zona glomerulosa; k, kidney; m, adrenal medulla.

Food Intake

Since differences in caloric intake may account for differences in body weight and/or composition, the rate of caloric consumption was measured in Lepr KO^{VMH} mice. Twelve week old female Lepr KO^{VMH} were housed individually and their daily caloric intake on LF chow was measured daily for seven days, after which they were switched to a HF diet and caloric intake was measured for an

equal amount of time (Figure 18). While no significant difference in caloric intake was seen on the LF diet, a small, but significant, difference was seen on the HF diet – with Lepr KO^{VMH} mice eating 1.8 ± 0.06 kcal/day more than Lepr WT mice (Figure 18A). No significant differences in food consumption or feeding efficiency (ratio of weight change to caloric intake) on either LF or HF diet were seen (Figure 18B). In a separate experiment, cumulative caloric intake over an extended period of time significantly differed on the HF diet (Figure 18C).

Energy Expenditure

Locomotor Activity

Increased weight results from an increased energy intake to output ratio. To evaluate the contribution of decreased energy output to the increased adiposity of Lepr KO^{VMH} mice, locomotor activity was evaluated using both wheel-running and photobeam break assays. Twelve week old, female Lepr KO^{VMH} mice showed a modest decrease in wheel-running activity on both a LF and HF diet, though this was not statistically significant (Figure 19B). Like Lepr WT mice, Lepr KO^{VMH} mice increased their locomotor activity in response to a HF challenge. As well, Lepr KO^{VMH} mice appeared to have a normal circadian pattern of activity (Figure 19A). As well, there appears to be little difference between Lepr KO^{VMH} and Lepr WT mice in a photobeam assay, which assesses fine locomotor activity and home cage behavior (Figure 20). While Lepr KO^{VMH} mice have a decreased rearing

activity (movement in the vertical direction), especially on a HF diet, the difference does not reach statistical significance (Figure 20B).

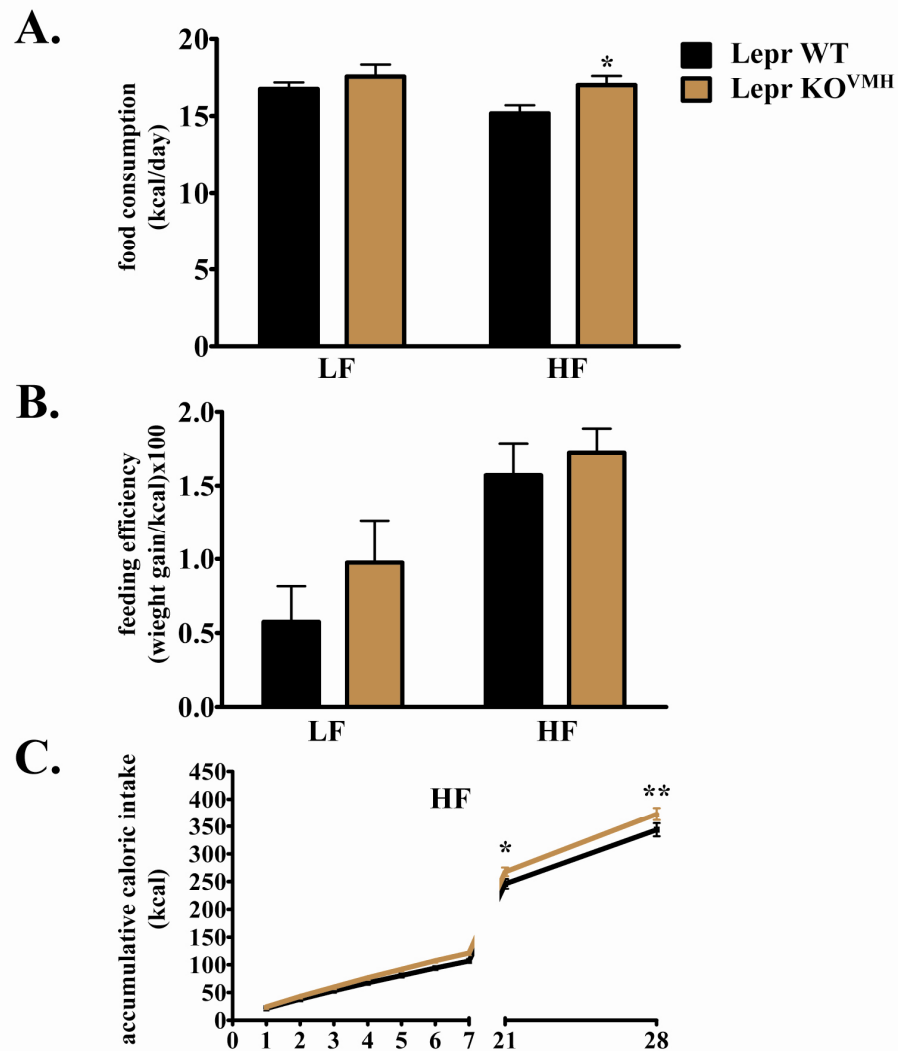


Figure 18. Caloric intake of Lepr KO^{VMH} mice.(A) Caloric intake of twelve-week-old female Lepr KO^{VMH} and Lepr WT mice was measured for seven days before and after the transition from LF to HF diet and average daily caloric consumption was calculated. (B) Feeding efficiency of twelve-week-old female Lepr KO^{VMH} and Lepr WT mice on LF and HF diet. (C) Cumulative

caloric intake of twelve-week-old female Lepr KO^{VMH} and Lepr WT mice over 4 weeks after transition to HF diet.

Metabolic rate

To evaluate the metabolic rate of Lepr KO^{VMH} mice, twelve-week-old female Lepr KO^{VMH} mice and controls were subjected to indirect calorimetry (Figure 21). Mice on LF diet were monitored for three days, after which they were transitioned to HF diet and monitored for at least three days. On LF diet, there was no discernable difference in the metabolic rate of Lepr KO^{VMH} and Lepr WT mice, as assessed by O₂ consumption. However, when transitioned to a HF diet, Lepr KO^{VMH} mice exhibit a defective adaptive thermogenic response. While Lepr WT mice show an increase of 15% in O₂ consumption, Lepr KO^{VMH} mice increase their O₂ consumption by only 8% (Figure 21A). In response to a HF challenge, Lepr WT demonstrate a shift from carbohydrate based metabolism to a more fatty acid based metabolism, as seen by the decrease in respiratory exchange ratio (RER). This substrate response appears to be intact in Lepr KO^{VMH} mice, as there is no significant difference in the RER of Lepr KO^{VMH} and Lepr WT mice on either LF or HF diet (Figure 21B).

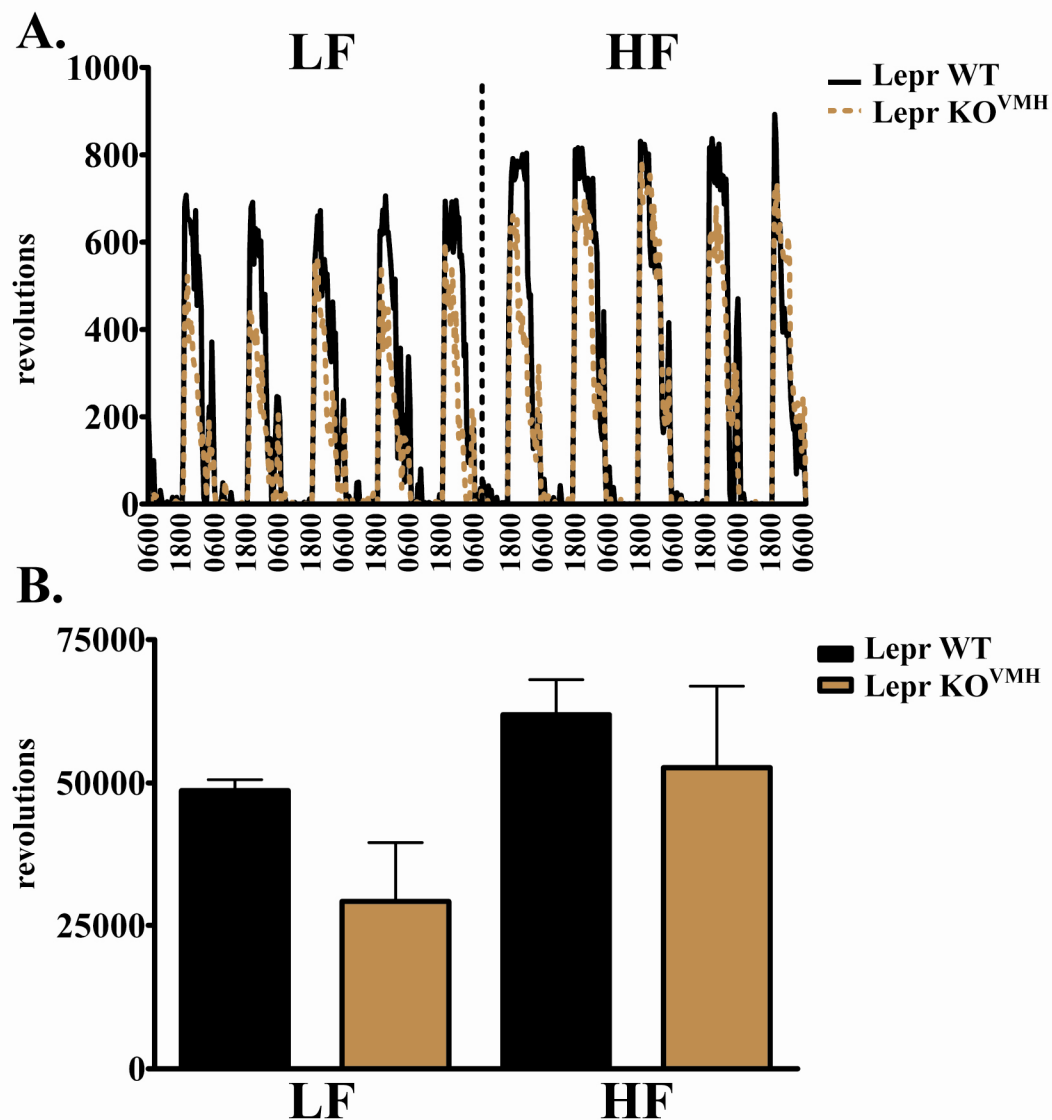


Figure 19. Wheel running activity of Lepr KO^{VMH} mice. Locomotor activity of twelve-week-old Lepr KO^{VMH} and Lepr WT females was measured over at least five consecutive days on both LF and HF diet and reported as the total number of wheel revolutions. (A) Shows circadian rhythm of activity with 0600 and 1800 representing lights on and off times, respectively. (B) shows total revolutions over five days. Results are given as the mean \pm S.E.M., $n = 4$ in each group.

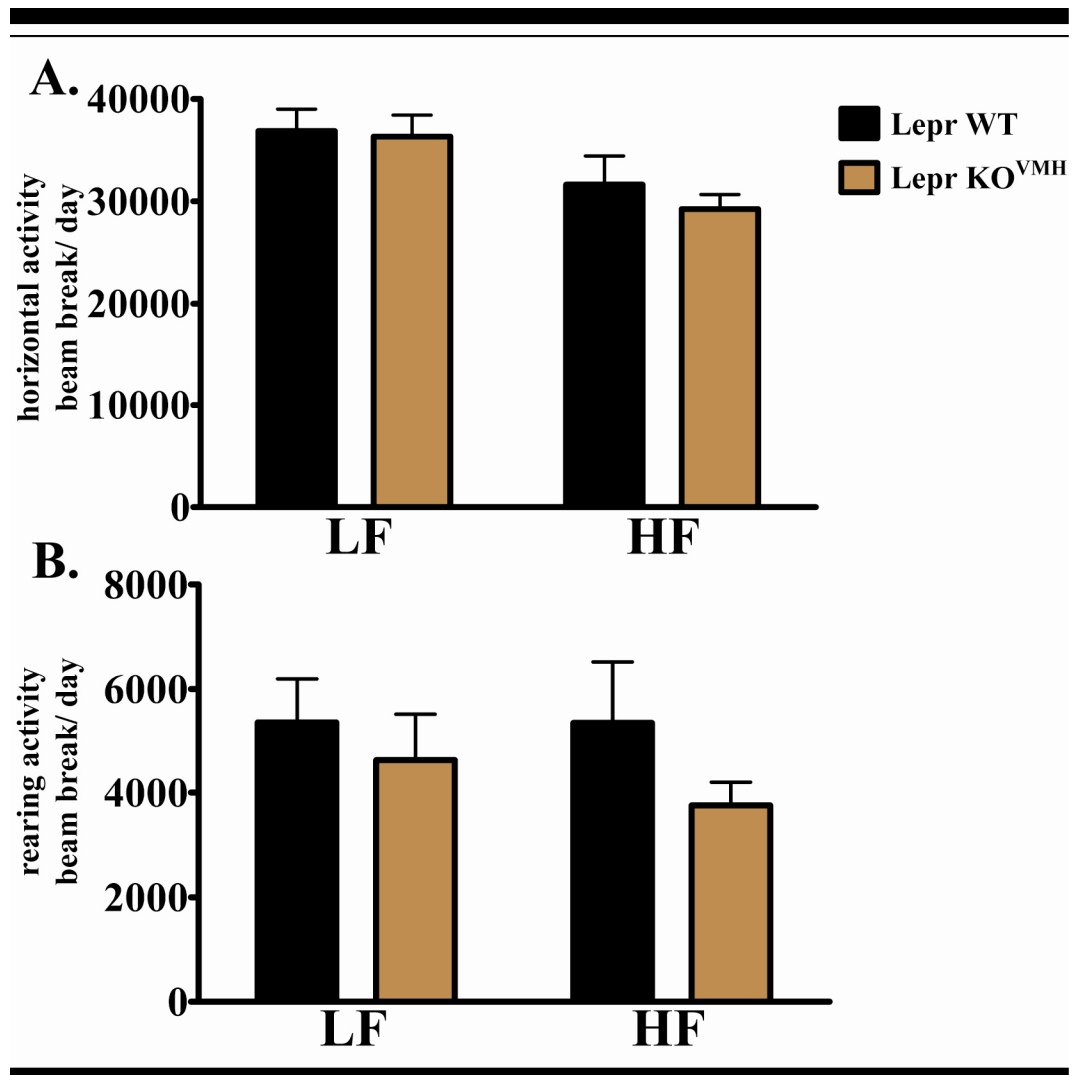


Figure 20. Fine locomotor activity of Lepr KO^{VMH} mice. Locomotor activity of twelve-week-old Lepr KO^{VMH} and Lepr WT females was measured over at least three consecutive days on both LF and HF diet and reported as the number of photobeam breaks per day. Locomotor activity in both the horizontal (A) and vertical (B) plane was measured. Results are given as the mean ± S.E.M., n = 6 in each group.

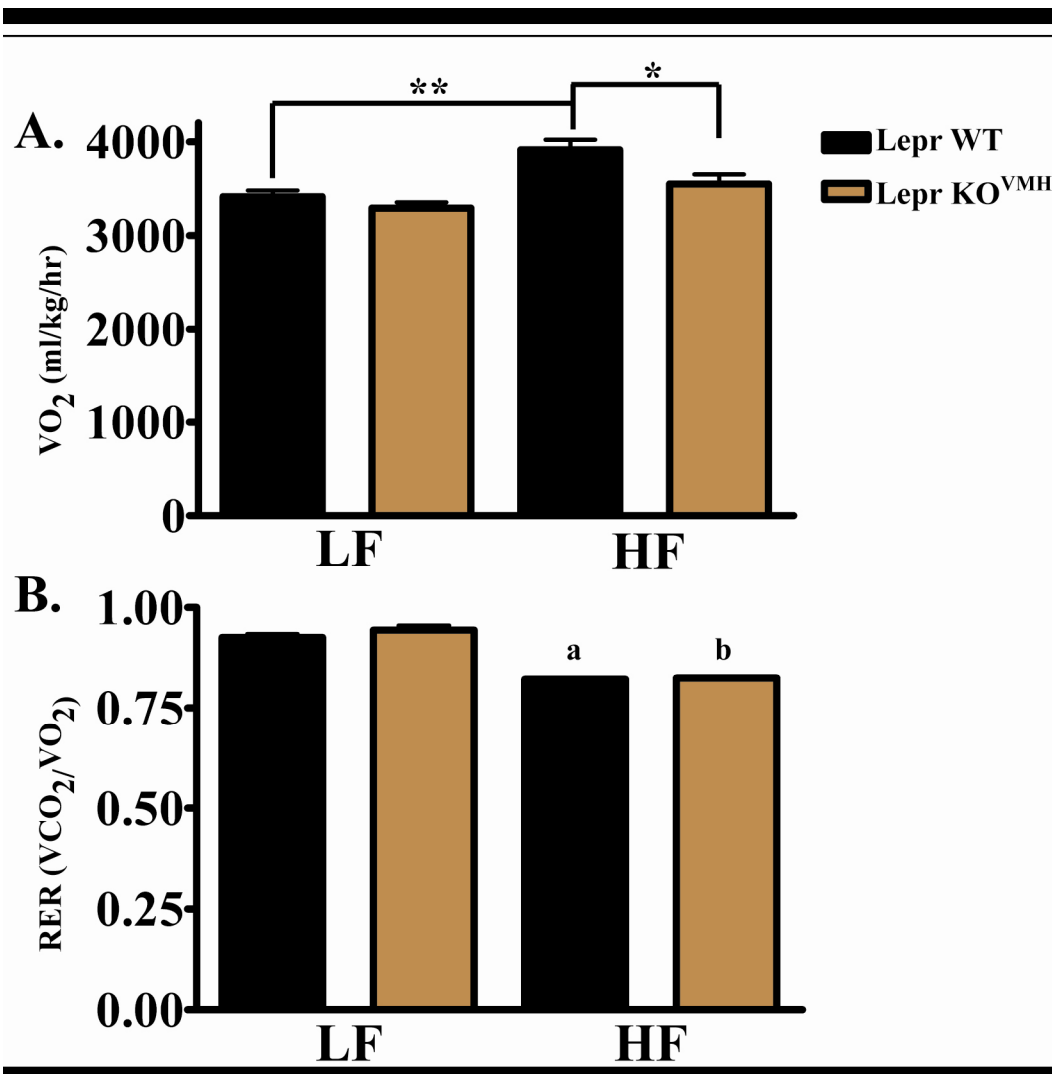


Figure 21. Metabolic rate and respiratory exchange ratio of Lepr KO^{VMH} mice.(A) VO_2 consumption was measured in twelve-week-old Lepr KO^{VMH} and Lepr WT females on LF and HF diets. (B) RER was calculated from VCO_2 and VO_2 rates. Results are given as the mean \pm S.E.M., $n = 6$ in each group; Statistical significance was determined by ANOVA. * $P < 0.05$, ** $P < 0.01$, ^a $P < 0.05$ compared to WT LF, ^b $P < 0.05$ compared to KO LF.

Glucose Homeostasis

Ob/ob and *db/db* mice both exhibit severe primary disturbances in glucose homeostasis (Coleman and Hummel, 1974; Herberg and Coleman, 1977). While no differences in fasting glucose are apparent, glucose tolerance tests (GTT)

performed on twelve-week-old mice fed a LF diet show significant glucose intolerance in both male and female $\text{Lepr KO}^{\text{VMH}}$ (Figure 22).

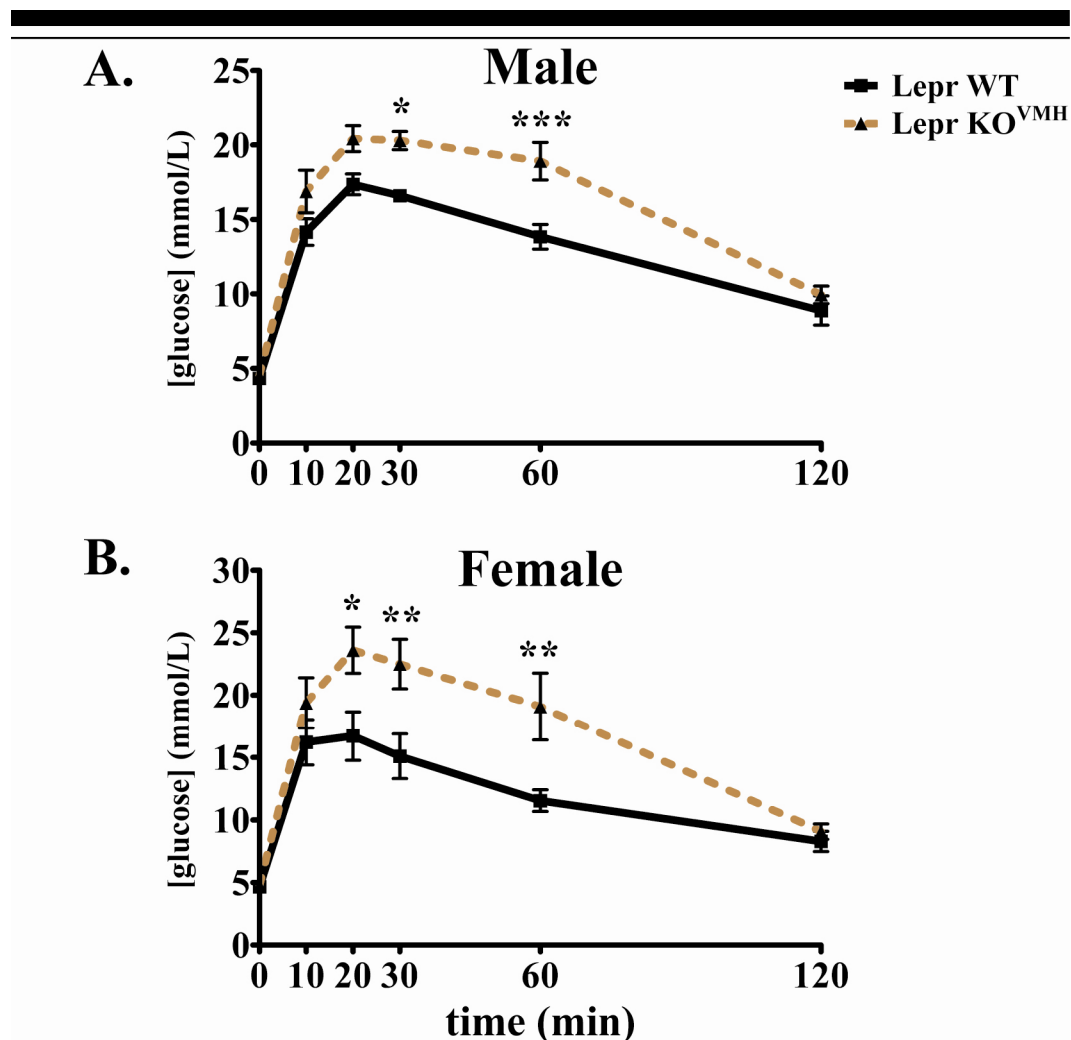


Figure 22. Glucose tolerance of adult $\text{Lepr KO}^{\text{VMH}}$ mice. Twelve-week-old $\text{Lepr KO}^{\text{VMH}}$ (triangle) and Lepr WT (square) mice fed LF diet were fasted for 12-16 hrs and given an i.p. bolus of glucose (1.5 mg per gram body weight). Whole blood glucose levels were measured thereafter. The results represent the mean \pm S.E.M for at least seven animals in each group. * $P < 0.05$, ** $P < 0.01$, *** $P < 0.001$ by ANOVA.

Closer examination of twelve-week-old Lepr KO^{VMH} mice showed that even at this age on a LF diet, these mice already have a significantly increased adipose mass. By 12 weeks, female Lepr KO^{VMH} mice have 65% more than adipose tissue than Lepr WT littermates. This suggests that, despite having similar weights, the glucose intolerance of Lepr KO^{VMH} mice may be secondary to the increased adiposity.

To determine if the glucose intolerance of twelve-week-old Lepr KO^{VMH} mice is a primary or secondary consequence to loss of VMH LEPRs, glucose homeostasis was examined in 4-week-old female Lepr KO^{VMH} mice, an age where no significant increase in body adipose is seen (data not shown). In the fed state, 4-week-old Lepr KO^{VMH} females are euglycemic despite having significantly elevated insulin levels (~two-fold, Figure 23A,B). In the fasting state (~12-16 hrs), Lepr KO^{VMH} mice trend towards hypoglycemia and hyperinsulinemia, through neither reaches statistical significance.

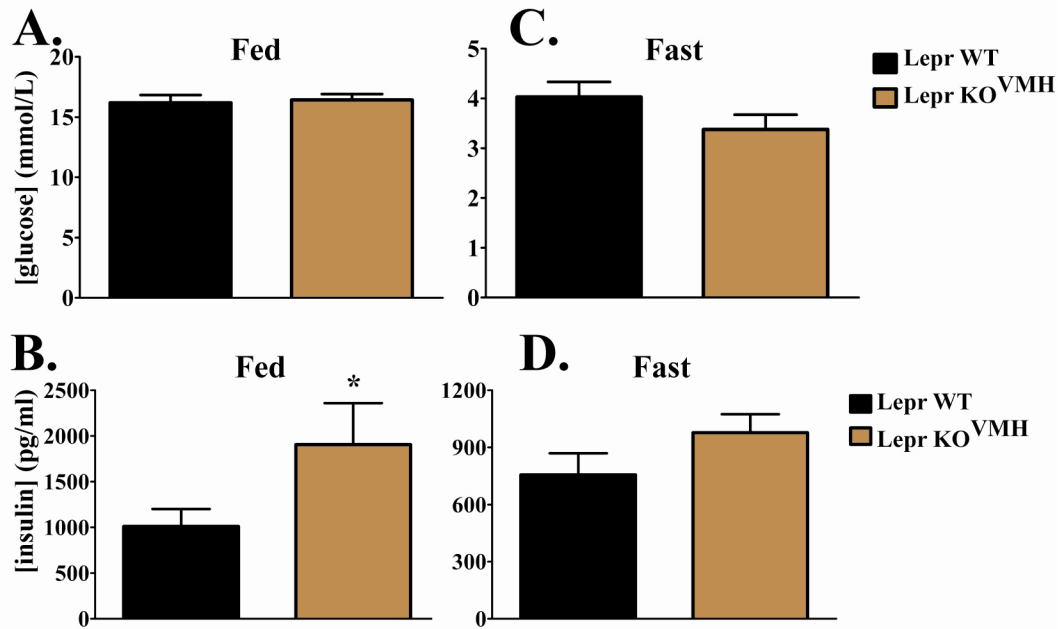


Figure 23. Fed and fasting glucose and insulin levels of Lepr KO^{VMH} mice. (A) Blood was drawn from the tail vein of four-week-old female Lepr KO^{VMH} and Lepr WT mice fed LF diet at 0900 hours in a fed state (A, B) or after a 16 hour fast (C, D). Glucose levels (A, C) were measured using a handheld glucometer and insulin levels were measured by ELISA. The results represent the mean ± S.E.M for at least seven animals in each group. Statistical significance was determined by two-way ANOVA. *P<0.05.

To further evaluate glucose homeostasis in Lepr KO^{VMH} mice, 4-week-old mice were subjected to GTTs (Figure 24). Interestingly, 4-week-old Lepr KO^{VMH} females had an improved glucose tolerance compared to their Lepr WT littermates (Figure 24A). In order to examine the reason for this improved glucose tolerance, plasma insulin levels were measured thirty minutes after a glucose bolus was given to a separate cohort of 4-week-old Lepr KO^{VMH} females. Consistent with the results of the GTT, Lepr KO^{VMH} females had significantly elevated levels of insulin thirty minutes after a glucose dose (Figure 24B).

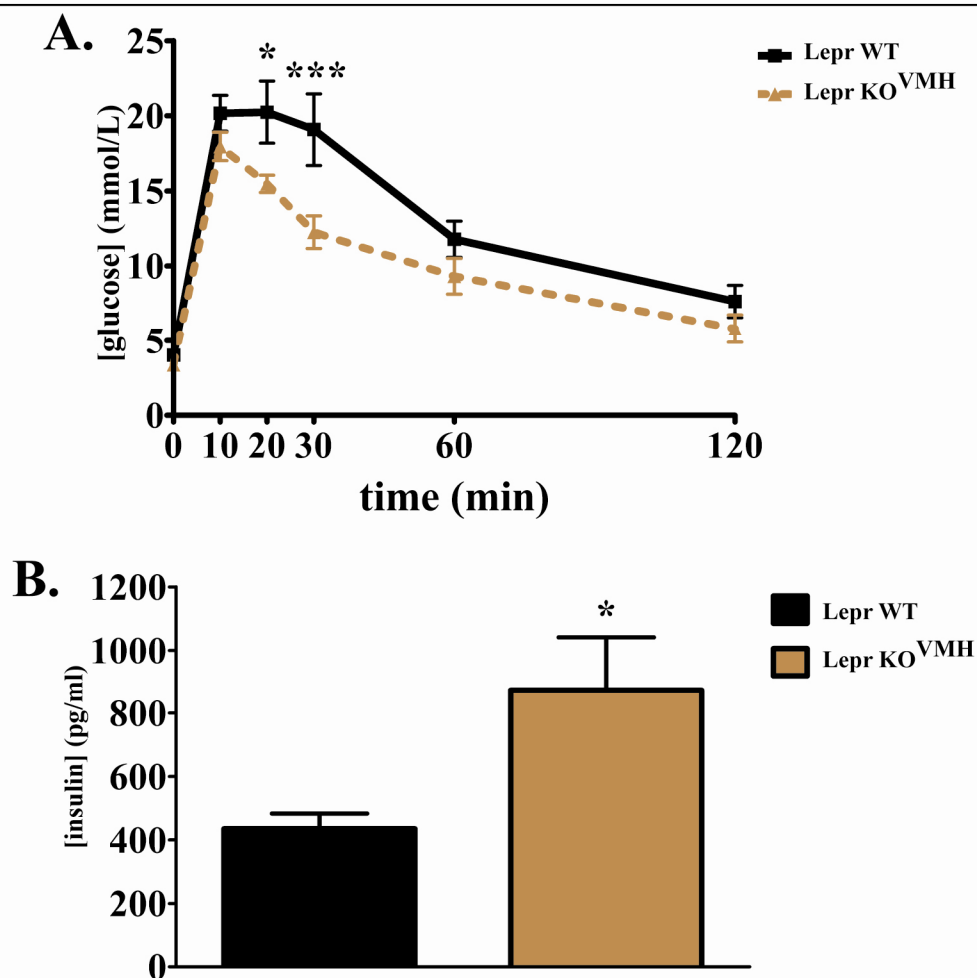


Figure 24. Glucose tolerance of weanling Lepr KO^{VMH} mice. (A) Four-week-old female Lepr KO^{VMH} (triangle) and Lepr WT (square) mice fed LF diet were fasted for 12-16 hours and given an i.p. bolus of glucose (1.5 mg per gram body weight). Whole blood glucose levels were measured thereafter. The results represent the mean \pm S.E.M for at least seven animals in each group. Statistical significance was determined by two-way analysis of variance (B) Four-week-old female Lepr KO^{VMH} and Lepr WT mice were given an i.p. bolus of glucose (1.5 mg per gram bodyweight). Thirty minutes after the injection blood was drawn and plasma insulin measured by ELISA. Results represent the mean \pm S.E.M of at least seven mice. Statistical significance was determined by unpaired two-tailed Student's t test. * $P < 0.05$, *** $P < 0.001$ by ANOVA.

CONCLUSION

Loss of LEPRs in the SF-1 positive neurons of the VMH results in a susceptibility to DIO. This susceptibility results from subtle defects in both food intake and energy expenditure. Unlike Lepr WT mice, Lepr KO^{VMH} mice fail to suppress food intake when transitioned from a LF to HF diet. Though the difference is small, the increased caloric consumption integrated over time, undoubtedly contributes to the increased fat stores of Lepr KO^{VMH} mice. As well, Lepr KO^{VMH} mice have defective adaptive thermogenic response. While Lepr WT mice increase their metabolic rate in response to a HF challenge, Lepr KO^{VMH} mice fail to do so. The failure of Lepr KO^{VMH} mice to modify food intake and metabolic expenditure in response to a high fat challenge results in a positive energy balance, increased adiposity, and obesity.

These studies demonstrate, however, that in addition to being susceptible to DIO, Lepr KO^{VMH} mice also exhibit a primary metabolic syndrome. This is supported by the fact that even when raised on a LF diet Lepr KO^{VMH} mice exhibit significantly increased adiposity – this in spite of there being no detectable differences in food intake or energy expenditure. That this increased adiposity is pathological is demonstrated by the mild steatosis and dyslipidemia of Lepr KO^{VMH} mice.

As well, Lepr KO^{VMH} mice show signs of abnormal glucose homeostasis. At 20 weeks of age, Lepr KO^{VMH} mice are hyperleptinemic and hyperinsulinemic. These mice are not overtly diabetic as they are able to maintain normal fed and fasting glucose levels. However, as early as 12 weeks of age, Lepr KO^{VMH} mice are glucose intolerant and have increased adipose mass. The hyperinsulinemia appears to be a primary result of inactivation of VMH LEPRs as it is detectible in weanling Lepr KO^{VMH} mice with very little body fat. Lepr KO^{VMH} mice appear not to have increased basal insulin secretion, as they are able to suppress insulin in response to fasting. Rather, the hyperinsulinemia of Lepr KO^{VMH} mice appears to be an exaggerated response to blood glucose levels – a postprandial hyperinsulinemia. Whether this hyperinsulinemia is a primary cause of the increased adiposity seen in Lepr KO^{VMH} mice, however, remains to be determined.

CHAPTER 5

Conclusions and Future Directions

CONCLUSIONS

Fifty years ago, the idea that obesity would become the largest threat to human health in the United States was unimaginable. Today, obesity has penetrated every socioeconomic level and brought with it the severe medical consequences of diabetes, hypertension, and cardiovascular disease. In response to this epidemic, the scientific community has become increasingly interested in understanding the physiology of energy homeostasis. The discovery of leptin and its receptor has greatly extended our understanding of central mechanisms governing these processes.

Despite much progress, however, it has become apparent in the recent years that we are just beginning to understand the complex neural circuitry through which leptin exerts its effects. While much attention has been given to the arcuate nucleus and the neural circuits that interface with it, our understanding of other leptin responsive regions of the brain is limited. In this report I show that LEPRs within the VMH play an important role in the adaptation to dietary fat. As well, LEPRs in the VMH contribute to the partitioning of energy stores, diverting calories away from fat storage and toward other uses.

Understanding the mechanisms by which leptin effects these changes in metabolism is certainly pertinent to human health and disease. Most obesity is a

result, not of monogenetic obesity syndromes, but an increase in caloric intake, particularly foods that are high in fat content. The study of DIO models, such as the *Lepr* KO^{VMH} mice, will lead to better understanding of gene-environment interactions and the role of such interactions in producing complex metabolic syndromes.

Other VMH leptin models

Using a genetic approach similar to that described here, Elmquist, Lowell, and colleagues reported that leptin acutely depolarized and increased the firing rate of neurons within the VMH and that mice lacking LEPRs within SF-1 neurons of the VMH were susceptible to DIO (Dhillon et al., 2006). Of considerable importance, the conditional *Lepr* allele and the SF-1 Cre transgene used in these studies were derived completely independently; in fact, the conditional *Lepr* allele used by the Dhillon et. al. flanks exons 17 and 17', again producing an apparent complete loss of function following Cre-mediated recombination. Given the use of completely independently-derived transgenic reagents, the close parallels between their results and this study, serve as a striking example of the utility of the Cre-loxP strategy to provide valid results regarding tissue-specific effects of gene disruption.

While the present study largely confirms the previous finding that *Lepr*s within the VMH mediate resistance to DIO, some differences between the two

studies should be noted. In the previous study, increased body weight was seen in Lepr KO^{VMH} mice fed a LF diet, while no increased body weight on the LF diet was observed here. Several explanations for this discrepancy may exist. First, the genetic backgrounds may account for some of the observed differences. While the previous report used mice with a mixed genetic background, mice used here were backcrossed onto a C57BL/6 background for at least five generations and thus may be considered congenic. C57BL/6J mice are themselves highly vulnerable to DIO (Alexander et al., 2006; Collins et al., 2004), which may explain why the weights of WT mice used in this study exceeded the weights of the KO mice used in the previous study, especially on a high fat diet.

Subtle differences in diets may also contribute to the differences in weight gain between the two studies. The previous study used a LF diet containing 12.5% kcal from fat, whereas here, a LF chow containing 9.5% kcal from fat was used. Given the sensitivity to DIO that these mice display, a 30% relative difference in dietary fat content may account for the discrepant results. Thus, on the LF diet used in this study, no detectible difference in food intake, energy expenditure, or body weight was detectible between Lepr KO^{VMH} and WT mice.

Comparison of Lepr KO^{VMH} and MC3R KO mice

Because leptin is known to regulate melanocortin signals in the arcuate nucleus, it is plausible that leptin might function in an analogous manner in the

VMH. Thus, it is interesting to note the similarities between the *Lepr* KO^{VMH} mice and melanocortin deficient mice, particularly the MC3R KO model. While MC4R deficient mice exhibit an obesity phenotype including hyperphagia, increased adiposity and linear growth, as well as sensitivity to increased dietary fat (Butler and Cone, 2003; Sutton et al., 2006), mice lacking MC3R exhibit a predominantly metabolic syndrome. Unlike the MC4R KO mice, MC3R mice show an obesity phenotype only in response to increased dietary fat (Chen et al., 2000; Sutton et al., 2006). Interestingly, MC3R mice fed a LF diet show dramatically increased fat mass in the face of limited weight gain – identical to the phenotype reported here for the *Lepr* KO^{VMH} mice (Butler et al., 2000; Sutton et al., 2006). Also similar to *Lepr* KO^{VMH} mice, MC3R KO mice are normophagic on LF diet, but become mildly hyperphagic when transitioned to HF diet (Butler, 2006). Butler reported that this diet induced hyperphagia was limited to the lights-on period, though this circadian effect was not investigated in *Lepr* KO^{VMH} mice. In addition, both *Lepr* KO^{VMH} mice and MC3R KO mice are hyperleptinemic and slightly hyperinsulinemic with normal corticosterone levels (Chen et al., 2000).

The role of MC3R in the regulation of locomotor movement remains unsettled. While one group reported decreased activity only in females (Chen et al., 2000), a separate group reported decreased activity only in males (Butler et al., 2000). As reported here, the role of VMH LEPRs on locomotor activity is also unclear. While some decreased locomotor activity was seen in male and female

Lepr KO^{VMH} mice, the differences failed to reach statistical significance. Further, the studies reported here were done using 12-week-old females that already showed significant increases in body fat content. Thus, differences in locomotor activity, if real, may be secondary to the decrease in lean body mass to body weight ratio and not a result of differential autonomic output in Lepr KO^{VMH} mice.

There are some noted differences between the phenotypes of MC3R KO and Lepr KO^{VMH} mice. Butler et al. reported a significant increase in the RER of MC3R mice transitioned to HF diet, indicating a defect in transitioning to fatty acid oxidation (Butler, 2006; Butler et al., 2000). Using the RER values of MC3R KO and WT mice, Butler showed MC3R mice have a positive fat balance (ratio of fat intake to fat oxidation) when fed a high fat diet. In contrast, Lepr KO^{VMH} mice, while failing to increase O₂ consumption in response to a HF challenge, lowered their RER normally. The RER phenotype in MC3R is subtle however, as it was observed by only one of the first two groups to describe the MC3R KO. Also, the RER effect seems to be very age and background dependent (Butler, 2006).

Hyperinsulinemia of Lepr KO^{VMH} mice

While it is generally accepted that increases in body adiposity lead to insulin resistance and hyperinsulinemia (Porte et al., 1998), others argue that hyperinsulinemia may, in some cases, be a causative factor of both obesity and

Type II diabetes mellitus. Several lines of evidence support this position. First, insulin significantly upregulates the rates of adipocytic and hepatic lipogenesis through both the long term expression of lipogenic genes and activation of lipogenic enzymes (Kersten, 2001). Rats fed a high glycemic diet had higher insulin secretion and higher body fat than those fed a low carbohydrate diet. As well, there is some evidence in humans that hyperinsulinemic states, especially postprandial hyperinsulinemia, early in life are predictive of future weight gain (Le Stunff and Bougneres, 1994; Sigal et al., 1997). In diabetic patients as well, insulin therapy tends to be associated with weight gain (Heller, 2004). Thus, proponents of this line of thinking would suggest that primary defects giving rise to hyperinsulinemia lead to increased adiposity which in turn, leads to a cycle of insulin resistance and increased insulin secretion in an attempt to maintain euglycemia. Unless broken, this cycle continues until decompensation occurs and overt diabetes results. Such evidence has led many to advocate, including some in academia, low-carbohydrate diets to temper the influence of insulin on weight gain (Foster et al., 2003; Samaha et al., 2003; Slyper, 2004; Wylie-Rosett et al., 2004). However, much of the evidence for insulin-induced obesity tends to be correlative and very controversial. Thus, the mechanistic relationship between hyperinsulinemia and obesity remains unclear and is an area of intense debate (Lara-Castro and Garvey, 2004; Porte et al., 1998).

A number of obese mouse models exhibit hyperinsulinemia. In *db/db* mice, hyperinsulinemia has been documented at a very early age, before the onset of hyperphagia and obesity (Coleman and Hummel, 1974). Hyperinsulinemia also occurs in *A^y*, MC3R, and MC4R KO mice, and as an acute response to pharmacologic antagonists of the melanocortin system (Chen et al., 2000; Huszar et al., 1997; Warbritton et al., 1994). As reported here, *Lepr* KO^{VMH} mice also exhibit hyperinsulinemia. This hyperinsulinemia is present at weaning and seems to be particularly associated with food intake. Though the mechanism of the hyperinsulinemia has not been demonstrated here, it is likely that the hyperinsulinemia is a primary effect from the loss of VMH LEPRs since the hyperinsulinemia precedes the increased adiposity. Regardless of mechanism, *Lepr* KO^{VMH} mice may prove to be an excellent model for studying the effect of hyperinsulinemia on obesity. This is especially true as *Lepr* KO^{VMH} mice do not exhibit the confounding hyperphagia that is present in many other models.

FUTURE DIRECTIONS

While this work has demonstrated that VMH LEPRs play an integral role in caloric partitioning and are necessary for the normal physiologic adaptations to dietary fat, the mechanisms by which leptin promotes these responses remain unexplored. It would be interesting to pursue several lines of investigation with regard to diet-induced thermogenesis in *Lepr* KO^{VMH} mice.

Diet-induced thermogenesis

Diet-induced thermogenesis, or the increase in energy expenditure in response to increased caloric intake, is mediated in part by the upregulation of mitochondrial uncoupling proteins (UCPs) within the brown adipose tissue of mice. UCP-1 expression and activity appear to be increased by sympathetic nerve activity and activation of β -adrenergic receptors on brown adipocytes (Cannon and Nedergaard, 2004; Lowell and Spiegelman, 2000). Several studies have shown that sympathetic nerve activity (SNA) is reduced in many models of obesity including *ob/ob* mice. Leptin increases the sympathetic nerve activity to brown adipose tissue while starvation reduces activity (Haynes et al., 1997). To conclusively demonstrate that *Lepr* KO^{VMH} mice have a defect in diet-induced thermogenesis, the SNA BAT could be measured using multifiber recording. This could be done on *Lepr* KO^{VMH} mice under several different conditions including LF and HF diet, and fasting. As well, *Lepr* KO^{VMH} and *Lepr* WT mice could be given injections of leptin, MTII (melanocortin agonist), or SHU9119 (melanocortin antagonist) and the response of their BAT SNA recorded. In order to examine a second modality of adaptive thermogenesis, the SNA of *Lepr* KO^{VMH} mice subjected to a cold challenge could also be measured. Cold, as with increases in caloric intake, has been shown to upregulate UCP activity and BAT thermogenesis (Lowell and Spiegelman, 2000). Finally, the expression of genes

involved in adaptive thermogenesis such as UCP-1, UCP-2, and PGC-1 α could be assessed by qRT-PCR in LF and HF fed Lepr KO^{VMH} and Lepr WT mice.

Lipogenesis

Lepr KO^{VMH} mice appear to have increased rates of lipogenesis, although this has not been empirically demonstrated in the current study. To evaluate the rate of lipogenesis, Lepr KO^{VMH} and Lepr WT mice would be given a dose of ³H₂O and the rate of ³H incorporation into fatty-acids can be determined as described previously (Hems et al., 1975). A similar experiment, using ¹⁴C-glucose could also be performed. Since the shuttling of glucose into fatty acid synthesis pathways is acutely an insulin-dependent process, this assay would not only assess rates of lipogenesis, but also the insulin sensitivity status of Lepr KO^{VMH} tissues. Therefore, it would be interesting to perform this experiment in both weanling and adult Lepr KO^{VMH} mice. Briefly, Lepr KO^{VMH} and Lepr WT mice would be given injections of a ¹⁴C-glucose tracer, both with and without a simultaneous bolus of D-glucose. After 30 minutes, WAT, BAT, liver and muscle could be resected, lipids extracted, and incorporation of ¹⁴C measured using a scintillation counter. For comparison, the incorporation of ¹⁴C into glycogen could also be assessed. Either experiment, ³H or ¹⁴C incorporation, could also be performed under conditions of pharmacological manipulation to assess the effect of leptin or melanocortins on the output. Finally, the expression of genes involved

lipogenesis including FAS, SREBP-1c, PPAR γ , PGC-1 α , DGAT, and SCD-1, should be assessed by qRT-PCR.

Neuronal Circuitry of VMH LEPRs – Role of MC3R

As mentioned above, the phenotype of the Lepr KO^{VMH} mice closely resembles that of the MC3R KO mice. In addition, MC3R is highly expressed in the VMH. It is easy to speculate therefore, that MC3R is downstream of VMH leptin signaling. However, with the tools now available, it is technically difficult to assess this possible relationship. First, there are no good antibodies for either MC3R or LEPR, though pSTAT3 can be used as a good surrogate for LEPR activity. This makes histological examination of any spatial relationship difficult. In addition, the mechanism of leptin action in the VMH is unknown; specifically, does leptin regulate the levels of melanocortin ligands, or given the expression of MC3R in the VMH, does it regulate the expression of the receptor itself?

This last question may be addressed using *in situ* expression analysis of *Mc3r*. This may be done under several conditions including LF and HF diet, and fasting. In Lepr WT mice one would expect, if leptin regulates the *Mc3r* expression, that expression levels would be lower in mice fasted or fed a LF diet. HF diet, with its resulting hyperleptinemia, should result in increased levels of *Mc3r* expression. Perhaps more informative would be to compare the expression levels in Lepr KO^{VMH} and Lepr WT mice given exogenous leptin injections.

Functional assessment of melanocortin involvement in VMH LEPR signaling may be approached using pharmacologic techniques. If differences were observed in the rates of lipogenesis, as assessed by the radiolabeling experiments outlined above, these assays may prove useful as readout of melanocortin stimulation and/or inhibition. If loss of LEPR signaling in the VMH creates a functional blockade in melanocortin signaling, the administration of MTII may be able to rescue the phenotype of *Lepr* KO^{VMH} mice, reducing the incorporation of radiolabel into lipid. Unfortunately, MTII is a non-specific melanocortin agonist and would therefore also stimulate MC4R. This may complicate the interpretation of any results and comparisons may need to be made with MC4R and MC3R KO mice to tease out MC3R-specific effects. However, perhaps the best evidence of MC3R role in the VMH could come from a VMH-specific knockout of *Mc3r*. This could readily be accomplished by crossing the SF-1/Cre transgenic mouse described here with a conditional, floxed allele of *Mc3r*. An MC3R KO^{VMH} mouse with a phenotype similar to the *Lepr* KO^{VMH} mouse would be strong evidence that leptin signaling through the VMH is mediated, at least in part, through MC3R.

Hyperinsulinemia

Given the proverbial chicken-and-egg controversy of hyperinsulinemia and obesity, it would be interesting to evaluate the role of hyperinsulinemia in the development of the *Lepr* KO^{VMH} adiposity. Inoue et al. demonstrated that

transplantation of pancreatic β -cells into chemically-induced diabetic rats, prevented the hyperinsulinemia and development of obesity in VMH lesioned rats. A similar experiment could be tried with the Lepr KO^{VMH} mice. Lepr KO^{VMH} mice would be given an injection of streptozotocin, which destroys pancreatic β -cells. Subsequently, isolated β -cells from a WT mouse could be placed under the renal capsule. This experiment could be used to answer two questions regarding glucose homeostasis in Lepr KO^{VMH} mice. First, if done in young mice, it could demonstrate whether the enhanced postprandial insulin secretion is neurally mediated. Second, by following β -cell transplanted Lepr KO^{VMH} mice, the role of insulin in the development of adiposity may be assessed. If such an experiment were to prove technically feasible, one could also repeat the ¹⁴C-labeled glucose experiments mentioned above to evaluate the role of postprandial hyperinsulinemia in the partitioning of glucose into fat stores.

Other gene knockouts

In conclusion, Lepr KO^{VMH} mice are a new genetic model of obesity which exhibits a mild metabolic syndrome including increased adiposity, mild steatosis, dyslipidemia, hyperinsulinemia, and aberrant adaptive thermogenesis. These mice should prove useful in further investigating the region-specific role of leptin as a master regulator of energy homeostasis and metabolism.

In addition, the SF-1/Cre transgenic mice should also prove useful for future work, both as a tool for VMH gene knockouts and for investigating the role of a variety of genes in the adrenal and gonads. Indeed, several such studies are currently in progress and knockouts of β -catenin, LXR, FXR, and FGFR2 are being evaluated. The resulting animal models should provide greater insight into a number of systems responsible for regulating animal physiology and development.

BIBLIOGRAPHY

- Adage, T., Scheurink, A.J., de Boer, S.F., de Vries, K., Konsman, J.P., Kuipers, F., Adan, R.A., Baskin, D.G., Schwartz, M.W., and van Dijk, G. (2001). Hypothalamic, metabolic, and behavioral responses to pharmacological inhibition of CNS melanocortin signaling in rats. *J Neurosci* 21, 3639-3645.
- Ahima, R.S., and Hileman, S.M. (2000). Postnatal regulation of hypothalamic neuropeptide expression by leptin: implications for energy balance and body weight regulation. *Regul Pept* 92, 1-7.
- Ahima, R.S., and Osei, S.Y. (2004). Leptin signaling. *Physiol Behav* 81, 223-241.
- Ahima, R.S., Prabakaran, D., Mantzoros, C., Qu, D., Lowell, B., Maratos-Flier, E., and Flier, J.S. (1996). Role of leptin in the neuroendocrine response to fasting. *Nature* 382, 250-252.
- Ahlskog, J.E., and Hoebel, B.G. (1973). Overeating and obesity from damage to a noradrenergic system in the brain. *Science* 182, 166-169.
- Alexander, J., Chang, G.Q., Dourmashkin, J.T., and Leibowitz, S.F. (2006). Distinct phenotypes of obesity-prone AKR/J, DBA2J and C57BL/6J mice compared to control strains. *Int J Obes* 30, 50-59.
- Allison, D.B., Kaprio, J., Korkeila, M., Koskenvuo, M., Neale, M.C., and Hayakawa, K. (1996). The heritability of body mass index among an international sample of monozygotic twins reared apart. *Int J Obes Relat Metab Disord* 20, 501-506.
- Altman, J., and Bayer, S.A. (1986). The development of the rat hypothalamus. *Adv Anat Embryol Cell Biol* 100, 1-178.
- Anand, B.K., and Brobeck, J.R. (1951). Hypothalamic control of food intake in rats and cats. *Yale J Biol Med* 24, 123-140.
- Aravich, P.F., and Sclafani, A. (1983). Paraventricular hypothalamic lesions and medial hypothalamic knife cuts produce similar hyperphagia syndromes. *Behav Neurosci* 97, 970-983.

- Bailey, P., and Bremer, F. (1921). Experimental diabetes insipidus. *Arch Intern Med* 28, 773-803.
- Balthasar, N., Coppari, R., McMinn, J., Liu, S.M., Lee, C.E., Tang, V., Kenny, C.D., McGovern, R.A., Chua, S.C., Jr., Elmquist, J.K., *et al.* (2004). Leptin receptor signaling in POMC neurons is required for normal body weight homeostasis. *Neuron* 42, 983-991.
- Banks, W.A., McLay, R.N., Kastin, A.J., Sarmiento, U., and Scully, S. (1999). Passage of leptin across the blood-testis barrier. *Am J Physiol* 276, E1099-1104.
- Bates, M.W., Nauss, S.F., Hagman, N.C., and Mayer, J. (1955). Fat metabolism in three forms of experimental obesity; body composition. *Am J Physiol* 180, 301-303.
- Bernardis, L.L., and Skelton, F.R. (1965). Growth and obesity following ventromedial hypothalamic lesions placed in female rats at four different ages. *Neuroendocrinology* 1, 265-275.
- Bingham, N.C., Verma-Kurvari, S., Parada, L.F., and Parker, K.L. (2006). Development of a steroidogenic factor 1/Cre transgenic mouse line. *Genesis* 44, 419-424.
- Bjorbaek, C., El-Haschimi, K., Frantz, J.D., and Flier, J.S. (1999). The role of SOCS-3 in leptin signaling and leptin resistance. *J Biol Chem* 274, 30059-30065.
- Bjorbaek, C., Uotani, S., da Silva, B., and Flier, J.S. (1997). Divergent signaling capacities of the long and short isoforms of the leptin receptor. *J Biol Chem* 272, 32686-32695.
- Bogerd, A.M., Franklin, A., Rice, D.A., Schimmer, B.P., and Parker, K.L. (1990). Identification and characterization of two upstream elements that regulate adrenocortical expression of steroid 11 beta-hydroxylase. *Mol Endocrinol* 4, 845-850.
- Borg, W.P., During, M.J., Sherwin, R.S., Borg, M.A., Brines, M.L., and Shulman, G.I. (1994). Ventromedial hypothalamic lesions in rats suppress counterregulatory responses to hypoglycemia. *J Clin Invest* 93, 1677-1682.

- Borg, W.P., Sherwin, R.S., During, M.J., Borg, M.A., and Shulman, G.I. (1995). Local ventromedial hypothalamus glucopenia triggers counterregulatory hormone release. *Diabetes* 44, 180-184.
- Borszcz, G.S. (2006). Contribution of the ventromedial hypothalamus to generation of the affective dimension of pain. *Pain* 123, 155-168.
- Branda, C.S., and Dymecki, S.M. (2004). Talking about a revolution: The impact of site-specific recombinases on genetic analyses in mice. *Dev Cell* 6, 7-28.
- Brobeck, J.R., Tepperman, J., and Long, C.N.H. (1943). Experimental hypothalamic hyperphagia in the albino rat. *Yale J Biol Med* 15, 831-853.
- Buettner, C., Poci, A., Muse, E.D., Etgen, A.M., Myers, M.G., Jr., and Rossetti, L. (2006). Critical role of STAT3 in leptin's metabolic actions. *Cell metabolism* 4, 49-60.
- Bultman, S.J., Michaud, E.J., and Woychik, R.P. (1992). Molecular characterization of the mouse agouti locus. *Cell* 71, 1195-1204.
- Butler, A.A. (2006). The melanocortin system and energy balance. *Peptides* 27, 281-290.
- Butler, A.A., and Cone, R.D. (2003). Knockout studies defining different roles for melanocortin receptors in energy homeostasis. *Ann N Y Acad Sci* 994, 240-245.
- Butler, A.A., Kesterson, R.A., Khong, K., Cullen, M.J., Pelleymounter, M.A., Dekoning, J., Baetscher, M., and Cone, R.D. (2000). A unique metabolic syndrome causes obesity in the melanocortin-3 receptor-deficient mouse. *Endocrinology* 141, 3518-3521.
- Campfield, L.A. (2000). Central mechanisms responsible for the actions of OB protein (leptin) on food intake, metabolism and body energy storage. *Front Horm Res* 26, 12-20.
- Campfield, L.A., Smith, F.J., Guisez, Y., Devos, R., and Burn, P. (1995). Recombinant mouse OB protein: evidence for a peripheral signal linking adiposity and central neural networks. *Science* 269, 546-549.

- Cannon, B., and Nedergaard, J. (2004). Brown adipose tissue: function and physiological significance. *Physiol Rev* 84, 277-359.
- Canteras, N.S., Simerly, R.B., and Swanson, L.W. (1994). Organization of projections from the ventromedial nucleus of the hypothalamus: a *Phaseolus vulgaris*-leucoagglutinin study in the rat. *J Comp Neurol* 348, 41-79.
- Carpenter, K.M., Hasin, D.S., Allison, D.B., and Faith, M.S. (2000). Relationships between obesity and DSM-IV major depressive disorder, suicide ideation, and suicide attempts: results from a general population study. *Am J Public Health* 90, 251-257.
- Chateau, D., Plas-Roser, S., and Aron, C. (1981). Follicular growth, ovulatory phenomena and ventromedial nucleus lesions in the rat. *Endokrinologie* 77, 257-268.
- Chehab, F.F., Lim, M.E., and Lu, R. (1996). Correction of the sterility defect in homozygous obese female mice by treatment with the human recombinant leptin. *Nat Genet* 12, 318-320.
- Chehab, F.F., Mounzih, K., Lu, R., and Lim, M.E. (1997). Early onset of reproductive function in normal female mice treated with leptin. *Science* 275, 88-90.
- Chen, A.S., Marsh, D.J., Trumbauer, M.E., Frazier, E.G., Guan, X.M., Yu, H., Rosenblum, C.I., Vongs, A., Feng, Y., Cao, L., *et al.* (2000). Inactivation of the mouse melanocortin-3 receptor results in increased fat mass and reduced lean body mass. *Nat Genet* 26, 97-102.
- Chen, G., Koyama, K., Yuan, X., Lee, Y., Zhou, Y.T., O'Doherty, R., Newgard, C.B., and Unger, R.H. (1996). Disappearance of body fat in normal rats induced by adenovirus-mediated leptin gene therapy. *Proc Natl Acad Sci U S A* 93, 14795-14799.
- Chen, P., Li, C., Haskell-Luevano, C., Cone, R.D., and Smith, M.S. (1999). Altered expression of agouti-related protein and its colocalization with neuropeptide Y in the arcuate nucleus of the hypothalamus during lactation. *Endocrinology* 140, 2645-2650.

- Cheung, C.C., Clifton, D.K., and Steiner, R.A. (1997). Proopiomelanocortin neurons are direct targets for leptin in the hypothalamus. *Endocrinology* 138, 4489-4492.
- Choi, G.B., Dong, H.W., Murphy, A.J., Valenzuela, D.M., Yancopoulos, G.D., Swanson, L.W., and Anderson, D.J. (2005). Lhx6 delineates a pathway mediating innate reproductive behaviors from the amygdala to the hypothalamus. *Neuron* 46, 647-660.
- Chua, S.C., Jr., Chung, W.K., Wu-Peng, X.S., Zhang, Y., Liu, S.M., Tartaglia, L., and Leibel, R.L. (1996). Phenotypes of mouse diabetes and rat fatty due to mutations in the OB (leptin) receptor. *Science* 271, 994-996.
- Clark, J.T., Kalra, P.S., Crowley, W.R., and Kalra, S.P. (1984). Neuropeptide Y and human pancreatic polypeptide stimulate feeding behavior in rats. *Endocrinology* 115, 427-429.
- Cohen, P., Zhao, C., Cai, X., Montez, J.M., Rohani, S.C., Feinstein, P., Mombaerts, P., and Friedman, J.M. (2001). Selective deletion of leptin receptor in neurons leads to obesity. *J Clin Invest* 108, 1113-1121.
- Cohen, R.S., and Pfaff, D.W. (1992). Ventromedial hypothalamic neurons in the mediation of long-lasting effects of estrogen on lordosis behavior. *Prog Neurobiol* 38, 423-453.
- Coleman, D.L. (1973). Effects of parabiosis of obese with diabetes and normal mice. *Diabetologia* 9, 294-298.
- Coleman, D.L., and Hummel, K.P. (1967). Studies with the mutation, diabetes, in the mouse. *Diabetologia* 3, 238-248.
- Coleman, D.L., and Hummel, K.P. (1969). Effects of parabiosis of normal with genetically diabetic mice. *Am J Physiol* 217, 1298-1304.
- Coleman, D.L., and Hummel, K.P. (1974). Hyperinsulinemia in pre-weaning diabetes (db) mice. *Diabetologia* 10 Suppl, 607-610.
- Collins, S., Martin, T.L., Surwit, R.S., and Robidoux, J. (2004). Genetic vulnerability to diet-induced obesity in the C57BL/6J mouse: physiological and molecular characteristics. *Physiol Behav* 81, 243-248.

- Cone, R.D. (2005). Anatomy and regulation of the central melanocortin system. *Nat Neurosci* 8, 571-578.
- Cowley, M.A., Pronchuk, N., Fan, W., Dinulescu, D.M., Colmers, W.F., and Cone, R.D. (1999). Integration of NPY, AGRP, and melanocortin signals in the hypothalamic paraventricular nucleus: evidence of a cellular basis for the adipostat. *Neuron* 24, 155-163.
- Cowley, M.A., Smart, J.L., Rubinstein, M., Cerdan, M.G., Diano, S., Horvath, T.L., Cone, R.D., and Low, M.J. (2001). Leptin activates anorexigenic POMC neurons through a neural network in the arcuate nucleus. *Nature* 411, 480-484.
- Cox, J.E., and Powley, T.L. (1977). Development of obesity in diabetic mice paired with lean siblings. *J Comp Physiol Psychol* 91, 347-358.
- Cullinan, W.E., and Zaborszky, L. (1991). Organization of ascending hypothalamic projections to the rostral forebrain with special reference to the innervation of cholinergic projection neurons. *J Comp Neurol* 306, 631-667.
- Cummings, D.E., and Schwartz, M.W. (2000). Melanocortins and body weight: a tale of two receptors. *Nat Genet* 26, 8-9.
- Dellovade, T.L., Young, M., Ross, E.P., Henderson, R., Caron, K., Parker, K., and Tobet, S.A. (2000). Disruption of the gene encoding SF-1 alters the distribution of hypothalamic neuronal phenotypes. *J Comp Neurol* 423, 579-589.
- Dhillon, H., Zigman, J.M., Ye, C., Lee, C.E., McGovern, R.A., Tang, V., Kenny, C.D., Christiansen, L.M., White, R.D., Edelstein, E.A., *et al.* (2006). Leptin Directly Activates SF1 Neurons in the VMH, and This Action by Leptin Is Required for Normal Body-Weight Homeostasis. *Neuron* 49, 191-203.
- Dielenberg, R.A., Hunt, G.E., and McGregor, I.S. (2001). "When a rat smells a cat": the distribution of Fos immunoreactivity in rat brain following exposure to a predatory odor. *Neuroscience* 104, 1085-1097.

- Elmquist, J.K., Ahima, R.S., Elias, C.F., Flier, J.S., and Saper, C.B. (1998a). Leptin activates distinct projections from the dorsomedial and ventromedial hypothalamic nuclei. *Proc Natl Acad Sci U S A* 95, 741-746.
- Elmquist, J.K., Bjorbaek, C., Ahima, R.S., Flier, J.S., and Saper, C.B. (1998b). Distributions of leptin receptor mRNA isoforms in the rat brain. *J Comp Neurol* 395, 535-547.
- Emery, D.E., and Moss, R.L. (1984). Lesions confined to the ventromedial hypothalamus decrease the frequency of coital contacts in female rats. *Horm Behav* 18, 313-329.
- Fan, W., Boston, B.A., Kesterson, R.A., Hruby, V.J., and Cone, R.D. (1997). Role of melanocortinergic neurons in feeding and the agouti obesity syndrome. *Nature* 385, 165-168.
- Fei, H., Okano, H.J., Li, C., Lee, G.H., Zhao, C., Darnell, R., and Friedman, J.M. (1997). Anatomic localization of alternatively spliced leptin receptors (Ob-R) in mouse brain and other tissues. *Proc Natl Acad Sci U S A* 94, 7001-7005.
- Flegal, K.M., Carroll, M.D., Ogden, C.L., and Johnson, C.L. (2002). Prevalence and trends in obesity among US adults, 1999-2000. *JAMA* 288, 1723-1727.
- Foster, G.D., Wyatt, H.R., Hill, J.O., McGuckin, B.G., Brill, C., Mohammed, B.S., Szapary, P.O., Rader, D.J., Edman, J.S., and Klein, S. (2003). A randomized trial of a low-carbohydrate diet for obesity. *N Engl J Med* 348, 2082-2090.
- Friedman, J.M. (2004). Modern science versus the stigma of obesity. *Nat Med* 10, 563-569.
- Fuchs, S.A., Edinger, H.M., and Siegel, A. (1985a). The organization of the hypothalamic pathways mediating affective defense behavior in the cat. *Brain Res* 330, 77-92.
- Fuchs, S.A., Edinger, H.M., and Siegel, A. (1985b). The role of the anterior hypothalamus in affective defense behavior elicited from the ventromedial hypothalamus of the cat. *Brain Res* 330, 93-107.

- Gantz, I., Konda, Y., Tashiro, T., Shimoto, Y., Miwa, H., Munzert, G., Watson, S.J., DelValle, J., and Yamada, T. (1993a). Molecular cloning of a novel melanocortin receptor. *J Biol Chem* 268, 8246-8250.
- Gantz, I., Miwa, H., Konda, Y., Shimoto, Y., Tashiro, T., Watson, S.J., DelValle, J., and Yamada, T. (1993b). Molecular cloning, expression, and gene localization of a fourth melanocortin receptor. *J Biol Chem* 268, 15174-15179.
- Ghilardi, N., Ziegler, S., Wiestner, A., Stoffel, R., Heim, M.H., and Skoda, R.C. (1996). Defective STAT signaling by the leptin receptor in diabetic mice. *Proc Natl Acad Sci U S A* 93, 6231-6235.
- Giraldo, P., and Montoliu, L. (2001). Size matters: use of YACs, BACs and PACs in transgenic animals. *Transgenic Res* 10, 83-103.
- Gold, R.M. (1973). Hypothalamic obesity: the myth of the ventromedial nucleus. *Science* 182, 488-490.
- Gossen, M., and Bujard, H. (2002). Studying gene function in eukaryotes by conditional gene inactivation. *Annu Rev Genet* 36, 153-173.
- Hakansson, M.L., Brown, H., Ghilardi, N., Skoda, R.C., and Meister, B. (1998). Leptin receptor immunoreactivity in chemically defined target neurons of the hypothalamus. *J Neurosci* 18, 559-572.
- Halaas, J.L., Gajiwala, K.S., Maffei, M., Cohen, S.L., Chait, B.T., Rabinowitz, D., Lallone, R.L., Burley, S.K., and Friedman, J.M. (1995). Weight-reducing effects of the plasma protein encoded by the obese gene. *Science* 269, 543-546.
- Han, P.W., Lin, C.H., Chu, K.C., Mu, J.Y., and Liu, A.C. (1965). Hypothalamic obesity in weanling rats. *Am J Physiol* 209, 627-631.
- Hatano, O., Takakusu, A., Nomura, M., and Morohashi, K. (1996). Identical origin of adrenal cortex and gonad revealed by expression profiles of Ad4BP/SF-1. *Genes Cells* 1, 663-671.
- Haynes, W.G., Morgan, D.A., Walsh, S.A., Mark, A.L., and Sivitz, W.I. (1997). Receptor-mediated regional sympathetic nerve activation by leptin. *J Clin Invest* 100, 270-278.

- Heintz, N. (2000). Analysis of mammalian central nervous system gene expression and function using bacterial artificial chromosome-mediated transgenesis. *Hum Mol Genet* 9, 937-943.
- Heller, S. (2004). Weight gain during insulin therapy in patients with type 2 diabetes mellitus. *Diabetes Res Clin Pract* 65 *Suppl 1*, S23-27.
- Hems, D.A., Rath, E.A., and Verrinder, T.R. (1975). Fatty acid synthesis in liver and adipose tissue of normal and genetically obese (ob/ob) mice during the 24-hour cycle. *Biochem J* 150, 167-173.
- Herberg, L., and Coleman, D.L. (1977). Laboratory animals exhibiting obesity and diabetes syndromes. *Metabolism* 26, 59-99.
- Hervey, G.R. (1959). The effects of lesions in the hypothalamus in parabiotic rats. *J Physiol* 145, 336-352.
- Hetherington, A.W., and Ranson, S.W. (1940). Hypothalamic lesions and adiposity in the rat. *Anat Rec* 78, 149-172.
- Hetherington, A.W., and Ranson, S.W. (1941). The relation of various hypothalamic lesions to adiposity and other phenomena in the rat. *Am J Physiol* 133, 326-327.
- Hetherington, A.W., and Ranson, S.W. (1942a). Effect of early hypophysectomy on hypothalamic obesity. *Endocrinology* 31, 30-34.
- Hetherington, A.W., and Ranson, S.W. (1942b). The relation of various hypothalamic lesions to adiposity in the rat. *J Comp Neurol* 76, 475-499.
- Hetherington, A.W., and Ranson, S.W. (1944). Non-production of hypothalamic obesity in the rat by lesions rostral or dorsal to the ventro-medial hypothalamic nuclei. *J Comp Neurol* 80, 33-45.
- Hirasawa, M., Nishihara, M., and Takahashi, M. (1996a). Neural activity in the VMH associated with suppression of the circulatory system in rats. *Physiol Behav* 59, 1017-1023.

- Hirasawa, M., Nishihara, M., and Takahashi, M. (1996b). The rostral ventrolateral medulla mediates suppression of the circulatory system by the ventromedial nucleus of the hypothalamus. *Brain Res* 724, 186-190.
- Hoggard, N., Mercer, J.G., Rayner, D.V., Moar, K., Trayhurn, P., and Williams, L.M. (1997). Localization of leptin receptor mRNA splice variants in murine peripheral tissues by RT-PCR and in situ hybridization. *Biochem Biophys Res Commun* 232, 383-387.
- Hubschle, T., Thom, E., Watson, A., Roth, J., Klaus, S., and Meyerhof, W. (2001). Leptin-induced nuclear translocation of STAT3 immunoreactivity in hypothalamic nuclei involved in body weight regulation. *J Neurosci* 21, 2413-2424.
- Hughes, A.M., and Tolbert, B.M. (1958). Oxidation of acetate, glucose, or glycine to carbon dioxide in mice exhibiting the hereditary obesity syndrome. *J Biol Chem* 231, 339-345.
- Hummel, K.P., Dickie, M.M., and Coleman, D.L. (1966). Diabetes, a new mutation in the mouse. *Science* 153, 1127-1128.
- Huszar, D., Lynch, C.A., Fairchild-Huntress, V., Dunmore, J.H., Fang, Q., Berkemeier, L.R., Gu, W., Kesterson, R.A., Boston, B.A., Cone, R.D., *et al.* (1997). Targeted disruption of the melanocortin-4 receptor results in obesity in mice. *Cell* 88, 131-141.
- Ikeda, Y., Lala, D.S., Luo, X., Kim, E., Moisan, M.P., and Parker, K.L. (1993). Characterization of the mouse FTZ-F1 gene, which encodes a key regulator of steroid hydroxylase gene expression. *Mol Endocrinol* 7, 852-860.
- Ikeda, Y., Luo, X., Abbud, R., Nilson, J.H., and Parker, K.L. (1995). The nuclear receptor steroidogenic factor 1 is essential for the formation of the ventromedial hypothalamic nucleus. *Mol Endocrinol* 9, 478-486.
- Ikeda, Y., Shen, W.H., Ingraham, H.A., and Parker, K.L. (1994). Developmental expression of mouse steroidogenic factor-1, an essential regulator of the steroid hydroxylases. *Mol Endocrinol* 8, 654-662.
- Ingalls, A.M., Dickie, M.M., and Snell, G.D. (1996). Obese, a new mutation in the house mouse. *Obes Res* 4, 101.

- Joseph, S.A., and Knigge, K.M. (1968). Effects of VMH lesions in adult and newborn guinea pigs. *Neuroendocrinology* 3, 309-331.
- Karpova, T., Presley, J., Manimaran, R.R., Scherrer, S.P., Tejada, L., Peterson, K.R., and Heckert, L.L. (2005). A FTZ-F1-containing yeast artificial chromosome recapitulates expression of steroidogenic factor 1 in vivo. *Mol Endocrinol* 19, 2549-2563.
- Kennedy, G.C. (1950). The hypothalamic control of food intake in rats. *Proc R Soc Lond B Biol Sci* 137, 535-549.
- Kennedy, G.C. (1953). The role of depot fat in the hypothalamic control of food intake in the rat. *Proc R Soc Lond B Biol Sci* 140, 578-596.
- Kersten, S. (2001). Mechanisms of nutritional and hormonal regulation of lipogenesis. *EMBO Rep* 2, 282-286.
- King, B.M. (2006). The rise, fall, and resurrection of the ventromedial hypothalamus in the regulation of feeding behavior and body weight. *Physiol Behav* 87, 221-244.
- Kloek, C., Haq, A.K., Dunn, S.L., Lavery, H.J., Banks, A.S., and Myers, M.G., Jr. (2002). Regulation of Jak kinases by intracellular leptin receptor sequences. *J Biol Chem* 277, 41547-41555.
- Lara-Castro, C., and Garvey, W.T. (2004). Diet, insulin resistance, and obesity: zoning in on data for Atkins dieters living in South Beach. *J Clin Endocrinol Metab* 89, 4197-4205.
- Le Stunff, C., and Bougneres, P. (1994). Early changes in postprandial insulin secretion, not in insulin sensitivity, characterize juvenile obesity. *Diabetes* 43, 696-702.
- Lee, G.H., Proenca, R., Montez, J.M., Carroll, K.M., Darvishzadeh, J.G., Lee, J.I., and Friedman, J.M. (1996). Abnormal splicing of the leptin receptor in diabetic mice. *Nature* 379, 632-635.
- Leedy, M.G., and Hart, B.L. (1985). Female and male sexual responses in female cats with ventromedial hypothalamic lesions. *Behav Neurosci* 99, 936-941.

- Leibowitz, S.F., Hammer, N.J., and Chang, K. (1981). Hypothalamic paraventricular nucleus lesions produce overeating and obesity in the rat. *Physiol Behav* 27, 1031-1040.
- Levin, B.E., Dunn-Meynell, A.A., and Routh, V.H. (1999). Brain glucose sensing and body energy homeostasis: role in obesity and diabetes. *Am J Physiol* 276, R1223-1231.
- Levin, N., Nelson, C., Gurney, A., Vandlen, R., and de Sauvage, F. (1996). Decreased food intake does not completely account for adiposity reduction after ob protein infusion. *Proc Natl Acad Sci U S A* 93, 1726-1730.
- Lewandoski, M. (2001). Conditional control of gene expression in the mouse. *Nat Rev Genet* 2, 743-755.
- Loten, E.G., Rabinovitch, A., and Jeanrenaud, B. (1974). In vivo studies on lipogenesis in obese hyperglycaemic (ob-ob) mice: possible role of hyperinsulinaemia. *Diabetologia* 10, 45-52.
- Lowell, B.B., and Spiegelman, B.M. (2000). Towards a molecular understanding of adaptive thermogenesis. *Nature* 404, 652-660.
- Lu, D., Willard, D., Patel, I.R., Kadwell, S., Overton, L., Kost, T., Luther, M., Chen, W., Woychik, R.P., Wilkison, W.O., *et al.* (1994). Agouti protein is an antagonist of the melanocyte-stimulating-hormone receptor. *Nature* 371, 799-802.
- Luo, X., Ikeda, Y., Lala, D., Rice, D., Wong, M., and Parker, K.L. (1999). Steroidogenic factor 1 (SF-1) is essential for endocrine development and function. *J Steroid Biochem Mol Biol* 69, 13-18.
- Luo, X., Ikeda, Y., and Parker, K.L. (1994). A cell-specific nuclear receptor is essential for adrenal and gonadal development and sexual differentiation. *Cell* 77, 481-490.
- Majdic, G., Young, M., Gomez-Sanchez, E., Anderson, P., Szczepaniak, L.S., Dobbins, R.L., McGarry, J.D., and Parker, K.L. (2002). Knockout mice lacking steroidogenic factor 1 are a novel genetic model of hypothalamic obesity. *Endocrinology* 143, 607-614.

- Marks, D.L., and Cone, R.D. (2001). Central melanocortins and the regulation of weight during acute and chronic disease. *Recent Prog Horm Res* 56, 359-375.
- Matkovic, V., Ilich, J.Z., Badenhop, N.E., Skugor, M., Clairmont, A., Klisovic, D., and Landoll, J.D. (1997). Gain in body fat is inversely related to the nocturnal rise in serum leptin level in young females. *J Clin Endocrinol Metab* 82, 1368-1372.
- Mayer, J. (1952). The glucostatic theory of regulation of food intake and the problem of obesity. *Bull New Engl Med Cent* 14, 43-49.
- Mayer, J. (1955). Regulation of energy intake and the body weight: the glucostatic theory and the lipostatic hypothesis. *Ann N Y Acad Sci* 63, 15-43.
- McClellan, K.M., Parker, K.L., and Tobet, S. (2006). Development of the ventromedial nucleus of the hypothalamus. *Front Neuroendocrinol*.
- Melanson, K.J., Westerterp-Plantenga, M.S., Saris, W.H., Smith, F.J., and Campfield, L.A. (1999). Blood glucose patterns and appetite in time-blinded humans: carbohydrate versus fat. *Am J Physiol* 277, R337-345.
- Mercer, J.G., Hoggard, N., Williams, L.M., Lawrence, C.B., Hannah, L.T., Morgan, P.J., and Trayhurn, P. (1996). Coexpression of leptin receptor and preproneuropeptide Y mRNA in arcuate nucleus of mouse hypothalamus. *J Neuroendocrinol* 8, 733-735.
- Miller, M.W., Duhl, D.M., Vrieling, H., Cordes, S.P., Ollmann, M.M., Winkes, B.M., and Barsh, G.S. (1993). Cloning of the mouse agouti gene predicts a secreted protein ubiquitously expressed in mice carrying the lethal yellow mutation. *Genes Dev* 7, 454-467.
- Mizuno, T.M., Makimura, H., Silverstein, J., Roberts, J.L., Lopingco, T., and Mobbs, C.V. (1999). Fasting regulates hypothalamic neuropeptide Y, agouti-related peptide, and proopiomelanocortin in diabetic mice independent of changes in leptin or insulin. *Endocrinology* 140, 4551-4557.

- Mizuno, T.M., and Mobbs, C.V. (1999). Hypothalamic agouti-related protein messenger ribonucleic acid is inhibited by leptin and stimulated by fasting. *Endocrinology* 140, 814-817.
- Morohashi, K., Tsuboi-Asai, H., Matsushita, S., Suda, M., Nakashima, M., Sasano, H., Hataba, Y., Li, C.L., Fukata, J., Irie, J., *et al.* (1999). Structural and functional abnormalities in the spleen of an mFtz-F1 gene-disrupted mouse. *Blood* 93, 1586-1594.
- Mountjoy, K.G., Mortrud, M.T., Low, M.J., Simerly, R.B., and Cone, R.D. (1994). Localization of the melanocortin-4 receptor (MC4-R) in neuroendocrine and autonomic control circuits in the brain. *Mol Endocrinol* 8, 1298-1308.
- Mountjoy, K.G., Robbins, L.S., Mortrud, M.T., and Cone, R.D. (1992). The cloning of a family of genes that encode the melanocortin receptors. *Science* 257, 1248-1251.
- Munzberg, H., Huo, L., Nillni, E.A., Hollenberg, A.N., and Bjorbaek, C. (2003). Role of signal transducer and activator of transcription 3 in regulation of hypothalamic proopiomelanocortin gene expression by leptin. *Endocrinology* 144, 2121-2131.
- Myers, M.G., Jr. (2004). Leptin receptor signaling and the regulation of mammalian physiology. *Recent Prog Horm Res* 59, 287-304.
- Naeser, P. (1974). Function of the adrenal cortex in obese-hyperglycemic mice (gene symbol ob). *Diabetologia* 10, 449-453.
- Nishizuka, M., and Pfaff, D.W. (1989). Intrinsic synapses in the ventromedial nucleus of the hypothalamus: an ultrastructural study. *J Comp Neurol* 286, 260-268.
- Ogden, C.L., Flegal, K.M., Carroll, M.D., and Johnson, C.L. (2002). Prevalence and trends in overweight among US children and adolescents, 1999-2000. *JAMA* 288, 1728-1732.
- Ollmann, M.M., Wilson, B.D., Yang, Y.K., Kerns, J.A., Chen, Y., Gantz, I., and Barsh, G.S. (1997). Antagonism of central melanocortin receptors in vitro and in vivo by agouti-related protein. *Science* 278, 135-138.

- Porte, D., Jr., Seeley, R.J., Woods, S.C., Baskin, D.G., Figlewicz, D.P., and Schwartz, M.W. (1998). Obesity, diabetes and the central nervous system. *Diabetologia* 41, 863-881.
- Puhl, R.M., and Brownell, K.D. (2003). Psychosocial origins of obesity stigma: toward changing a powerful and pervasive bias. *Obes Rev* 4, 213-227.
- Reilly, M.P., and Rader, D.J. (2003). The metabolic syndrome: more than the sum of its parts? *Circulation* 108, 1546-1551.
- Rice, D.A., Mouw, A.R., Bogerd, A.M., and Parker, K.L. (1991). A shared promoter element regulates the expression of three steroidogenic enzymes. *Mol Endocrinol* 5, 1552-1561.
- Rios, M., Fan, G., Fekete, C., Kelly, J., Bates, B., Kuehn, R., Lechan, R.M., and Jaenisch, R. (2001). Conditional deletion of brain-derived neurotrophic factor in the postnatal brain leads to obesity and hyperactivity. *Mol Endocrinol* 15, 1748-1757.
- Roselli-Reh fuss, L., Mountjoy, K.G., Robbins, L.S., Mortrud, M.T., Low, M.J., Tatro, J.B., Entwistle, M.L., Simerly, R.B., and Cone, R.D. (1993). Identification of a receptor for gamma melanotropin and other proopiomelanocortin peptides in the hypothalamus and limbic system. *Proc Natl Acad Sci U S A* 90, 8856-8860.
- Rosen, E.F. (1968). Amygdaloid complex and medial hypothalamic nucleus functioning in food regulation. *Physiol Behav* 3, 567-570.
- Ryan, N.K., Van der Hoek, K.H., Robertson, S.A., and Norman, R.J. (2003). Leptin and leptin receptor expression in the rat ovary. *Endocrinology* 144, 5006-5013.
- Ryan, N.K., Woodhouse, C.M., Van der Hoek, K.H., Gilchrist, R.B., Armstrong, D.T., and Norman, R.J. (2002). Expression of leptin and its receptor in the murine ovary: possible role in the regulation of oocyte maturation. *Biol Reprod* 66, 1548-1554.
- Saad, M.F., Damani, S., Gingerich, R.L., Riad-Gabriel, M.G., Khan, A., Boyadjian, R., Jinagouda, S.D., el-Tawil, K., Rude, R.K., and Kamdar, V. (1997). Sexual dimorphism in plasma leptin concentration. *J Clin Endocrinol Metab* 82, 579-584.

- Samaha, F.F., Iqbal, N., Seshadri, P., Chicano, K.L., Daily, D.A., McGrory, J., Williams, T., Williams, M., Gracely, E.J., and Stern, L. (2003). A low-carbohydrate as compared with a low-fat diet in severe obesity. *N Engl J Med* 348, 2074-2081.
- Sambrook, J., and Russell, D.W. (2001). *Molecular Cloning: A Laboratory Manual*, 3 edn (Cold Spring Harbor, Cold Spring Harbor Laboratory Press).
- Saper, C.B., Chou, T.C., and Elmquist, J.K. (2002). The need to feed: homeostatic and hedonic control of eating. *Neuron* 36, 199-211.
- Sauer, B., and Henderson, N. (1988). Site-specific DNA recombination in mammalian cells by the Cre recombinase of bacteriophage P1. *Proc Natl Acad Sci U S A* 85, 5166-5170.
- Shima, Y., Zubair, M., Ishihara, S., Shinohara, Y., Oka, S., Kimura, S., Okamoto, S., Minokoshi, Y., Suita, S., and Morohashi, K. (2005). Ventromedial hypothalamic nucleus-specific enhancer of Ad4BP/SF-1 gene. *Mol Endocrinol* 19, 2812-2823.
- Shinoda, K., Lei, H., Yoshii, H., Nomura, M., Nagano, M., Shiba, H., Sasaki, H., Osawa, Y., Ninomiya, Y., Niwa, O., *et al.* (1995). Developmental defects of the ventromedial hypothalamic nucleus and pituitary gonadotroph in the Ftz-F1 disrupted mice. *Dev Dyn* 204, 22-29.
- Sigal, R.J., El-Hashimy, M., Martin, B.C., Soeldner, J.S., Krolewski, A.S., and Warram, J.H. (1997). Acute postchallenge hyperinsulinemia predicts weight gain: a prospective study. *Diabetes* 46, 1025-1029.
- Slyper, A.H. (2004). The pediatric obesity epidemic: causes and controversies. *J Clin Endocrinol Metab* 89, 2540-2547.
- Soriano, P. (1999). Generalized lacZ expression with the ROSA26 Cre reporter strain. *Nat Genet* 21, 70-71.
- Spanswick, D., Smith, M.A., Groppi, V.E., Logan, S.D., and Ashford, M.L. (1997). Leptin inhibits hypothalamic neurons by activation of ATP-sensitive potassium channels. *Nature* 390, 521-525.

- Stallings, N.R., Hanley, N.A., Majdic, G., Zhao, L., Bakke, M., and Parker, K.L. (2002). Development of a transgenic green fluorescent protein lineage marker for steroidogenic factor 1. *Mol Endocrinol* 16, 2360-2370.
- Stanley, B.G., Chin, A.S., and Leibowitz, S.F. (1985). Feeding and drinking elicited by central injection of neuropeptide Y: evidence for a hypothalamic site(s) of action. *Brain Res Bull* 14, 521-524.
- Stellar, E. (1954). The physiology of motivation. *Psychol Rev* 61, 5-22.
- Sutton, G.M., Trevaskis, J.L., Hulver, M.W., McMillan, R.P., Markward, N.J., Babin, M.J., Meyer, E.A., and Butler, A.A. (2006). Diet-genotype interactions in the development of the obese, insulin-resistant phenotype of C57BL/6J mice lacking melanocortin-3 or -4 receptors. *Endocrinology* 147, 2183-2196.
- Swerdloff, R.S., Batt, R.A., and Bray, G.A. (1976). Reproductive hormonal function in the genetically obese (ob/ob) mouse. *Endocrinology* 98, 1359-1364.
- Tartaglia, L.A. (1997). The leptin receptor. *J Biol Chem* 272, 6093-6096.
- Tartaglia, L.A., Dembski, M., Weng, X., Deng, N., Culpepper, J., Devos, R., Richards, G.J., Campfield, L.A., Clark, F.T., Deeds, J., *et al.* (1995). Identification and expression cloning of a leptin receptor, OB-R. *Cell* 83, 1263-1271.
- Vaisse, C., Halaas, J.L., Horvath, C.M., Darnell, J.E., Jr., Stoffel, M., and Friedman, J.M. (1996). Leptin activation of Stat3 in the hypothalamus of wild-type and ob/ob mice but not db/db mice. *Nat Genet* 14, 95-97.
- van der Kroon, P.H., Boldewijn, H., and Langeveld-Soeter, N. (1982). Congenital hypothyroidism in latent obese (ob/ob) mice. *Int J Obes* 6, 83-90.
- Warbritton, A., Gill, A.M., Yen, T.T., Bucci, T., and Wolff, G.L. (1994). Pancreatic islet cells in preobese yellow *Avy*^{-/-} mice: relation to adult hyperinsulinemia and obesity. *Proc Soc Exp Biol Med* 206, 145-151.
- Wilding, J.P., Gilbey, S.G., Bailey, C.J., Batt, R.A., Williams, G., Ghatei, M.A., and Bloom, S.R. (1993). Increased neuropeptide-Y messenger ribonucleic

- acid (mRNA) and decreased neurotensin mRNA in the hypothalamus of the obese (ob/ob) mouse. *Endocrinology* *132*, 1939-1944.
- Woods, S.C., Seeley, R.J., Porte, D., Jr., and Schwartz, M.W. (1998). Signals that regulate food intake and energy homeostasis. *Science* *280*, 1378-1383.
- Wylie-Rosett, J., Segal-Isaacson, C.J., and Segal-Isaacson, A. (2004). Carbohydrates and increases in obesity: does the type of carbohydrate make a difference? *Obes Res* *12 Suppl 2*, 124S-129S.
- Xu, B., Goulding, E.H., Zang, K., Cepoi, D., Cone, R.D., Jones, K.R., Tecott, L.H., and Reichardt, L.F. (2003). Brain-derived neurotrophic factor regulates energy balance downstream of melanocortin-4 receptor. *Nat Neurosci* *6*, 736-742.
- Yang, X.W., Model, P., and Heintz, N. (1997). Homologous recombination based modification in *Escherichia coli* and germline transmission in transgenic mice of a bacterial artificial chromosome. *Nat Biotechnol* *15*, 859-865.
- Yen, T.T., Allan, J.A., Yu, P.L., Acton, M.A., and Pearson, D.V. (1976). Triacylglycerol contents and in vivo lipogenesis of ob/ob, db/db and Avy/a mice. *Biochim Biophys Acta* *441*, 213-220.
- Zhang, Y., Proenca, R., Maffei, M., Barone, M., Leopold, L., and Friedman, J.M. (1994). Positional cloning of the mouse obese gene and its human homologue. *Nature* *372*, 425-432.
- Zhao, L., Bakke, M., Krimkevich, Y., Cushman, L.J., Parlow, A.F., Camper, S.A., and Parker, K.L. (2001). Steroidogenic factor 1 (SF1) is essential for pituitary gonadotrope function. *Development* *128*, 147-154.

VITAE

Nathan Christian Bingham was born in Provo, Utah, on April 5, 1973, the son Michael Wayne Bingham and Arlene Wells Bingham. He graduated from Irvington High School, Fremont, California in 1991. From May of 1993 to May of 1995, he worked as missionary for the Church of Jesus Christ of Latter-day Saints in Montreal, Quebec, Canada. In the fall of 1995 he began his studies at Brigham Young University in Provo, Utah, where he received the degree of Bachelor of Arts with a major in History and minor in Chemistry in April, 1999. In June, 1999, he entered the Medical Scientist Training Program at the University of Texas Southwestern Medical Center, Dallas, Texas. After completing two years of medical training, he entered the Graduate School of Biomedical Sciences, Division of Cell and Molecular Biology in August, 2001. After completing his dissertation work, he began the clinical portion of his M.D. training in January, 2007. Nathan married Danielle Nicole De Graw in February 1996. They are the proud parents of two sons, Chaid Daniel and Avram Christian, and a daughter, Kennis Nicole.

Permanent Address: 3309 Wareham Circle
Richardson, TX 75082